BLL ID NO' –

The Voltammetric Determination
of Phosphate and Silicate
in Washing Powders.

G.C.Cripps, B.Sc., M.Sc.

A Doctoral thesis submitted in partial requirement
for the award of Doctor of Philosophy degree of the
Loughborough University of Technology.

Supervisor: Dr.A.G.Fogg, B.Sc., Ph.D., A.R.T.C.S.,
C.Chem., F.R.I.C.

Dept. of Chemistry

October 1982.

Contents

Acknowledgements

I would like to thank my supervisor Dr. Arnold Fogg and my industrial supervisor Dr. Brian Birch for their help and guidance throughout the past two years. I would like to thank Barbara Watkins for typing this thesis and the staff of the Chemistry Department at Loughborough for their technical support.

Permission has been granted by the following publishers for the reproduction of diagrams in the introductory section. Permission has been obtained from authors where requested by the publisher.

The American Chemical Society, Washington DC; Figures 3 and 16.
Marcel Dekker, Inc., New York; Figures 23-26.
Elsevier Scientific Publishing Company, Amsterdam; Figures 27, 28, 29, 32 and 33.
Elsevier Sequoia, SA., Lausanne; Figures 10, 29, 30, 37-39.
Ganthier-Villars, Paris; Figure 40.
McGraw-Hill Book Company, New York; Figures 14 and 15.
Pergamon Press, Oxford; Figures 2a, 2b, 4.
The Royal Society, London; Figures 20-22.
The Royal Society of Chemistry, London; Figure 36.
The Society for Applied Spectroscopy, Frederick MD; Figure 35.
Springer-Verlag, Heidelburg; Figure 34.
Technicon, Basingstoke, Figure 12.
John Wiley and Sons, Inc., New York; Figures 5-9, 11, 17, 19, 31.

But I grow old always learning many things.

(Plutarch, Solom, xxxi)

Summary

In this work previous static and flow injection voltammetric methods for the determination of phosphate and silicate have been developed for the determination of total phosphate and soluble silicate in commercial washing powders. The method is based on the electrochemical reduction of heteropoly acids at + 0.3 v. (vs. SCE) at a glassy carbon electrode. Anionic detergents are a constituent of washing powders and are found to reduce markedly the differential pulse voltammetric peak currents obtained for 12-molybdophosphate and 12-molybdosilicate in aqueous solutions. Use of a sample solution 40 - 50% in ethanol was found to prevent this interference. By this method soluble silicate has been determined in unhydrolysed solutions of washing powders and total phosphate in hydrolysed solutions using both static and flow injection modes.

The flow injection analysis method for silicate requires the reaction coil to be heated in a water bath at 60°, very little reaction taking place at room temperature. Thus it is possible to determine phosphate with the reaction coil at room temperature without interference from silicate. The flow injection system developed for silicate determination initially involved a converging stream of mannitol solution to prohibit phosphate interference. The use of mannitol was subsequently found to be unnecessary as the level of free phosphate in unhydrolysed samples is not high enough to interfere with the silicate determination. The reagent stream used was the same for both silicate and phosphate analysis.

The differential pulse voltammograms for 12-phosphomolybdate and 12-silicomolybdate are sufficiently different to observe one in the presence of the other. An attempt was made to determine phosphate

and silicate simultaneously; this was only partially successful. The heteropoly acids used for these determinations exhibit different voltammograms with variation of pH and ethanol content of the test solutions. The α and β isomers of phospho- and silicomolybdates were thus identified by different pulse voltammetry. The heteropoly acids showed an ability to be adsorbed onto the surface of the working electrode, and this was the subject of a brief study.

An attempt has been made to combine an autoanalyzer hydrolysis coil with the flow injection system developed. A completely automated system for total phosphate has met with some success.

Introduction

The analytical chemistry of phosphates and silicates has been dominated for many years by the method of forming a heteropoly acid and reducing it to form a "heteropoly blue" compound which is detected colorimetrically (Boltz and Howell 1978). The colorimetric methods have been developed for automatic and flow injection analysis (Grasshoff, 1971; Ruzicka and Hansen, 1981) mainly for phosphates. This introduction reviews the chemistry of heteropoly acids and their electrochemical behaviour at carbon electrodes, together with an overview of flow injection methods.

1. The Analysis of Silicates.

This work confines itself to the analysis of soluble silicates, in particular the sodium silicates which were employed in the washing powder industry as additives. A quarter of the United Kingdom's production of sodium silicates is used in the manufacture of detergents (Dent Glasser, 1982). In the solid phase the structures of the metasilicate hydrates ($Na_2SiO_3.xH_2O$) are well known; all contain the dihydrogen orthosilicate ion, $H_2SiO_4^{--}$ (tetrahedral). In solution, at low concentrations ($<10^{-2}$M) monomeric species are thought to exist at all pH values.

The analytical chemistry of silicon and its compounds has been reviewed by Bennett (1977) and Myshiyaeva and Krasnoschekov (1974). Apart from heteropoly techniques other methods have been used to determine silicates, e.g., gravimetry, titrimetry, potentiometry and indirect spectroscopic detection, ultra violet (Truedell and Boltz, 1963) and atomic absorption (Kirkbright et al, 1967; Ramakrishna, 1969; Simon and Boltz, 1975; Sand et al, 1976). Indirect methods usually entail the extraction of a heteropolyacid with an organic solvent, for example, iso-butyl acetate.

Recently, Alimarin et al (1981) has reviewed the electrochemical methods in the analytical chemistry of heteropoly compounds including a list of voltammetric methods for silicon. These methods have been applied to the analysis of metals and metal ores as well as to solutions and organic solvents (Pottkamp and Umland, 1971). The most recent application is that of Iyer et al (1981) who can detect traces of silica in water down to 10 μg/litre, by anodic stripping voltammetry.

Interference to silicate analysis is affected by phosphorus which is often present in high concentrations and to a lesser extent the trace elements arsenic and germanium. It is possible to detect all four when present in the same sample. Hahn and Wagenknecht (1961) detected arsenic, germanium, phosphorus and silicon by amperometric titration at different potentials. Other workers have reported these elements by selective extraction of heteropoly acids with organic solvents followed by polarographic (Bazzi and Boltz, 1976; Fujinaga and Maguosa, 1978), colorimetric (Paul, 1965) or atomic absorption spectroscopic analysis (Kirkbright et al, 1967). Mcdonald and Van de Voort (1968) separated silicate from phosphate by precipitation of phosphomolydbate leaving silicomolybdate in solution. Several workers have managed by control of pH to selectively form silicomolybdate in the presence of phosphate (Greenfield, 1959; Shen and Dryoff, 1962; Sarkar, 1981). However reduction of any phosphomolybdate formed by an organic acid (e.g. citric, oxalic or tartaric) is the usual mode of removing interfering phosphate species.

2. The Analysis of Phosphates.

In this work we are concerned with the analysis of total phosphate in washing powders. Most of the phosphate in washing powders is present as sodium triphosphate in the range 5-25% w/w; it is used as a base for the synthetic surfactant (e.g. sodium alkyl benzyl sulphonate producing a more efficient cleansing agent (Toy, 1976).

Phosphates exist as phosphorus atoms surrounded by four oxygen atoms. The oxygen atoms may be shared between two phosphorus atoms to produce P - O - P bonds, these are called condensed phosphates (cf. polymeric forms of silicon). Compounds containing a few phosphorus atoms (1 - 6) are readily soluble in water forming anions; higher polyphosphates (10 - 25 phosphorus atoms) are more inert and vitreous in nature (Corbridge, 1978). Polyphosphates are able to sequester metal ions such as Mg^{++} and Ca^{++} which are responsible for the hardness in water.

The analysis of phosphates like silicates has been dominated by the colorimetric determination of an "heteropoly blue" complex (Boltz and Howell, 1978). Other methods, gravimetry, titrimetry and X-ray fluorescence have been reviewed by Halman (1972) and Young (1976). Crawford et al (1973) estimated phosphate by atomic absorption spectroscopy of a complex formed with magnesium. Two other sets of workers, Zaugg and Knox (1966) and Kumamura (1967) also used atomic absorption spectroscopy, but on the heteropolyacid compound. Lueck and Boltz (1958) extracted the heteropolyacid from aqueous solution into diethyl ether and iso-butanol then measured the ultra-violet spectrum. Alimarin (1981) has recently reviewed electrochemical techniques. Similarly, with the analysis of silicates, the determination of phosphate by an heteropolyacid method is interfered with by its homologues, silicate, arsenate and germanate. Only silicate is usually present in large enough quantities to have any effect. Mercuric mercury has also been observed to interfere at low levels (Tillman and Syers, 1975). Extraction procedures and control of pH can eliminate interferences. Johnson (1971) eliminated arsenate interference by reducing to arsenite which does not form a heteropoly compound. Two sets of workers have determined silicate and phosphate simultaneously. Shen and Dryoff (1962) measured the rates of formation of the "heteropoly blue" against absorbance and correlated against standards of phosphate and silicate. Downes (1978) has developed an automatic technique for phosphate in the presence of arsenic, silicon and mercuric ions. The arsenate and mercury are removed by thiosulphate in acid solution and the silicate by including a tartrate in the reagent stream.

Analysing total phosphate involves the hydrolysis of higher condensed phosphates to orthophosphate so that a heteropoly compound can be produced. The hydrolysis process is time consuming and is a possible source of error. The hydrolysis of condensed phosphates is discussed below.

3. Condensed Phosphates.

The term "condensed phosphate" is used to describe all phosphates whose acids contain less water than orthophosphoric acid (Greenfield and Clift, 1975). Condensed phosphates can be divided into two main groups, "poly" or "chain" phosphates which can be defined by the empirical formula

$$H_{(n+2)}P_nO_{(3n+1)}$$

and "meta" or "cyclic" phosphates with the general formula, $(HPO_3)_n$.

The experimental study described later concentrates on the detergent constituent sodium tripolyphosphate (TPP), $Na_5P_3O_{10}$, the simplest linear condensed phosphate. Condensed phosphates have been the subject of two recent texts by Greenfield and Clift (1975) and Kulaev (1979). Both works include a study of the structure of condensed phosphates, but a more extensive work was published by Thilo (1965). The structures of two simple species are shown below (fig. 1).

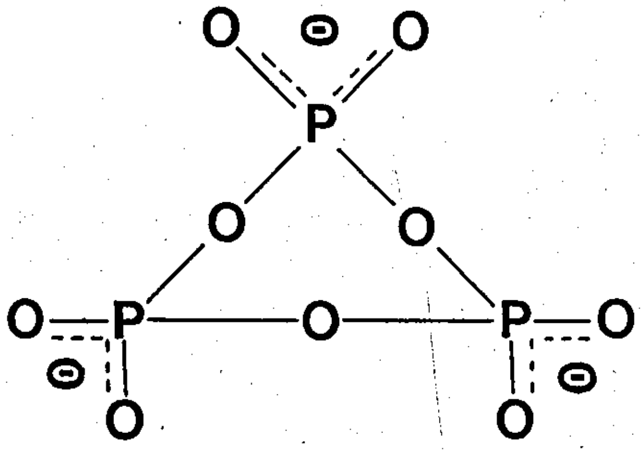

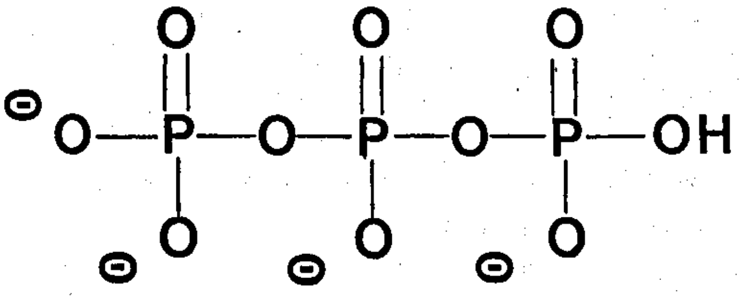

So called "ultraphosphates" also exist as cross linked species containing phosphorus atoms linked to three others by three oxygen atoms in a "tertiary arrangement".

3a. Complexing Properties.

The major chemical property of the condensed phosphates is their ability to sequester metal ions. Most general texts deal with this topic (Corbridge, 1978; Griffith et al, 1973; Halmann, 1972; Toy, 1976). Recently Yoza et al (1975, 1980a) and Crawford et al (1973) have applied this complexing property to analytical procedures for the determination of magnesium. Condensed phosphates have been shown to complex nearly all the heavy metals (Werner and Ebert, 1977) present in the natural aqueous environment. Reynolds and Rogers (1949) and Rogers and Reynolds (1949) observed similar chemistry with pyrophosphate forming insoluble products with most cationic species. Polyphosphate anions have also been shown to associate with larger complex species such as the hexamminocobalt (III) ion, $[Co(NH_3)_6{}^{3+}$, (Matsuura, 1974). Salts of alkali metals are soluble in water, whereas salts of divalent species (e.g. Ba^{++}, Mg^{++}, Pb^{++}) are generally insoluble. Condensed phosphates are stable in neutral solution conditions.

3b. Hydrolysis of Condensed Phosphates.

Hydrolysis occurs in solutions which are not neutral. The P - O - P bond liberates about 3Kj/mol for all types of phosphates upon hydrolysis.

The hydrolysis of polyphosphates has been extensively studied as it is a prerequisite step in their analysis. The degradation of sodium tripolyphosphate for example, is a two-stage process:

(i) $P_3O_{10}{}^{5-} \rightarrow P_2O_7{}^{4-} + PO_4{}^{3-}$

(ii) $P_2O_7{}^{4-} \rightarrow 2PO_4{}^{3-}$

One triphosphate molecule does not break down to these orthophosphate units directly. The simultaneous hydrolysis of two P - O - P bonds does not occur, the intermediate product being the pyrophosphate species. Larger polyphosphates behave in a similar fashion. With cyclic phosphates, however, the first step is the scission of the ring structure. The rate of formation of orthophosphate from polyphosphates in solution is a function of pH and temperature.

Figures 2a and 2b. The hydrolysis of sodium triphosphate (Greenfield and Clift, 1975).

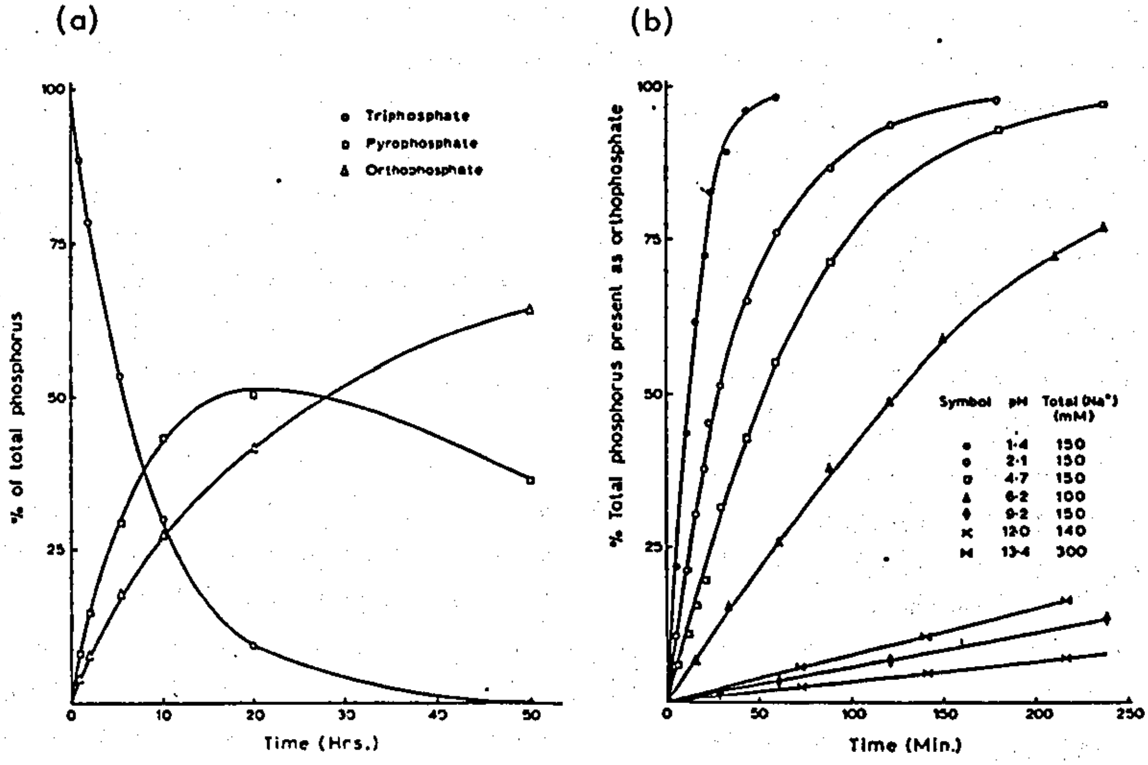

. Distribution of phosphate species during the hydrolysis of sodium triphosphate, 100°C, pH 9.2.

. Hydrolysis of sodium triphosphate (10 mM), 100°C, distilled water.

The swiftest hydrolysis has been shown to occur at pH 1.5 and 100°C. Slower hydrolysis will occur under alkaline conditions. Figures 2(a) and 2(b) demonstrate the change in rate of hydrolysis with pH. The half reaction time ($t\frac{1}{2}$) for the hydrolysis of a straight chain polyphosphate at pH 1.0 is 10 minutes. Cyclic phosphates degrade to best effect at pH 3.5 (Huffman and Fleming, 1960). The conditions for hydrolysis have been summarised in the form of a nomograph by Griffith (1959) (see fig. 3). Several attempts to catalyse the hydrolysis of polyphosphates have been made in order to accelerate the reaction. However the use of metal ions of copper, zinc and molybdate have not improved the acid digestion method. Recently Haight et al (1979) and Imamura et al (1979) used permanganate to oxidise vanadopolyphosphate and manganese(II)polyphosphate to vanadium(V) and manganese(III) respectively. This results in the release of an orthophosphate unit from the polyphosphate chain. Fast hydrolysis rates have also been claimed for biological mechanisms, using phosphatase extracted from E.Coli, yeast and pea plants (Josse, 1966; Pierpoint, 1957). Enzymatic hydrolysis is reviewed by Kulear (1979) in his recent text. These methods are generally applied to the hydrolysis of biological chemicals such as adenosine triphosphate (ATP) and the analysis of pyrophosphate (Silcox and McCarty, 1973; Baykor and Araera, 1982). The phosphatases employed can be highly specific. The rate of hydrolysis catalysed by unspecific enzymes, however, is not fast enough to challenge the efficiency of acid digestion. Both inorganic and biological hydrolysis occur in the natural environment. In the latter case the energy carrying molecule ATP loses phosphate groups in such a process. Hydrolysis of phosphates in surface waters has been studied by Clesceri

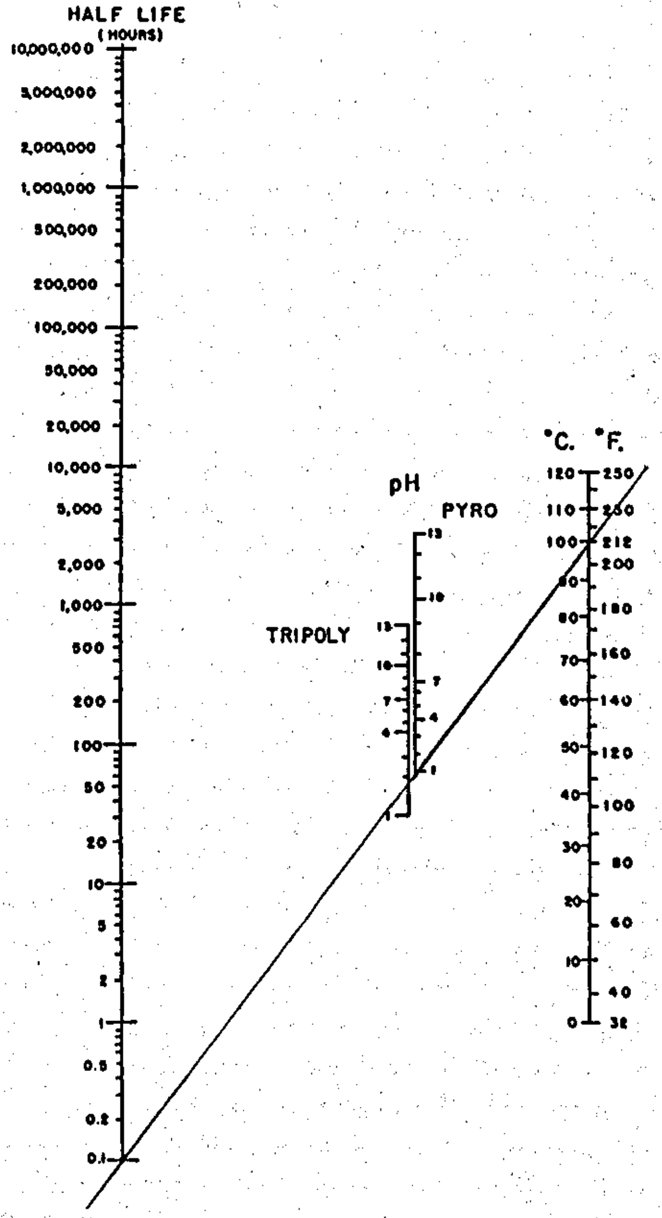

Figure 3. A nomograph of the conditions for hydrolysis of polyphosphates. The line superimposed cuts the scales at 100°C, 1.8 pH and 0.1 hours (Griffith, 1959).

and Lee (1965 (a), (b)), Roux and Boutin (1975), and Aiba and Ohtake (1976). In a polluted river such as the Rhine the half life of tripolyphosphate is approximately 2 days (Werner and Ebert, 1977).

3c. Analysis of Condensed Phosphates.

The usual mode for analysis of condensed phosphates is hydrolysis to orthophosphate via acid digestion followed by colorimetric determination as phosphomolybdate. Whilst this method is efficient for inorganic forms of phosphate, organic or biological material, such as surface water samples, require more drastic methods (e.g. ultra violet irradiation and autoclaving). Harwood et al (1969) have reviewed methods for total phosphate analysis.

It is often necessary to determine individual polyphosphates. Recently methods have been developed based on an HPLC separation using anion-exchange columns, followed by acid hydrolysis and colorimetric detection (Scott and Haight, 1975; Yoza et al, 1975, 1980a, b). Other chromatographic methods have been used, including thin layer techniques and unforced anion exchange. Specific determinations have been carried out using enzymatic hydrolysis. Highly specific phosphatases have been employed to analyse for pyrophosphate (Silcox and McCarty, 1973; Bloemers et al 1970) and trimetaphosphate (Meyerhof et al, 1953). Some chemical methods have been used. For example Hoffman and Saracz (1962) separated ortho, pyro and metaphosphates by producing complexes with the aid of chloranilic acid salts.

Gravimetric methods have been employed, but have never been completely satisfactory due to the similarity of the properties of the different polyphosphates. These methods use the precipitation of the phosphate with heavy metals. Zinc can be used to separate pyrophosphate as a precipitate from a solution also containing ortho- and triphosphate.

The titration curves of the free acids of polyphosphates can be used to distinguish between species (Greenfield and Clift, 1975) (see fig. 4 below).

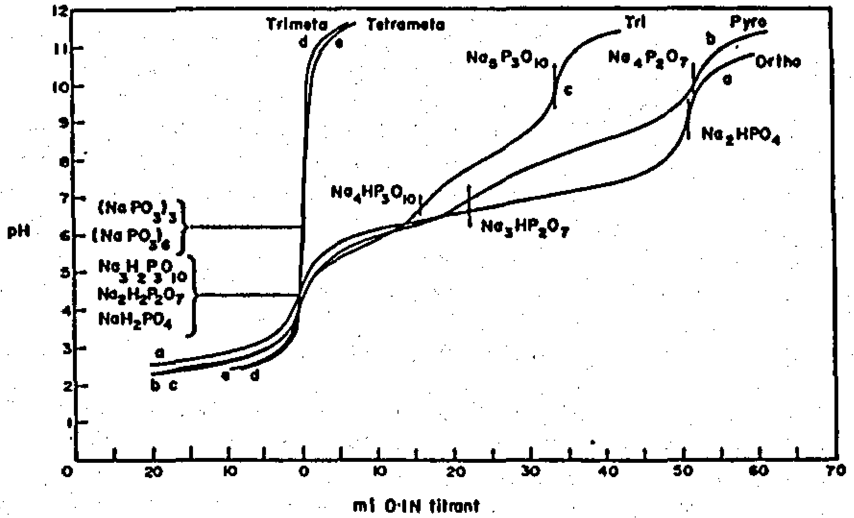

Potentiometric titration curves of orthophosphate, pyrophosphate, triphosphate, trimetaphosphate and tetrametaphosphate from alkaline pH.

Figure 4. (Greenfield and Clift, 1975).

Electrochemical detection with which this work is concerned has been used only to a limited extent. One amperometric method depends on the insolubility of cadmium pyrophosphate, another is the amperometric titration with hexammine cobalt(III)chloride (Laitenen and Burdett, 1951). Buyers (1958) used a conductimetric method to determine ortho-, pyro- and triphosphate in admixture. The method relies on the fact that orthophosphate reacts with 3 moles of silver ions (Ag^+), pyro 4 moles and tri 5 moles. More pertinent to this study is the use of polarographic methods. Al-Sulimany and Townsend (1973) determined triphosphate by the reduction of the cadmium wave which is proportional to the triphosphate present in the sample. A similar indirect method was developed by Shaw and Townsend (1972) using the reduction of the octyltin wave in the presence of triphosphate. The effect of phosphates, particularly pyrophosphate, on polarographic waves has been extensively studied. Rogers and Reynolds (1949) and Reynolds and Rogers (1949) studied a wide range of transition and heavy metals' polarographic behaviour in the presence of phosphates. More recent work has come from Townsend (see above), Cox and Cheng (1974) on iron and Costley and Farr (1968) on zinc and lead.

The use of some of the above techniques have been developed for flow injection and auto analyzer methods; these are discussed later.

4. Flow Injection Analysis.

Flow injection analysis has been developed in the main by Ruzicka and Hansen over the past eight years and their work together with other contributors has been reviewed by them in a recent publication (Ruzicka and Hansen, 1981) and volume 114 of Analytica Chimica Acta.

Flow injection analysis (FIA) entails the injection of liquid samples into a continuous flowing non-segmented stream, usually consisting of suitable reagents to enable detection at a flow through cell. The flow through cell is most popularly a spectrophotometric or electrochemical device. We can make a direct comparison with the air-segmented autoanalysis methods. Figures 5, 6, 7 compare and contrast simple FIA and air-segmented methods. The pump manifold is simpler for a FIA system. Quite often only one stream is required whereas automatic methods need

5.

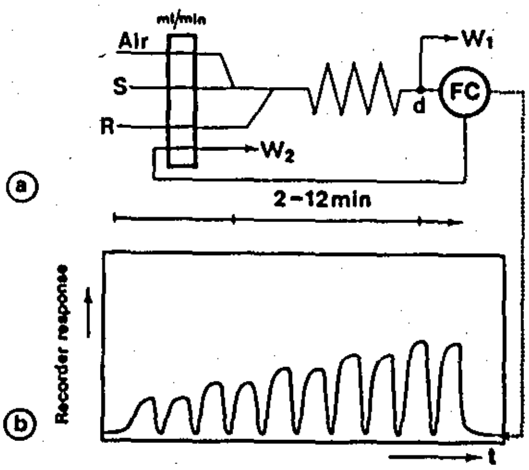

Air-segmented continuous flow system (*a*) designed for the same function as the FIA system of Figs. 2.1 and 2.2. The record in (*b*) shows the analysis of five samples with progressively increasing analyte content.

6.

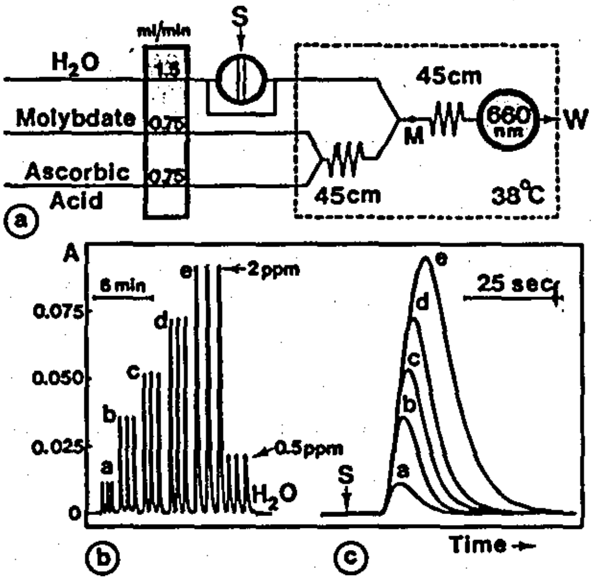

(*a*) Manifold for high-sensitivity determination of phosphate. The sample is injected into an inert carrier stream (water) merged with the reagent solution, and after mixing in the reaction coil is measured spectrophotometrically. To obtain effective mixing without excessive dispersion of the sample solution, a mixing point M is inserted immediately following the confluence point. All tubes are 0.5 mm ID. To increase the rate of reaction, the system is thermostated at 38°C. (*b*). At the left are the records obtained by injecting increasing volumes of sample of a 2 ppm P-PO_4 standard solution (S_v being: a, 23 µl; b, 70 µl; c, 115 µl; d, 180 µl; and e, 320 µl), followed by the output for a 0.5 ppm P-PO_4 sample solution, where S_v = 320 µl. To the right are shown peaks a–e, recorded at high paper speed.

7.

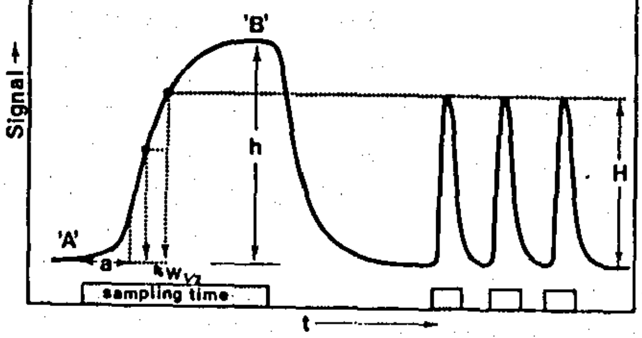

Sampling frequency, sampling time, and signal form as recorded in a continuous flow analyzer based on air-segmented stream (left) and the recorder output of a FIA system (right) (1). For details, see the text.

Figures 5, 6 and 7, (Ruzicka and Hansen, 1981) at least four. It is usual for flow rates in FIA to be much higher giving sharp and more reproducible responses. However tube lengths (or reaction coils) are longer and of a narrower bore. Bores are typically 0.3 - 0.8 mm internal diameter (i.d.) whereas autoanalysis will use tubes with diameters in the order of 2 mm. The air segments in the autoanalyzer system prevent the sample diffusing in the stream whilst the reaction is occurring. In FIA the narrower bore tubing and faster flow rates compensate for this. Thus with FIA the maximum number of discrete samples can be analyzed using the minimum quantities of reagent and sample in the shortest time by controlling flow rate and optimising the bore and length of the conduits of the system. FIA is often coupled with HPLC which is used to resolve many compounds into discrete bands. FIA is well suited for such applications with the ability to minimize band broadening and maintain the effectiveness of the HPLC. The performance of FIA is governed by the control of sample dispersion. The sensitivity can be adjusted by varying the volume of the sample injected, the i.d. and the length of the system. Degree of dispersion increases with tube length and decreases with diameter, so in contrast with air segmented methods residence time is increased in practice by slowing the flow rate as opposed to lengthening the reaction coils. Taking this idea to the extreme the flow can be stopped such that the sample slug is held in the reaction coil or the detector allowing for slow reaction rates or the study of reaction rates. As the readout in FIA is a measure of peak height dispersion can be defined as the ratio between the original sample concentration and the concentration at the detector (or maximum peak height). Ratios in the range 2 - 10 are most frequently found in FIA. For example, for a dispersion ratio of 5 the sample will have been diluted by the reagent 5 times before detection.

FIA does not rely on measurement at a "steady state" as do air-segmented systems, but on reproducibility of sample injection, dispersion of the sample zone and the timing of the sample zone from injection to detection. A dispersion value of 10 corresponds to 50% of a "steady state" signal. As FIA operates usually well below the "steady state" and chemically not at equilibrium, certain slow chemical reactions may limit the use of the technique. The chemical reactions involved can be seen as a process of interaction, where concentration gradients are set up between the carrier stream and the core of the sample injection. Consequently the chemistry may be complicated and will depend initially upon the rate of mixing.

A simple version of FIA (see Fig. 8 below)

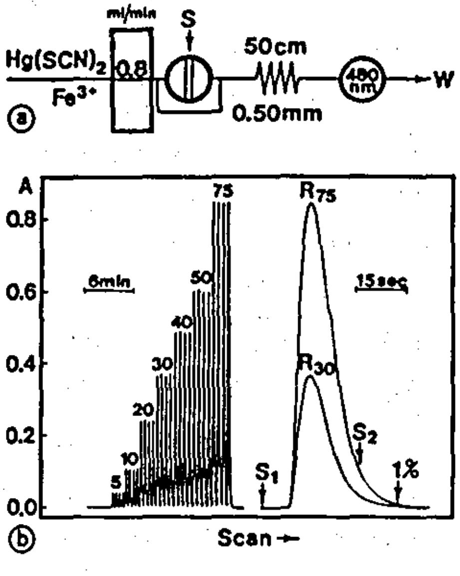

(a) Flow diagram for the spectrophotometric determination of chloride. S, point of sample injection; W, waste. *(b)* Record output showing chloride analysis in the range 5 to 75 ppm Cl with the system depicted in *(a)*. To demonstrate the reproducibility of measurement, each sample was injected in quadruplicate. Injected volume, 30 µl; sampling rate, approximately 130 samples/h. The fast scan of the 30 ppm sample (R_{30}) and the 75 ppm sample (R_{75}) on the right shows the extent of the carryover (less than 1%) if samples are injected in a span of 28 s (difference between S_1 and S_2).

Figure 8. (Ruzicka and Hansen, 1981).

consists of (1) Peristaltic Pump
(2) Injection Valve
(3) Reaction Coil
(4) Flow through detector.

Peristaltic pumps are preferred, in which high frequency pulsation of low amplitude generate low levels of noise by use of models operating at high speeds (≈ 40 rpm) employing at least 8 rollers on the rotating cylinder. If any pulsing is observed, it may be removed by the use of a pneumatic damper (Bergamin et al, 1978), a small reservoir (10 - 20 ml volume) is inserted in the system between pump and injection port. The introduction of the sample is effected usually by either injection through a septum or more popularly by means of a valve system which diverts the flow of the stream through a small volume of tubing (e.g. 100 μl) into which the sample had been introduced. The methods of detection are limited to spectrophotometry (Atomic Absorption, ultra violet, visible, fluorescence, flame photometry) or electrochemical methods (potentiometry or voltammetry). Spectrophotometric methods involve the passing of the stream through the optical cell of a suitable instrument. Electrochemical detectors consist of a working electrode (quite often carbon based) to which the carrier stream is presented, either flowing past the electrode or being "fired" at it in a wall-jet configuration (see Figures 9a, b, and 10). The basic difference between these methods of detection is that in spectrophotometric methods the signal achieved reflects the composition of the bulk of the solution, whereas electrochemical methods rely on the transport of electroactive species to the surface of the electrode. Hence the preference for the wall-jet type of detector. However excellent the system of FIA may be, malfunctions may sometimes occur. Poor reproducibility of the signal may occur from carry-over between injections, this can be eliminated by increasing the flow rate. Sluggish response may be due to

Figure 9. (Ruzicka and Hansen, 1981)

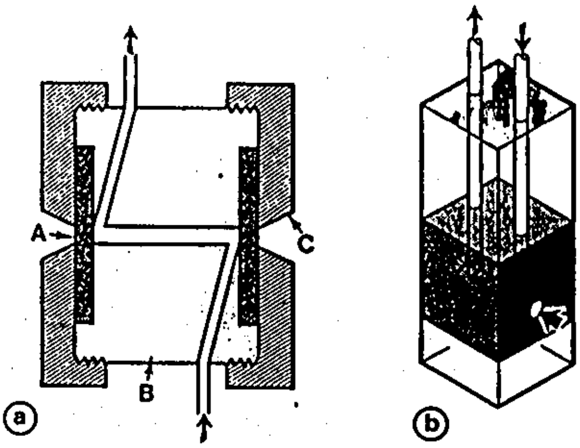

Spectrophotometric flow-through cells (*a*) Z, cell of the type used in HPLC: A, transparent windows; B, Teflon body; C, cell house. (*b*) Hellma cuvette which fits into most commercial photometers. The cells generally have an optical path length of 10 mm, but are available with different inner diameters (i.e., different volumes).

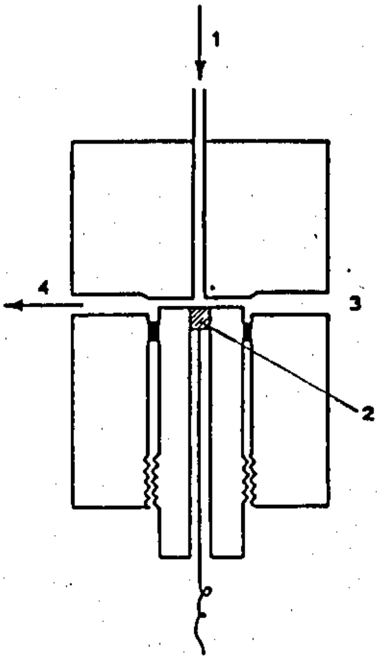

Figure 10. Wall Jet Electrode (Stulick and Pacakova 1981b).

1. Inlet
2. Working electrode
3. Position of Reference Electrode
4. Outlet and position of auxiliary electrode.

the dead volume of the detector being too large, a leak or blockage in the system or contamination of the detector. In the case of electrochemical detectors contamination of the electrode surface can manifest itself as baseline drift. Noisy signals can be the result of an electrically noisy pump or pulsation in the flow stream. The signal peak may become indistinct or doubled, this is due to insufficient mixing of the injected sample and the carrier stream; in this case reaction is only occurring at the interfaces of the sample bolus with the stream. Negative signals may be observed. This is due to dilution of the carrier stream by the sample injection, resulting in a decrease in the background signal.

Many analytical methods have been adapted to flow injection systems in recent years and several techniques have been developed: titrations, stopped flow analysis, merging zones, solvent extraction and gas diffusion.

5. Automatic Determination of Dissolved Phosphate and Silicate.

The automatic methods for determining phosphate and silicate nearly all use the formation of the heteropoly acid (yellow) or the reduction to a "heteropoly blue" compound for a flow colorimetric method. This generalisation applies equally to automatic air segmented and flow injection methods. A simple FIA system for phosphate can be seen in Figure 11, (Ruzicka and Hansen, 1981) using acidified molybdate and ascorbic acid to produce a heteropoly blue detected at 660 nm. Figure 12 shows a simple autoanalyser system for silicate (Grasshoff; 1970) using acidic molybdate as reagent stream, oxalic acid to mask interfering phosphate and metol to reduce the heteropoly acid to a blue compound.

However this study along with several others is concerned with total phosphate analysis which requires the hydrolysis and/or the separation of condensed phosphates (see previous section). Using the air segmented

Figure 11. (Ruzicka and Hansen, 1981)

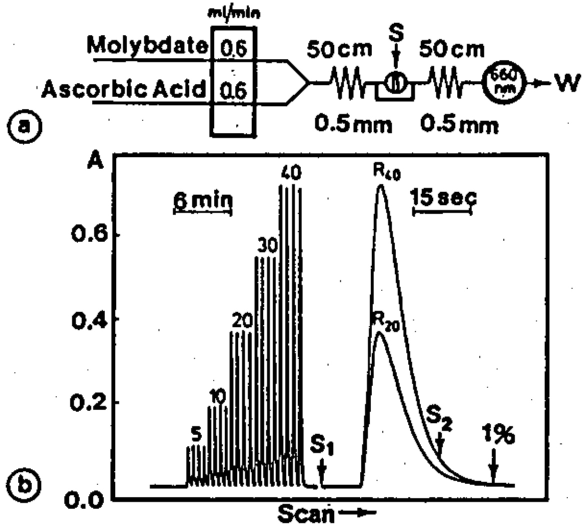

(a) FIA manifold for spectrophotometric determination of phosphate. The two reagents are premixed in the first coil, whereupon sample is injected (30 μl). All tubes are 0.5 mm ID. *(b)* Left: record obtained by injecting standards in quadruplicate, containing 5 to 40 ppm P-PO_4; the record to the right shows a scan where the time scale is expanded to show the peak shape when injecting 20 and 40 ppm solutions. Note that it takes only 15 s between sample injection S and peak maximum readout R, and another 15 s until the next sample (S_2) can be injected. Hence the signal will be below the 1% level before the next readout will be taken, and therefore there is no carryover even at a rate of 120 s/h.

Figure 12. Manifold for the continuous flow analysis of silicate (Grasshoff, 1971).

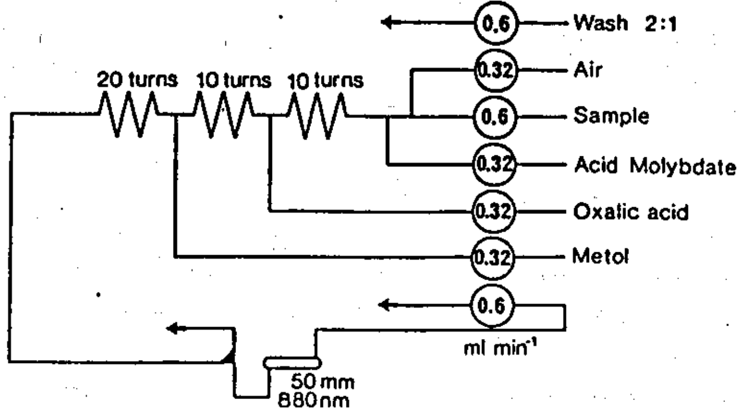

Technicon autoanalyser system most of all P - O - P bonds of the condensed phosphates are hydrolysed in an acidic medium (Nakamura et al 1980). However, Hirai et al (1979) claims 95% hydrolysis with his FIA system. One problem with the hydrolysis of condensed phosphates is whether different molecules are hydrolysed to the same degree and at a similar rate. It is known that the peak areas of the detector response are accurately proportional to the phosphorus contents of the samples. However it is also found that peak height will also give good calibrations. Peak heights are easier to analyse. Nakamura et al (1980) further claim that 80% of all condensed phosphates are hydrolysed to orthophosphate at 97°C; higher temperatures are required for the hydrolysis of all phosphates. Also it has been found that the signals at the detector may be amplified by the presence of sodium chloride in the stream flow, though no explanation is offered. Several workers have separated the condensed phosphates from a mixture using HPLC before hydrolysis. Hirai et al (1979, 1980) and Yamaguchi et al (1979) have eluted columns of ion exchange resin into an air segmented system. Surfactant is often added to the system to facilitate smoother flow through the system. In similar fashion FIA systems have been connected to HPLC apparatus (Hirai et al, 1981). All the above systems used acidified ammonium molybdate as reagent stream, but Basson et al (1981) used molybdovanadate to similar effect and Yoza et al (1980b) used indirectly complexes of cerium and magnesium with methylthymol blue and xylenol orange. As opposed to colorimetric detection Yoza et al (1975) eluted a column equilibrated in magnesium chloride solution through an atomic absorption spectrometer and the separate phosphates were analysed indirectly by the reduction in magnesium signal.

Hydrolysis is always carried out by the sample flowing through a long coil at high temperature under acid conditions or in the presence of the molybdate reagent (Downes 1978, Pavenello et al, 1977). However strong conditions are sometimes required, so Goulden and Brookshank (1975) and Osburn et al (1974) employed an ultra violet digester.

Similar methods have appeared for silicate determination (Wilson, 1965, Brewer and Riley, 1966; Truesdale and Smith, 1976), mostly for an air-segmented system, and only recently has any FIA work on silicate, been published. Hirai et al (1981) have described a FIA method with a heated reaction coil and colorimetric detection at 400 nm whilst Hori et al (1981) used colorimetric detection with a column electrode packed with glassy carbon fibre. The problem of phosphate interference is usually averted by manipulation of pH and the introduction of oxalic acid into the stream preventing formation of the phospho-complex with any excess molybdate reagent. Optimum conditions for promotion of the heteropoly acid β-silicomolydic acid are at pH 2.0.

6. Voltammetry.

The theory and analytical applications of voltammetry are discussed in detail in two recent texts by Bard and Faulkner (1980) and Bond (1980).

The electrochemical properties of solutions are the basis of a major series of analytical methods; voltammetry is one of these. Voltammetry (and polarography) are methods of studying the composition of dilute electrolytes by plotting current-voltage curves (see fig. 13). Usually the voltage applied to a small working electrode relative to a reference electrode is increased or decreased within the range - 2.0 - + 2.0 V; the resulting current charges are observed. Voltammetry is the general name for this technique; polarography is the term applied to voltammetric application of the dropping mercury electrode. Early voltammetry began with solid electrodes, the dropping mercury electrode did not come into use until 1923. The origins date back to 1893 with the novel work of Le Blanc on the electrolysis of metals and the decomposition voltages of acids and bases (see Adams, 1969). Soloman in 1897 was the first to use current-voltage curves and indicated the existence of limiting currents. There has been a growth of interest in solid electrode voltammetry since 1950; this is allied to the development of modern analytical techniques which employ such electrodes. Electrochemistry at solid electrodes has been discussed in detail by Adams (1969).

6a. Basic Principles.

Voltammetric methods are used to investigate phenomena associated with a passage of Faradaic current as a function of the voltage applied to a working electrode (e.g. Glassy Carbon, or Hanging Mercury Drop). Simple cells usually consist of two electrodes, but the passage of current requires modification to one of the electrodes (reference) or the introduction of a third electrode. The electrode

Figure 13. Typical DC Voltammagram

1×10^{-3}M $CdCl_3$ in 1M KNO_3

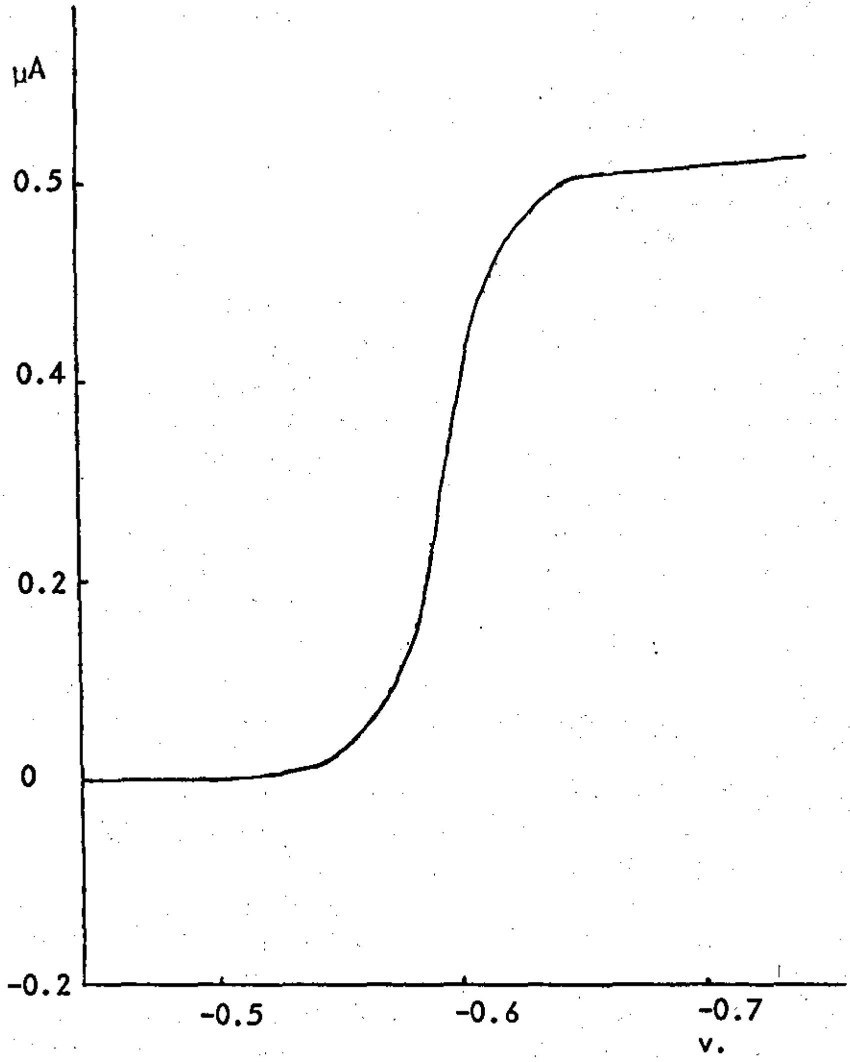

Figure 14. Ewing (1975).

Two- and three-electrode systems for voltammetry. Wkg, working electrode; Ref, reference electrode; Aux, auxiliary electrode.

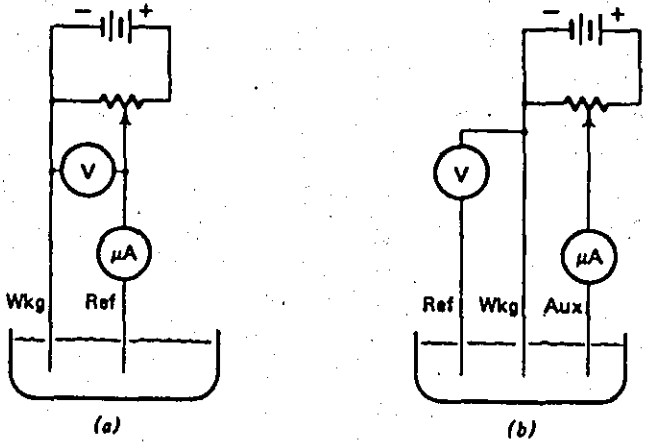

acting as both current carrier and reference must be of low resistance to minimise errors; a 10mV error can result from 10 μA passing through 1000Ω. Also the solution/electrode interface will have to have a much larger surface area than the working electrode so current density and polarization effects are maintained at a low level. The use of a third electrode is preferred; it can be a simple wire of platinum or silver, or mercury for example. The reference electrode since it does not carry current can be of any convenient form (e.g. the standard calomel electrode). The two and three electrode systems are depicted in fig. 14. The working electrode is made of inert material capable of passing an electrical current; the choice of which is governed largely by the likely range of potential it will be required to investigate. Figure 15 shows the range of limiting potentials for various working electrodes and the convention for plotting voltammetric curves. Carbon electrodes are more suited to positive potentials, whilst mercury electrodes are to negative potentials. Mercury is restricted to 0.25v on the positive side, due to anodic dissolution. Use of platinum is fairly restricted, the oxidation of water occurring at + 0.65v and hydrogen is liberated at - 0.45v, due to the high over-voltage for hydrogen evolution at mercury, it is not liberated until - 1.8v in acid conditions or - 2.3v in basic conditions.

Consider a static system, for example, a plane inert working electrode in a deaerated unstirred solution containing 0.1M K Cl and 1×10^{-3}M Pb^{++} with a saturated calomel reference electrode (SCE) and a platinum auxiliary electrode. The solution is deaerated because of interference from dissolved oxygen which exhibits two reduction reactions at - 0.05v and - 0.9v; however when working at positive

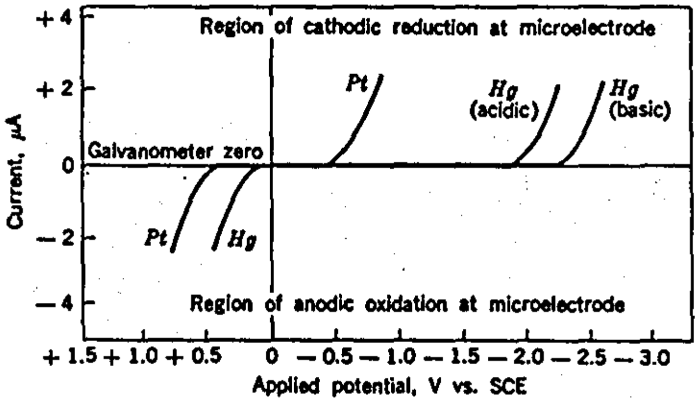

Conventions for plotting voltammetric curves. The curves labeled Pt or Hg indicate the approximate potential limits attainable at these electrodes.

Figure 15. The potential ranges for platinum and mercury working electrodes (Ewing, 1975).

Figure 16. The potential range for glassy carbon in various electrolytes (Zittel and Miller, 1965).

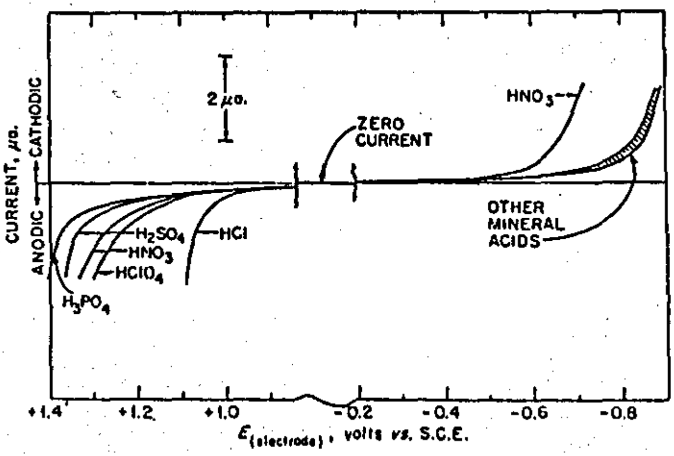

Usable potential range for G.C.E. in various mineral acids

Test conditions: acid concentration, 0.1 N
Voltage scan rate, 0.1 volt-min.$^{-1}$

potentials deaeration is not essential. If we apply 1.0v across the electrodes (with the working electrode negative) several things will happen. K^+ and Pb^{++} ions will start to move in the electric field towards the working electrode, any negative ions (e.g. Cl^-) will move in the opposite direction to the auxiliary electrode. At this potential Pb^{++} ions are reduced but K^+ ions are not. The K^+ ions form a sheath of about one ion thick on the electrode surface almost completely neutralising the field with respect to the bulk of the solution. The Pb^{++} ions will be discharged and deposited on the electrode, this can only happen by diffusion of the Pb^{++} ions to the vicinity of the electrode as the field has been neutralised by the K^+ ions. Correspondingly the movement of anions in the opposite direction slows to a low level equal to the diffusion of Pb^{++} ions. The rate of movement of species by diffusion is proportional to the concentration gradient, in calculus,

$$\frac{dC}{dt} = D\frac{d^2C}{dx^2}, \qquad (1)$$

this is Ficks Law.

C: Concentration of diffusing species.

D: Diffusion coefficient.

(t refers to time and x to distance).

Applying Fick's Law to the process of electrolysis gives the relation,

$$i = nFA\left(\frac{D}{\pi t}\right)^{\frac{1}{2}}.C \qquad (2)$$

i: electrolysis diffusion current at time t

n: number of electrons involved in the reaction at the electrode.

F: Faraday Constant (9.65×10^4 coulombs per mol)

C: Bulk concentration of the electroactive species in solution. The concentration is assumed to be zero at the electrode surface. The convention is to label i and n as positive for cathodic reactions and negative for anodic reactions (see fig. 16). The current is proportional to concentration, so that the current observed for a particular electrochemical reaction in voltammetry can generally be said to be diffusion limited. Potassium chloride is present as "supporting electrolyte", whose function is to prevent occurrence of a "migration current". If the electroactive species is charged, its mass transfer will be modified due to the passing of a current through the solution. Migration current can be positive, negative or zero depending on the charge of the electroactive species, and can affect the current observed due to the oxidation or reduction reactions occurring at the electrode. These reactions are called "faradaic processes" because they obey Faraday's Law. The magnitude of this current is governed by the mass transfer process and is limited mainly by diffusion and to a lesser extent by other processes, for example, electron transfer, chemical kinetics, and adsorption.

In the absence of an electroactive species (i.e. the working electrode is at a potential where the species in solution are not reduced or oxidised), charge cannot cross the electrode-solution interface and so the electrode behaves like a capacitor. When a potential is applied across a capacitor a current will flow until its charge (q, coulombs) satisfies the equation $C = q/_E$, where C is the capacitance (farads) and E is potential (volts). The electrode-solution interface (electrical double layer) behaves like a capacitor.

The electrical double layer is a whole array of charged species and oriented dipoles existing at the electrode-solution interface. Its structure only loosely resembles two charged layers. At given potentials the electrode-solution interface is characterized by a double layer capacitance. This is typically in the range 10-40 μF/cm^2; however unlike real capacitors this capacitance is often a function of potential. The solution side of the double layer is thought to be made up of several layers, the innermost being solvent molecules and specifically adsorbed species. This inner layer is often called the Helmholtz or Stern layer (see fig. 17 below).

Figure 17. The Electrical Double Layer
(Bard and Faulkner, 1980).

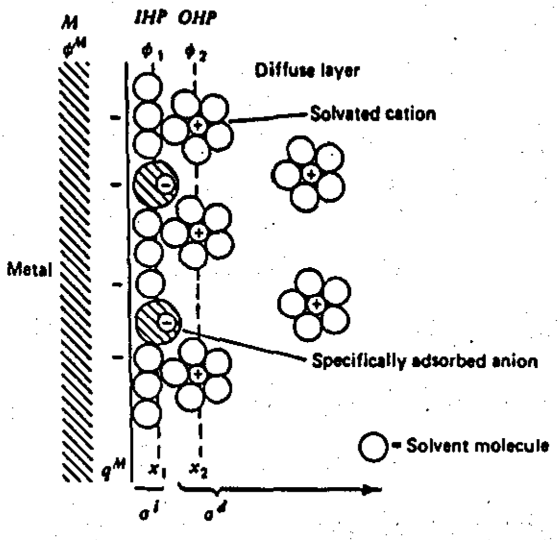

Proposed model of the electrode-solution, double-layer region.

The voltammogram of figure 16 represents the background current due to a solution of 0.01M sulphuric acid at a glassy carbon electrode. It is seen that infinite current flows between the potentials of 0 v. and 1.2 v. This slowly increasing current is termed the "residual current". It is present in all current-voltage curves to varying degrees and is composed of (1), the Faradaic current from electrochemical reactions, (2), the charging current as mentioned above, (3), currents from reactions of the electrode surface and (4), trace currents from impurities in the solution. No electrolyte is completely free of trace impurities which can be oxidised or reduced at the electrode. According to electrochemical rate theory (see for example Bond 1980) finite current will flow at potentials considerably removed from the point at which the sharp rise in current occurs. This Faradaic current is only a small portion of the residual current at a solid electrode. Mainly, residual currents are associated with extraneous processes primarily at the electrode surface. This may be connected with the past history of the electrode, for example, a layer of sorbed gas on the surface. Also the act of forming a sorbed gas layer may give rise to a residual current. Such effects at the electrode surface make up the bulk of residual currents at solid electrodes which may limit its use by masking the primary process under study.

6b. Modes of Voltammetry.

Figure 13 illustrates the standard practice of plotting a voltammogram (or current-voltage curve). It is conventional practice to run voltammograms by varying the applied potential and measuring the resulting current, which is normally expressed in microamperes (μA). Apart from the dropping mercury electrode (DME) and the hanging mercury drop electrode (HMDE) a variety of modes have been employed using solid electrodes.

(1) Stationary Electrodes, in (a) quiet solutions, (b) stirred solutions and (c) flowing electrolytes.

(2) Rotated Electrodes at a variety of rotation speeds.

(3) Vibrating systems.

(4) Ring disc electrodes in static, rotating and flowing systems.

6b.1 Linear Sweep and Cyclic Voltammetry.

Initially linear sweep voltammetry (LSV) was the rapid scanning of potential within the last half second of the lifetime of a mercury drop. Using solid electrodes the speed of the sweep can be reduced and varied to best effect as regards the experimental requirements. Rapid scan techniques give rise to a characteristic voltage-current curve shape (see fig. 18). The peak shape is so because the diffusion process is too slow to supply electroactive material to the electrode fast enough to keep up with the rapidly increasing potential; thus a steady state is never attained. The peak potential (E_p) is related to the half wave potential ($E_{½}$):

$$E_p = E_{½} - 1.1.\frac{RT}{nF} \qquad (4)$$

The current at the peak is given by an equation derived by Randles and Sevcik,

$$i_p = Kn^{3/2}\, A\, D_o^{½} C_o\, V^{½} \qquad (5)$$

where i_p = Current (μA)

A = Area of electrode (cm²)

V = Rate of potential change (V sec⁻¹)

k = Randles-Sevcik constant

C = Concentration of electroactive species in the bulk of the solution (mol/cm⁻¹)

D = Diffusion coefficient (cm² sec⁻¹)

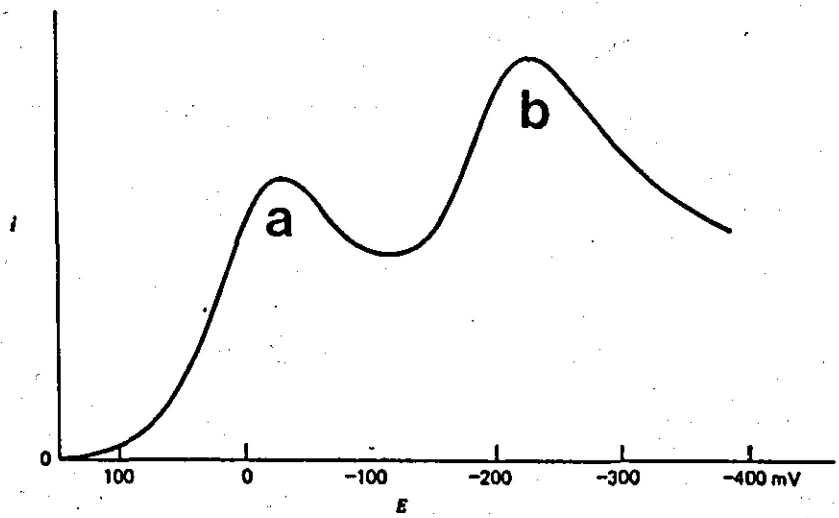

Figure 18. A linear sweep voltammogram of a mixture of electroactive species a and b.

Figure 19. A typical reversible cyclic voltammogram.

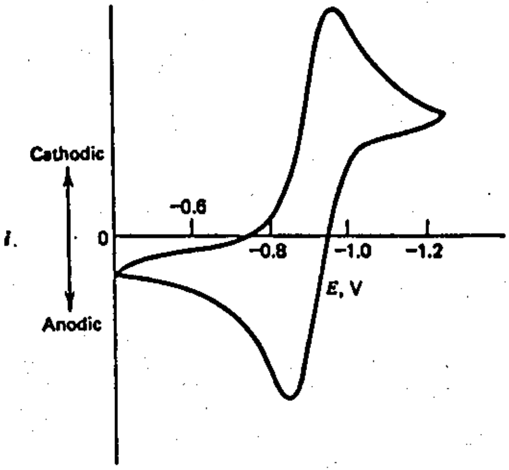

Cyclic voltammogram at a stationary Pt electrode of oxygen in pyridine

(Bard and Faulkner, 1980).

The value, i_p is directly proportional to the concentration, C.

Cyclic voltammetry is an extension of LSV. The direction of the potential scan is reversed following the reaction of interest occurring at the electrode. A triangular potential wave is applied as opposed to the single sweep which is just a simple ramp function. A typical curve is shown for a reversible system (fig. 19). If the electrochemical reaction is reversible then an anodic current will be observed equally opposite to the cathodic current seen when sweeping the potential in the opposite direction. The difference in potentials at which the current increases are observed is related to the number of electrons involved. For example a 2 electron reaction will show a difference of 0.28 v at 25°C; this can be predicted from equation (4).

A related method to those above is anodic stripping voltammetry (ASV). This is the combination of a concentration process where an electroactive species (quite often a trace metal) is reduced at a constant potential which is more negative than the half-wave potential of the species to be investigated. This results in the plating of this species on the solid electrode or an amalgamation if a HMDE is used. The concentration step is carried out for a precise time to ensure reproducibility followed by a potential sweep in order to oxidise the plated material; the resulting current is proportional to the concentration of the electroactive species in the original solution.

6b.2 Pulse Techniques.

Pulse methods of analysis have been the subject of two recent reviews by Osteryoung and Osteryoung (1981) and Borman (1982). In pulse voltammetry, millisecond pulses of successively increasing potential amplitude are applied to the working electrode, this is referred to as "normal pulse voltammetry" (NPV). The initial potential is such that no reaction takes place. The current is measured usually at the end of a pulse application. In DPV the potential is changed slightly between each pulse and the pulse itself is of constant amplitude. The current is measured just before and at a fixed time after the pulse, the difference in the current is recorded (N.B. the frequency of the pulses is usually in the range 0.5 - 10 secs). The shape of the current-voltage curves for NPV and DPV are compared to a conventional (DC) curve in figure 20.

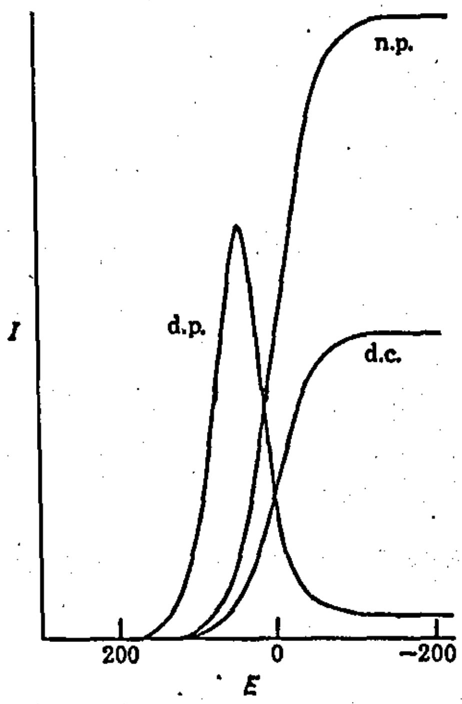

Figure 20. Comparison of c-v curves for various voltammetric modes (Osteryoung and Osteryoung, 1981).

The sensitivity of the NPV mode is about ten times that of the conventional method. The limiting current plateau in NPV and DC methods is directly proportional to the concentration of species in solution that has diffused to and reacted at the working electrode. The maximum current in DPV is likewise proportional to the concentration of material in the solution under test. The shape of the curve obtained from DPV is that of a derivative of the NPV or DC methods. The DPV is the most favoured method with a signal to noise ratio two order of magnitude less than the other modes the detection limit in analytical applications is likewise lower.

G.C.Barker is known as the father of pulse techniques (Barker and Gardner, 1960) because of his work in the fifties, but new techniques continue to emerge; for example reverse phase and square wave pulse voltammetry. In reverse pulse voltammetry, instead of conventionally scanning in the negative direction observing say for example the reduction of Fe(III), the scan is in the opposite direction beginning at a negative potential where Fe(III) is reduced at a diffusion controlled rate. Thus the reverse scan will observe the oxidation of Fe(III) that had been generated whilst the potential was at its initial value. Alternatively we could call this technique anodic stripping pulsed voltammetry. . Square wave voltammetry is another fast method, and has only been applied to a dropping mercury electrode, though it is equally applicable to a solid electrode. After the mercury drop has been allowed to grow for a precise time then a staircase with a square wave is applied (see fig. 21). The current is measured once in the forward pulse and once in the reverse pulse, and then displayed as the forward and reverse current on the difference (fig. 22). It is worth noting that the plots resemble that of a cyclic voltammogram and the difference current resembles the differential pulse method.

Figures 21 and 22. Osteryoung and Osteryoung, 1981.

21.

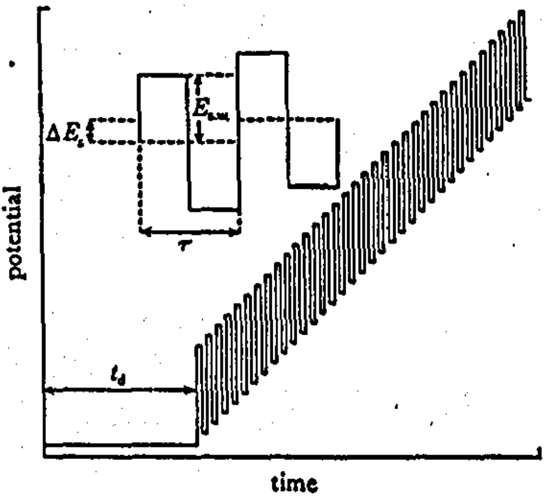

The square wave waveform. $E_{s.w.}$ is the square wave amplitude, ΔE_s the step height, τ the square wave period, and t_d the delay time at the initial potential before the initiation of the scan.

22.

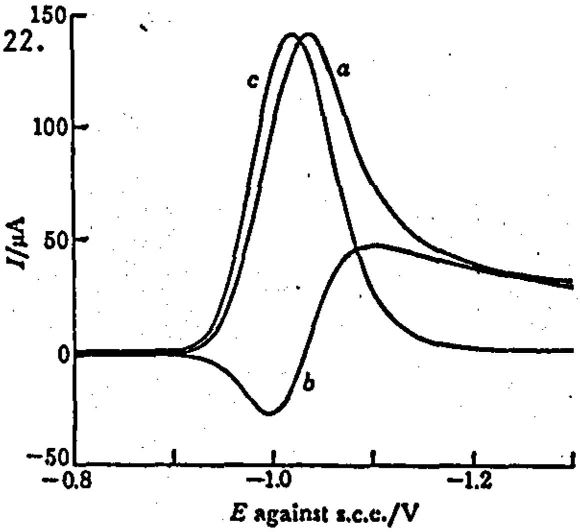

Square-wave voltammogram of 0.52 mM Zn^{II} in 0.1 M KNO$_3$; τ = 2 ms, ΔE = 5 mV, $E_{s.w.}$ = 25 mV. (a) forward current, (b) reverse current, (c) net current.

In conventional DC voltammetry the current wave fluctuates once the limiting current has been reached. Tast (or sampled d.c.) voltammetry eliminates this effect by sampling the current near the end of each pulse. Thus the DC method becomes more accurate though no more sensitive.

6c. Electrode Processes.

Two types of processes occur at electrodes. One kind is where charges (e.g. electrons) are transferred across the electrode-solution interface, which causes oxidation and reduction to occur. As these reactions are governed by Faraday's Law (i.e. the amount of chemical reaction caused by the flow of current is proportional to the amount of electricity passed), they are called faradaic processes. Processes such as adsorption and desorption can occur, and the structure of the electrode solution interface may be altered by changing potential or solution conditions. These are termed non-faradaic processes, and although charge does not cross the interface under these conditions, a current flows. An electrode process is said to be electrochemically reversible if the current measured for the reduction of a species (e.g. Fe(III) → Fe(II) is exactly equal and opposite for the reverse reaction (i.e. oxidation of Fe(II) to Fe(III) (see fig. 23). The chemical path connecting the two states (Fe(III) and Fe(II)) is thermodynamically reversible and the rate of electron transfer for both oxidation and reduction is fast enough so that at all points along the path the system is in equilibrium. For a reversible reaction the current-voltage curve can be defined in terms of the Nernst equation,

$$E = E^{o} + \frac{RT}{nF} \ln \frac{OX}{RED} \qquad (6)$$

Figure 23. A cyclic voltammogram for a system such as Fe(II)/Fe(III).

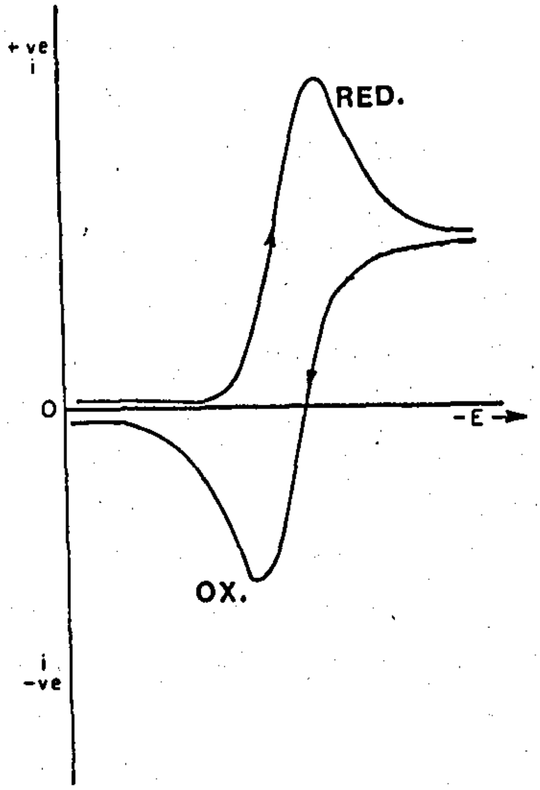

Figure 24.

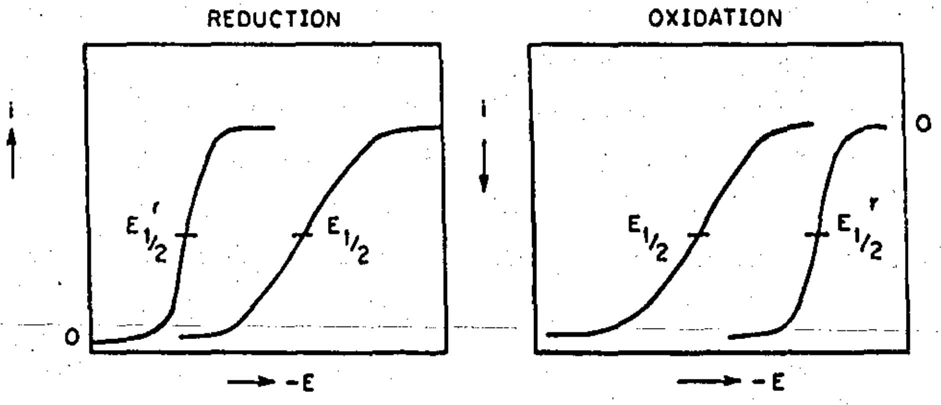

Differences between reversible ($E^r_{1/2}$) and irreversible ($E_{1/2}$) dc polarographic waves.

Bond (1980)

and diffusion equations relating current to concentration (discussed earlier). An electrode process may be irreversible due to either a slow electron transfer step, a slow chemical step, or adsorption, i.e. a deviation from the conditions of the reversible reaction. In the irreversible situation the pathway between oxidised and reduced states is not an equilibrium one. The irreversible reaction can be observed in the normal voltammetric mode to have a much slower rate of increase of current at the half wave potential ($E_{\frac{1}{2}}$) (see fig. 24), which is also displaced. The pathway is now defined by kinetic factors; the rate constants of the oxidation and reduction reactions.

So far we have only discussed heterogeneous reactions at the electrode surface (electrochemical reversibility). A homogeneous chemical reaction might occur before or after the charge transfer steps, for example, if the product of the electron transfer reacts with the solvent or when an electroactive species is formed from a non-active one. If the homogeneous reaction "chemically reversible" is coupled with a reversible charge transfer then the overall process is reversible and obeys the Nernst Equation (6). If the chemical reaction is irreversible then $E_{\frac{1}{2}}$ values will be perturbed by a factor pertaining to the homogeneous rate constant. The perturbation will be positive or negative depending on whether the chemical reaction precedes or follows the charge transfer.

Testa and Reinmuth (1961) classified chemical steps "C" and electron transfer steps "E". Thus we get the convenient notation of EC for a chemical reaction following an electrochemical one. Thus for a preceding reaction e.g.,

$$X \rightleftarrows A \qquad\qquad A + ne \rightleftarrows B$$

$$\underline{C}. \qquad\qquad\qquad \underline{E}.$$

A is reduced only at the electrode surface and so disturbs the equilibrium of the C reaction and so more A is produced and consequently converted to B at the electrode. So the current flowing will be a function of the rate of the chemical (homogeneous) reaction. For the EC reaction the current is a function of the electrode process and the rate a function of production of P in solution.

$$A + ne \rightleftarrows B \qquad\qquad B \rightleftarrows P$$

$$\underline{E}. \qquad\qquad\qquad \underline{C}.$$

6c.1 Regenerative Mechanisms.

In this type of process the original material is regenerated by a chemical reaction which occurs subsequently to the charge transfer step (E). In this case we can get electroactive material being reduced (or oxidised more than once) producing starting material at the electrode surface by chemical and diffusion processes. The limiting current flowing through the cell will be larger than the diffusion controlled value, the increase being a function of the rate constant of the chemical process (C). For example,

$$\begin{array}{lr} U(VI) + e \rightleftarrows U(V) & E. \\ 2U(V) \rightarrow U(VI) + U(IV) & C. \end{array}$$

In some media "C" is so slow that only "E" occurs and in others so fast that it goes to completion and the electrode process becomes equivalent to :

$$U(VI) + 2e \rightleftarrows U(IV).$$

Catalytical processes can occur, where the product of the electrode reaction (B) reacts with an inactive species (Z) to regenerate the active species "A".

$$\begin{tikzcd}
& A + ne \arrow[r, shift left] & B \arrow[l, shift left] & & \text{E.} \\
B + Z \arrow[r] & A \arrow[u] & & & \text{C.}
\end{tikzcd}$$

Thermodynamically if B can be oxidised by Z to A, then Z ought to be reduced at the electrode. However if this process for Z is very slow, electrochemical reduction can be far more negative than predicted by thermodynamics. Hence a catalytic process will enhance limiting currents to an extent governed by the speed of the catalytic reaction.

Adsorption Phenomena.

Non-linear calibration curves, inhibition of electrode processes, perturbation of waves and other undesirable effects which are the bane of the electroanalytical chemist, can all arise from adsorption processes at the surface of the working electrode. At the dropping mercury electrode such effects can largely be ignored, as the surface of the electrode is renewed every second or so.

There are two types of adsorption: nonspecific, where long range electrostatic forces disturb the distribution of ions near the electrode surface and specific, where a strong interaction between the adsorbate and the electrode material causes the formation of a layer on the electrode surface. Nonspecific adsorption affects the electrochemical response because it affects the concentration of the species as well as the potential distribution near the electrode. Specific adsorption can have several effects. If an electroactive species is adsorbed, the theory must be modified to cater for the fact that an electroactive species at the surface is at a relatively higher concentration than in the bulk of the solution. Also the adsorbed species may be more difficult to reduce than the same species in solution. If an inactive species is adsorbed then the electrochemical response will be altered, due to a blocking layer forming at the electrode surface. In addition a process of electrocatalysis may occur with the adsorption of an unreactive material which then dissociates into reactive fragments.

The relationship between the amount of substance adsorbed on the electrode per unit area (Γ_i), the activity in bulk solution (a) and the electrical state of the system at a given temperature is called an adsorption isotherm. A general form is given below,

$$a^A = a^B . e^{-\Delta G^o/RT} = \beta . a^B \qquad (7)$$

superscripts A and B refer to adsorbed and bulk situations respectively, ΔG^o is the standard free energy of adsorption. The Langmuir Isotherm assumes no interactions between adsorbed species, a homogeneous surface and at high bulk activities saturation coverage of the electrode by adsorbate (a monolayer) (Γ_s).

(8) $\dfrac{\Gamma_i}{\Gamma_s - \Gamma_i} = \beta a^B$, this isotherm can also be written in terms of fractional coverage of the electrode surface Θ, where $\Theta = \Gamma_i/\Gamma_s$ to give:

$$\frac{\Theta}{1 - \Theta} = \beta a^B \qquad (9)$$

If the rate of adsorption is fast, then equilibrium is set up at the electrode surface. This equilibrium may not be set up in cases such as the DME or LSV whose operation is of a rapid nature.

If a species is irreversibly adsorbed then cyclic voltammetry will show increase in current amplitude with repeated scan. If strong adsorption occurs a voltammogram may show an additional peak when the adsorbed material is reactive at a different potential. Also a peak may occur after the peak of an electroactive species, when a product of the electrode reaction is strongly adsorbed and is also reactive.

Adsorption of an electroinactive species can lead to poisoning of an electrode and form an impervious layer at the surface rendering the electrode inactive. However it is possible that reaction may occur at the "filmed" surface, the electrons being transferred though albeit at a slower rate. The "film" may have sites which are capable of catalyzing reactions, thus increasing the effectiveness of the electrode.

d. Instrumentation.

Classical DC methods were operated initially with two electrode systems (see fig. 14) where the cell is connected to a potentiometer from which a voltage is applied across the working and reference electrodes. The current passing is then observed on a galvometer.

Modern equipment is more sophisticated and has developed along with the improvement of voltammetric methods. The initial improvement was the three electrode system, this avoids problems of solution resistance (i.e. reducing solution IR drop) and provides greater flexibility in the location of the reference and working electrodes (see fig. 14). Potential control is between the working electrode and the reference, but the circuitry is arranged so that the cell current passes between the working and auxiliary electrodes.

Potentiostatic control is maintained using the type of circuitry (see fig. 25), using a high gain, high impact operational amplifier. The potential at the negative or inverting input is maintained at a level equal to the other input when the amplifier is connected in a feedback

25.

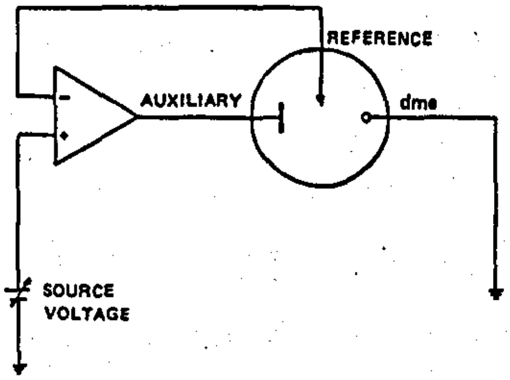

Three-electrode potentiostatic control system for polarography.

26.

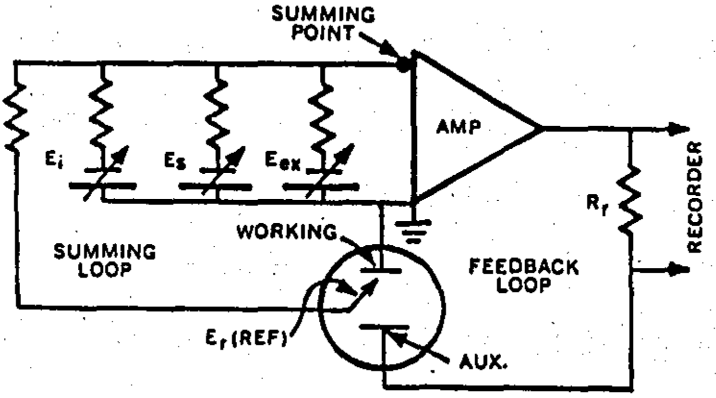

Potentiostatic system including input voltage and current readout.

Figures 25 and 26 (Bond, 1980).

configuration. No current will flow into the amplifier from the negative input, the amplifier behaving as if it had infinite input impedance. It is required that the output of the amplifier can be inverted so its polarity will be opposite to that of the negative input. Only a small difference of potential need be applied between the two inputs is required to obtain a measurable output due to the high gain of the amplifier.

When current passes through the solution, the solution becomes more positive relative to the ground. The reference electrode likewise becomes more positive, but the potential at the reference electrode is applied to the inverting or negative input of the amplifier which also becomes more positive, then the output will become negative. So we have a self-stabilising feedback system which automatically makes the potential of the reference electrode the same as that applied to the positive input of the amplifier from the source voltage. The potential across reference electrode and the ground is equivalent at all times to that applied by the source voltage to the positive input of the amplifier. As the working electrode is connected directly to the ground, the voltage across the cell is equal to the source voltage.

For operation the three electrode system requires an input voltage, a potentiostat, a control system and a current read out. Figure 26 shows the location of the cell in a potentiostatic system. All current flowing to the amplifier must flow through the feedback resistor to the output and then to ground. So the current is measured by this circuit but the working electrode is maintained at the ground potential at all times.

With the two electrode system the reference electrode requires low resistance and a reference potential not affected by the passage of current. Now any electrode with an impedance that gives reproducible potential at zero current conditions can be used. The widely used saturated calomel electrode may not be compatible with the chemistry of the test solution, so the SCE is kept remote of the test solution by employing salt bridge connectors (e.s. Sat. KCl/Agar). As KCl is not always soluble in nonaqueous solvents its use is not universal and the SCE will have to be replaced. The auxiliary electrode does not need to have a reproducible potential and can be made of any metal or inert material (e.g. Platinum, Graphite). There is the possibility of products from the auxiliary electrode diffusing to the working electrode. However the time scale of the experiment is usually too short for any interference to occur, so the electrode is usually placed in direct contact with the test solution.

7. Electrodes.

This review is confined to solid electrodes and in particular carbon based probes which are used in this project. Apart from carbon solid electrodes are usually constructed of a hard inert metal such as gold or platinum. The electrode can be stationary in a quiescent solution or one with forced convection or rotating in a quiet solution. Recently solid electrodes have been used as detectors for flow injection systems and HPLC effluent. The surface of the electrode is generally planar, but can be a variety of shapes, e.g. cylindrical or conical, depending upon the application.

Classical voltammetry (or polarography) was carried out at a DME or HMDE. The major difference to solid electrodes is that the mercury drop presents a constantly renewable surface. The surface conditions of the DME are highly reproducible, whereas the surface of a solid electrode may be altered by the electrochemical reactions occurring. Cleaning the surface of a solid electrode is very likely to alter the surface texture, the area and also the current as it is proportional to the surface area of the electrode. In some cases an insoluble film may be deposited on the electrode surface making results erratic and giving rise to peak current shifts. Generally the waves recorded at a DME are comparable to those at a stationery electrode within the potential limits of both electrode systems.

A range of materials for solid electrodes were investigated by Alder et al (1971) and Lund et al (1979). They found that glassy carbon, pyrolytic graphite and platinum perfomed the best out of all the materials tested. Carbon and platinum gave well defined oxidation peaks and showed little influence from surface effects. Boron carbide was tested and found to show a large anodic range comparable to carbon and platinum but the current generated was not reproducible. Dieker et al (1978) studied the residual currents of several solid electrodes in normal and differential pulse modes. The currents were recorded from a solution of 0.05M potassium chloride scanning from zero potential in both negative and positive directions. The electrodes tested were, glassy carbon (GCE), mercury (HMDE), carbon paste (CPE), platinum foil (PFE), gold foil (GFE), a paraffin impregnated graphite rod (IGE), and glassy carbon with a mercury film (GCHg). The largest residual current was exhibited by the gold electrode and the lowest by the carbon paste. The order of decreasing current was as follows : GFE, PFE, GCHg, IGE, GCE, and CPE. It is possible to obtain glassy carbon from different manufacturers of quite different qualities and so quite different residual currents.

7a. Carbon electrodes.

Carbon electrodes are very popular in electroanalytical techniques; they are robust, versatile, cheap and have a wide potential range. The best solid electrodes are those with low porosity. Untreated graphite electrodes are very porous, and give unreproducible results. Carbon electrodes are most often used in voltammetric studies, but have been used for potentiometric titrations, as a redox electrode and for acid-base titrations. Majer et al (1973) studied the potentiometric response of several different graphite, pyrolytic and glassy carbon electrodes and found that glassy carbon electrodes most closely resemble an ideal redox electrode.

Evseeva et al (1973) have also studied different carbon electrodes; glassy carbon, untreated graphite and graphite impregnated with paraffin or an epoxy compound. The impregnation of graphite will reduce the porosity factor by a factor of 4 with an epoxy compound and by 3 with paraffin. Evseeva et al show that residual current is lowest for less porous materials. The treating of graphite also extends the working region of such an electrode giving it a performance comparable to glassy carbon. Graphite electrodes' ability to adsorb certain classes of compound have made it possible to study the electrochemistry of reactants irreversibly adsorbed on the electrode surface. The graphite electrode is exposed to solutions containing the reactant for several minutes, followed by differential pulse or slow linear sweep voltammetry. This is achieved in the absence of any diffusing reactant in a solution of electrolyte. The more sensitive nature of DPV suggests use of this technique for quantitative purposes.

Glassy carbon is impermeable to gas, resistant to chemical attack and electrically conductive. Many of its properties are common with pyrolytic graphite but is isotropic rather than anisotropic. The material, glassy carbon is formed by means of a carefully controlled heating programme of a polymeric resin (e.g. phenol-formaldehyde) in an inert atmosphere. Carbonization starts at about 300°C and is complete after raising the temperature to 1200°C. This process is accompanied by a shrinkage factor of 50%. The whole process must proceed slowly to ensure that the gaseous products can diffuse to the surface. The structure of glassy carbon is made up of aromatic ribbon molecules oriented randomly and tangled in a complicated fashion (see fig. 27).

Figure 27. Lankelma and Poppe (1976).

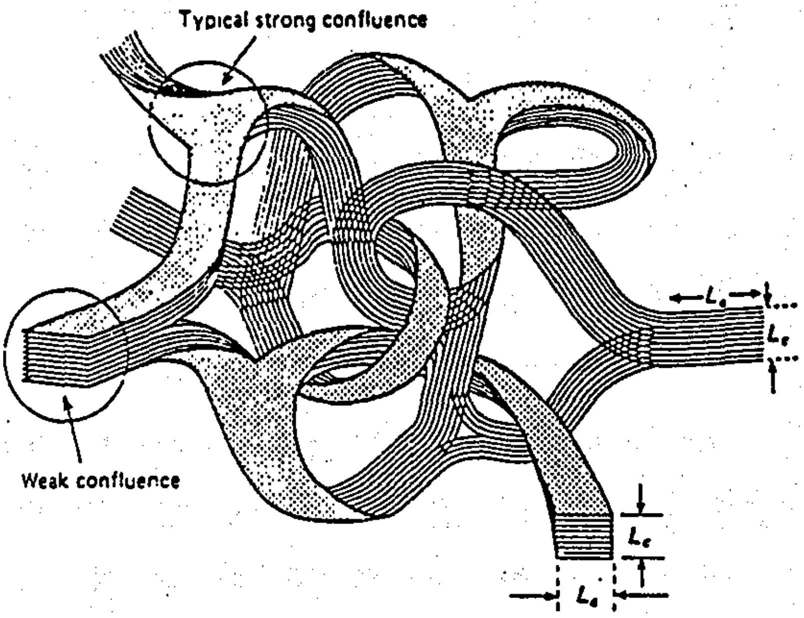

Schematic structural model for glassy carbon.

The electrical contact with glassy carbon is a simple metal pressure system (a spring) and because it is isotropic no specific orientation is required. Most stationary electrodes are susceptible to poisoning during voltammetry. Glassy carbon was found by Zittel and Miller (1965) not to show such properties in solutions of a selection of inorganic ions. However they do mention that it is necessary, when recording a wave with a glassy carbon electrode, to return the applied potential to the original value and to allow sufficient time for any material to be removed from the surface or for the double layer to disperse. Glassy carbon electrodes behave as if they are totally inert except that they are H^+ sensitive due to adsorption of oxygen or oxygen in solution.

Van der Linden and Dieker (1980) have reviewed the use of glassy carbon electrodes in electroanalytical chemistry. The application of glassy carbon to analytical work was first reported by Zittel and Miller (1965) with voltammetric work with various transition metal ions. Other techniques to which glassy carbon electrodes have been applied are : stripping voltammetry, amperometry, coulometry, potentiometry and flow through electrochemical detection (ECD).

Glassy carbon electrode surfaces can be oxidised to carbonyl and carboxyl groups,where substitutions can be affected by electrochemically active species (R) such as a porphyrin . The following reaction scheme presents the modification of an electrode surface (S)

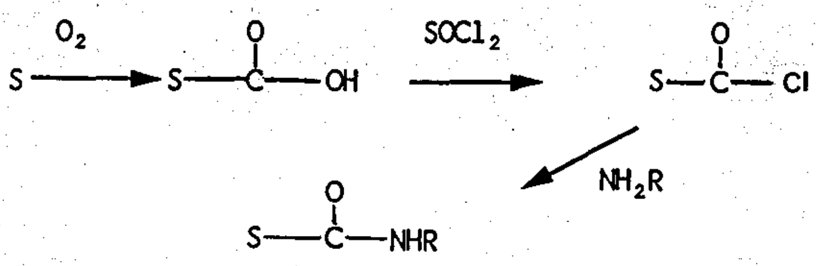

Systems can be synthesized which exert interesting and potentially useful electrocatalytic effects. Van der Linden and Dieker suggest some pretreatment of glassy carbon electrodes before reproducible results can be obtained. Depending on the quality of the material derived from the care of its preparation microscopic pitting can be observed in the surface. It is suggested that the surface is abraded with emery paper of ever increasing fineness followed by polishing with a silica or an alumina suspension. Functional groups attached to the surface may be removed in this fashion. Sometimes a simple wiping of the surface with a suitable solvent will rid the electrode of films and adsorbed species. The grade of glassy carbon is obviously variable as Majer et al (1973) found the surface of the electrode they were using not to show any pores or structure when studied under an electron microscope.

Carbon paste and wax impregnated electrodes have the advantage of the possibility of preparing a new surface, in a simple manner, which is unaffected by the history of the electrode. Another important advantage is the low background current which is smaller than that for glassy carbon and pyrolytic graphite electrodes. The preparation of carbon paste electrodes is simpler than wax impregnated electrodes. A well about 3mm deep is prepared in the end of a Teflon rod and a wire is run through the rod to form an electrical connection with a platinum plate, this forms the bottom of the well. A paste of graphite and nujol is prepared and then pressed into the well. It is tamped down forming a smooth and relatively firm surface. This construction is similar to the glassy carbon electrode.

Adams (1958) first introduced the carbon paste electrode which gained in popularity quickly as an alternative to other carbon electrodes. Linqvist (1974) has reviewed the way different grades of carbon paste can affect its operational parameters. Even with the same grade material it is very difficult to duplicate surface conditions exactly. A problem with paste electrodes is their stability. Murcoux et al (1965) have studied the likelihood of the nujol (or similar material) base being miscible with solvents or reactive towards the species in solution. Olson and Adams (1963) have described some applications of carbon paste electrodes to cathodic reductions and stripping voltammetry. For anodic oxidations carbon paste is very versatile, possessing virtually zero anodic residual current. The potential limits of carbon paste electrodes are - 1.1 v to + 1.1 v in 1M KCl.

Solid electrode voltammetry is more sensitive and faster than polarography at DME. It can be used for trace analysis in the stripping mode and to study the mechanism of electrode reactions. The cyclic potential scan makes it possible to investigate the products and detect intermediates in electrochemical reactions. Robustness and reproducibility are of prime importance when choosing an electrochemical sensor. Solid electrodes fulfill this requirement especially when applied to modern methods, for example, in flow injection analysis detectors.

8. Electrochemical detectors for flowing liquid systems.

The development of flow cells stems from the requirement for a sensitive detector of chromatography column effluents. In particular HPLC required a detector sensitive enough to match the high resolution of the column. Electrochemical detectors are now commonplace with HPLC systems, and have begun to replace colorimetric flow through cells on other automatic analytical set ups. The best detector will have a low dead volume, a low signal to noise ratio, a stable repeatable response and a fast and linear response over a wide range of concentrations.

Electrochemical detectors can be highly specific, for example, ion selective electrodes. The electrode fitted in a flow cell may be susceptible to adsorption, poisoning the electrode surface reducing long term stability and affecting the signal. The DME, as mentioned earlier is not troubled by poisoning being easily renewable, but is much noisier electrically. Electrochemical detectors (ECD) though very sensitive may suffer from poor resolution as similar species quite often are reduced at potentials close to each other.

Recently reviews of ECDs in flowing systems have been published by Hanekamp et al (1982), Rucki (1980) and Brunt (1981). The first electrochemical flow cell was produced by Mueller (1947) using a platinum microelectrode. This was followed by the DME flow cell by Kemula (1952), Mann (1957) and Blaedel and Todd (1958). Robertus et al (1958) applied a DME flow cell to the effluent of a chromatography column. Carbon based and other solid electrodes did not appear until the late sixties, one of the earliest was a carbon paste electrode described by Pungor and Szepesvary (1968).

8a. Design of Electrochemical Detectors.

Flow cells using solid electrodes favour two basic designs. The wall-jet electrode, for example the products of EDT Research and Metrohm and the thin layer coulometric detector of Kipp-Analytica. A recent paper by Burmitz (1980) has listed and compared commercially available electrochemical sensors (see fig. 28 a - d).

A linear relationship between current and concentration is only found where the potential is constant. However this is not always so, an IR drop may cause a decrease in the potential available at the interface of the working electrode and the solution. The IR drop will be caused if an electrical current flows (Lankelma and Poppe, 1976). No

Figure 28. A comparison of some commercially available electrochemical flow cells.

COULOMETRIC DETECTOR FOR HPLC

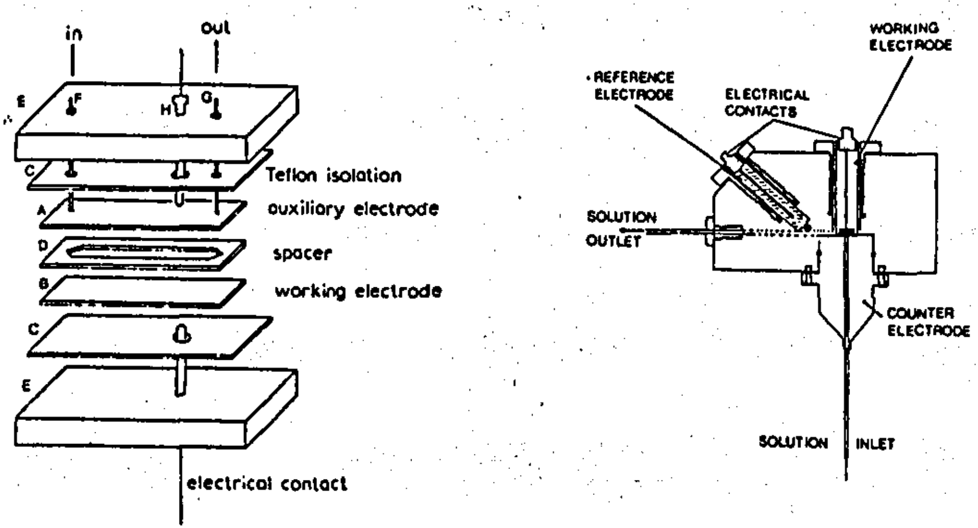

(Lankelma and Poppe, 1976).

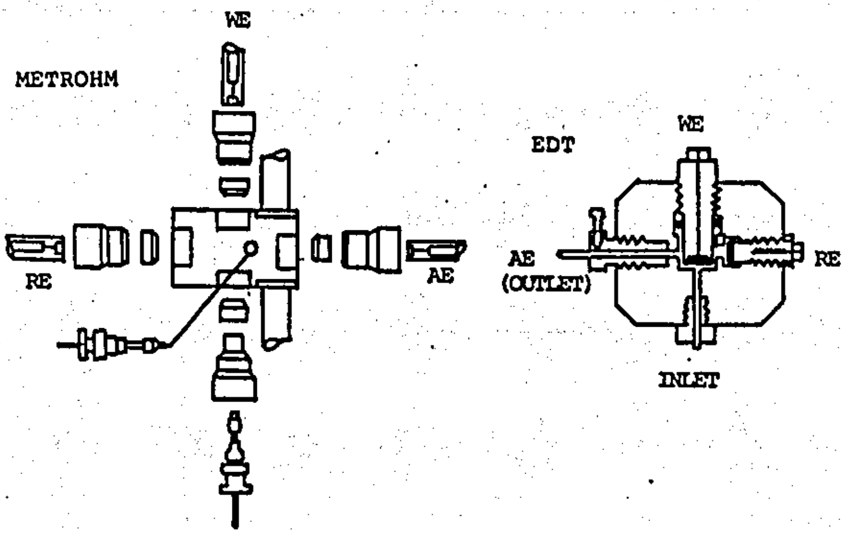

Comparison of electrochemical sensor designs using solid electrodes

(Burmitz, 1980).

problem is encountered when a solution of high conductivity is used; this is generally undesirable. The alternative is to use a cell in which the resistance between the working and reference electrodes is minimised. Using a three electrode system, as most modern cells do, the effect of the ohmic drop is suppressed making the use of low conductivity solutions viable.

Increasing the detector volume results in dilution of the sample bolus causing unwanted band broadening and peak reduction. The volume of the detection in total might be large, but the response volume must be kept small, ensuring a sharp response. The design and construction of ECDs have been discussed by Stulik and Pacakova (1981 a), Lankelma and Poppe (1976) and Fleet and Little (1974).

Apart from the wall jet electrode and the thin layer electrode various flow cells have been constructed with a DME, some of which predate HPLC. It is difficult to preserve the reliable function of the DME and keep a small dead volume. Figure 29 depicts a typical DME flow cell. Employing a very short drop time or an RC filter will reduce the current oscillations caused by the dropping of the mercury. A variety of shapes of electrodes for hydrodynamic systems have been evolved, for example, tubular and conical. The thin layer plate electrode, as described by Lankelma and Poppe (1976), has been used almost exclusively as a coulometric detector for the effluent of HPLC columns. The use of large area electrodes in a thin layer cell configuration makes a high degree of electrochemical conversion possible. The high surface area results in a signal 20 times higher than with amperometric detectors.

The electrode configuration found most effective is the wall-jet electrode, and it is this type which is used in this project. The principle of the wall-jet electrode was first described by Yamada and

Figure 29. Typical DME Flow Cell.

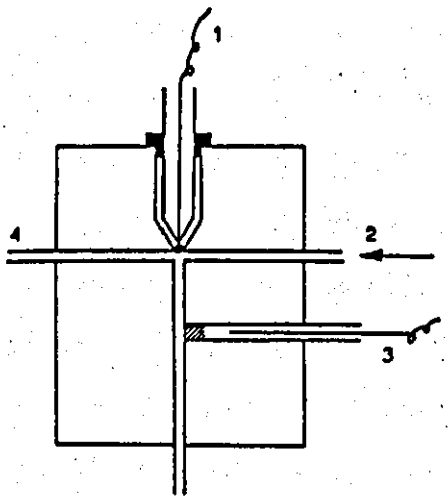

1. DME working electrode, 2. Inlet. 3. reference electrode, 4. outlet and auxiliary electrode (Stulick and Pacakova, 1981).

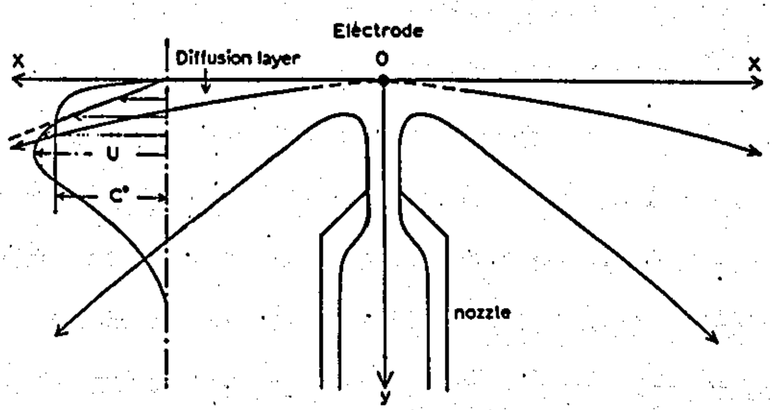

Figure 30. Schematic Representation of a wall jet electrode; u. velocity and c. concentration. (Yamada and Matsuda, 1973).

Matsuda (1973) and a schematic diagram of the velocity and concentration effects in a wall jet are depicted in figure 30, (see also fig. 28 c, d). The term wall-jet describes the flow due to a jet of fluid which spreads out over a plane surface. The wall jet electrode offers high sensitivity and low solution hold up which makes it suitable for measurements of flowing systems. The basic theory is expressed in the following two equations, where u is the radial velocity component in a Laminar wall jet,

$$u = {\frac{15M}{2vx^3}}^{\frac{1}{2}} f.(\eta) \qquad (10)$$

$$\text{where } \eta = {\frac{135M}{32v^3x^5}}^{\frac{1}{4}} . \, y \qquad (11)$$

x and y are distances along and normal to the electrode wall and v is the kinematic viscosity. M is the term for the flux of liquid estimated as,

$$M = \tfrac{1}{2} \text{ (velocity). (volume flow/radian)}^2$$

and f is a function of distance from the electrode surface. Yamada and Matsuda (1973) have produced an equation for the limiting diffusion current (I) for the wall-jet disc electrode and verified its dependance on the parameters in equation (12) below.

$$I = (1.6k)nFC^{o}D^{2/3}v^{-5/12}.\ V^{\frac{3}{4}}.\ a^{-\frac{1}{2}}.\ R^{\frac{3}{4}} \qquad (12)$$

The symbols are as for equations (5) and (11) plus,

R: radius of the electrode (assumed to be a disc)

a: diameter of jet nozzle.

V: volume flow rate of solution issuing from the nozzle,

and $k = (k')^{\frac{1}{4}}$ where k' is a proportional factor relating to M. Equation (12) does not have any parameter relating to the distance d between the nozzle of the jet to the electrode surface. The current does however decrease with increasing d, an effect which is most pronounced with low flow rates. Equation (12) indicates that the current is proportional to the bulk concentration of the solution, assuming all other parameters to be the same and that current is related to the flow rate. Yamada and Matsuda also confirmed the observation that current increased with increasing radius of electrode. The current is inversely proportional to the diameter of the nozzle, and depends on the viscosity of the solution. The diffusion coefficient is inversely proportional to the viscosity (Stokes-Einstein relation) and the kinematic viscosity is equal to the viscosity divided by the density, thus from equation (12) the limiting diffusion current (I) is inversely proportional to the $^{13}/_{12}$ power of viscosity.

The wall-jet electrode is highly sensitive, due to the rapid convective diffusional mass transfer. The dead volume can be varied and any type of solid electrode can be used. According to Fleet and Little (1974) it is remarkably free from problems caused by surface adsorption effects.

Several workers have designed and operated flow cells that incorporate two working electrodes. This type of system can be used to detect species at one electrode which are produced up stream at another (Bard and Faulkner, 1980). In this mode of operation each working electrode has its own reference and auxiliary electrode and accompanying circuitry (see fig. 31) for schematic diagram). Blank (1976) used a dual electrode system at different potentials to separate species which overlapped on a HPLC column, e.g. dopamines and catecholamines. Beauchamp et al (1980) have developed a multi-use flow cell incorporating wall jet and thin layer electrodes.

The mechanical limitations of the DME in flow cells coupled with

Figure 31. A schematic diagram of a dual electrode flow cell. (Bard and Faulkner, 1980).

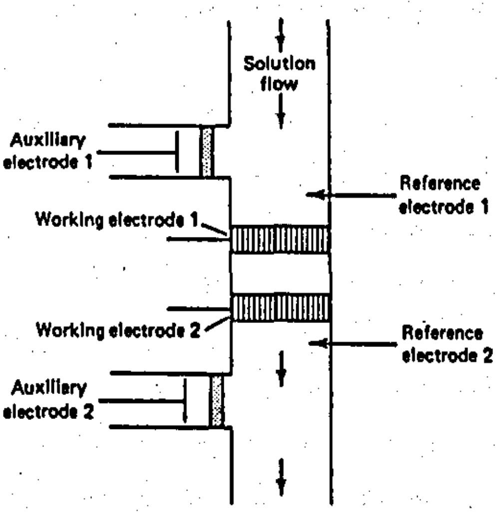

Figure 32. Electrochemical flow cell including a second auxiliary electrode (A2) required to supply cleaning pulses.

(Burmitz, 1980).

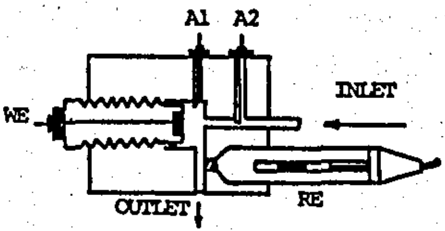

Electrochemical flow cell.

W.E. Working Electrode. R.E. Reference Electrode. A1 Auxiliary Electrode 1.
A2 Auxiliary Electrode 2.

its limited anodic range resulted in the development of the solid electrode (e.g. glassy carbon, impregnated graphite). The maintenance of a constantly active surface is the main problem, adsorption of products and reactants and film formation for example, contribute to variance in the performance of solid electrodes. Various techniques for cleaning the surface have been proposed, the most popular being mechanical abrasion which in effect removes the poisoned surface. Potential cycling is when the electrode is held at a potential at which any sorbed species are desorbed. Burmitz (1980) proposed two methods, firstly a scrubbing with a 20% methanol/buffer solution and secondly the application of a cleaning pulse of potential to the electrode. A electrochemical detector was constructed (see fig. 32) with two auxiliary electrodes, the cleaning pulse is applied between the second auxiliary electrode and the working electrode between sample zones of the stream.

8b. Types of electrode and their applications.

The thin layer configuration developed by Takata and Muto (1973) has found widespread use as a coulometric detector for HPLC. The most popular material for the electrode being glassy carbon, though other materials have been used; carbon cloth, carbon paste, platinum gauze, silver wire netting and Kel-F/graphite (Chesney et al, 1981). The wall-jet electrode is the other popular configuration, also using carbon electrodes. The application of electrochemical flow cells has been discussed in two recent papers by Ivaska and Ryan (1981), Toth et al (1981) and Van der Linden and Dieker (1980).

Glassy carbon electrodes are thus widely used for detectors applied to HPLC and flow injection analysis. Lankelma and Poppe (1976) have detected pharmaceuticals containing amine and ester groups, Dieker et al

(1979) analysing for natural biochemicals such as the catecholamines and Fogg and Bhanot (1981) studied synthetic food colouring compounds at glassy carbon electrode flow cells. Apart from this study the same research group has been using glassy carbon flow detectors analysing for bromide and nitrite (unpublished results).

Carbon paste electrodes have also been applied to HPLC effluent (Stulik et al, 1981b; Swartzfager, 1976). Carbon paste electrodes have also been used in the determination of catecholamines (Freed and Asmus, 1977) and food colours (Fogg and Bhanot, 1981). Other carbon based electrodes have been used in flow cells to a lesser extent. Wax impregnated graphite (Fenn et al 1978) and pyrolytic graphite (Wightman et al 1978) have been used in HPLC detectors and Pungor et al (1975) used graphite impregnated silicone rubber in a detector for continuous flow analysis. Strohl and Curran (1979) used a reticulated vitreous carbon electrode, where the stream flows through porous glassy carbon block. Wang and Dewald (1982) claim that such an electrode is 20 times as sensitive and 11 times less noisy than a conventional wall-jet electrode when detecting dopamine and ferricyanide. The surface area of their electrode is estimated at 1.26 cm^2 compared to the average area for a wall-jet electrode of 0.049 cm^2. Graphite has been used for tubular electrodes in both amperometric and coulometric detectors for liquid chromatography (Meschi et al, 1981 a, b), as pure graphite or as a polythene-carbon mixture (Armentrout et al, 1979).

The DME flow cell has seen relatively little application; a system described by Lund and Opheim (1975), Manekamp et al (1979 a,b) and Koen et al (1970) was used for liquid chromatography detection. Very recently Janata and Ruzicka (1982) have described a mercury micropool electrode for flow through systems (see fig. 33). They investigated d.c. voltammetry, rapid scan and amperometric titrations on a dispersed sample zone in motion. Chin and Chandran (1981) used a ring disc electrode in a wall-jet configuration, made of an inert metal (e.g. Platinum or Gold).. This detector has been used to study electrochemical reactions in the same fashion as the dual electrode system already described.

Figure 33. Electrochemical flow cell featuring a mercury pool electrode.

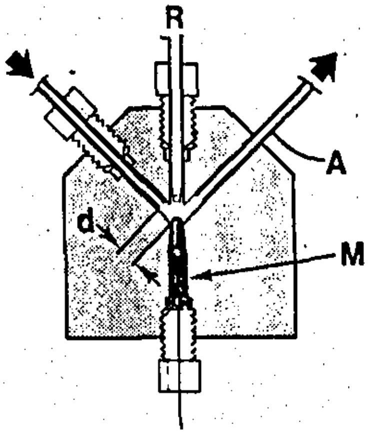

A. Outlet and Auxiliary electrode.
R. Reference electrode.
M. Micropool mercury working electrode.
d. 3mm.

8c. Modes of Operation.

The mode of operation is limited by the instrumentation and in order to achieve maximum sensitivity non-potentiostatic methods have be been employed Hanekamp et al, 1982); Swartzfager, 1976). These methods are usually pulse techniques, but AC measurement will also have the same effect of reducing the size of the reaction boundary layer, and so the signal becomes less dependent upon flow rate.

In pulse techniques the potential is applied in short pulses, thus reducing the time in which reaction is taking place at the surface of the electrode. This implies that the reaction layer is thinner and as current is proportional to the concentration gradient, a larger signal occurs. In the differential pulse mode the current is only measured for a short period at the end of each pulse. Hence, any capacitive currents are allowed to decay between pulses and a more favourable ratio between faradaic and capacitive currents is achieved. Capacitive currents are filtered out using a.c. measurements with a phase sensitive read-out. Dieker et al (1979) have compared d.c, normal pulse and differential pulse modes of operation. The d.c. mode was found to have the fastest response and the differential pulse mode the most sensitive but least reproducible. For all three modes the response time was independent of the flow rate above 0.9 ml/min, using both carbon paste and glassy carbon electrodes. D.C. detection was shown to have the lowest background noise. In d.c. and normal pulse modes all electrochemically active compounds that will react near to the applied potential contribute to the current observed. In differential pulse, particularly for reversible situations, the contribution of a certain compound will decrease quickly as the potential is shifted from the peak potential. Swartzfager published chromatograms demonstrating the selectivity of this method, but without any quantitative results. It is expected as the actual time of reaction with pulse methods is much less than for the d.c. mode, electrochemical adsorption will be reduced at the surface of the electrode. The DME may have an advantage over glassy carbon in pulse techniques due to the fast response of mercury to potential changes. As yet potentiostats do not provide the facility for differential and normal pulse operation and it is necessary to use polarographic instrumentation.

9. Heteropoly Acids and their salts.

Heteropoly compounds of molybdenum and tungsten have been of interest to chemists ever since 1826 when Berzelius first prepared ammonium 12-molybdophosphate. The 12-heteropolymolybdates with heteroatoms of As(V), P(V) and Si(IV) have been widely used for the colorimetric determination of the heteroatom. The heteropoly anions can be used themselves (usually yellow) or they can be reduced to an intensely coloured heteropoly blue compound. 12-Heteropolymolybdates are also used as industrial catalyst, flame retardants or as corrosion inhibitors. Other common anions of this group are the 6-, 9- and 18-heteropoly species. However this study will concentrate only on the 12-molybdophosphate and 12-molybdosilicate anions which are used in this work. Most of the studies on heteropoly acids have been on the molybdo- and tungsto-compounds, as in the review published by Tsigdinos (1978). Vanado-compounds have been investigated; they are usually mixed anions, such as vanadophosphomolybdate.

9a. Structure and Nature.

Heteropoly compounds generally have very high molecular weights for inorganic electrolytes, ranging to over 4000. The free acids and salts of heteropoly compounds are extremely soluble in water and sometimes very soluble in organic solvents. Generally the larger the cation the lower the solubility. For example the larger alkaline earth salts are insoluble. Ethers, alcohols and ketones are usually the best organic solvents. Dehydrated forms are readily soluble but hydrated forms are insoluble. The crystalline free acids and salts are always highly hydrated and are quite often highly coloured, occurring in many shades.

Heteropoly compounds are classified by the ratio of central atoms to the peripheral molybdenum atoms. Compounds with the same number of atoms in the anion are usually isomorphous and have similar properties. I.U.P.A.C. nomenclature uses this ratio as the prefix in naming the anions, with reference to the peripheral atoms, molybdo-, tungsto- or vanado-. For example 12-molybdophosphoric acid, which has the formula $[PMo_{12}O_{40}]^{3-}$. The general formula for 12-heteropoly acids is,

$$(X^{+n}\ Mo_{12}O_{40})^{(8-n)-}$$

where X can be P^{5+}, As^{5+}, Si^{4+}, Ge^{4+}

Molybdenum can be totally replaced by tungsten or partially by tungsten or vanadium to give a mixed species, the structural ratio is always maintained.

The structural chemistry of heteropoly acids has been discussed in detail by Weakley (1974) and Evans (1971). The structures of many heteropoly anions were determined originally by X-ray diffraction (Illingworth and Keggin, 1935). Each heteropoly anion contains a number of MoO_6 octahedra (M = Mo, W, V) sharing edges, curves and edges or corners and faces with one another. In addition every octahedron shares a corner with an XO_4 tetrahedron, an edge with an XO_6 octahedron on a face with an XO_{12} icosahedron (X = heteroatom). The 12-heteropolyacids have a structure postulated by Keggin in 1934 (see fig. 34), and have the overall tetrahedral symmetry of the central XO_4 groups. These M atoms are positioned at the corners of an almost regular cubo-octahedron. Although the anion is compact it will accommodate heteroions of radii ranging from 0.50Å (Al^{3+}) to 0.96Å (Cu^{+}) and non-metal heteroatoms of covalent radii 0.85Å (B) to 1.22Å (Ge). Experimental distances reported for X-O distances are (Weakley 1974), X = Si, 1.63; P, 1.71; Ga, 1.87; CoIII, 1.88 Å.

12-Heteropolyanions exist in two isomeric forms, the α and β structures.

Figures 34 and 35. The structure of 12-heteropolyacids.

34.

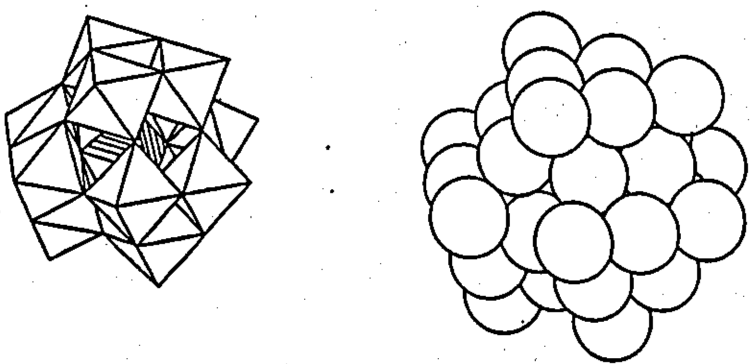

The $X^{+n}M_{12}O_{40}^{(8-n)-}$ anion: the Keggin structure. Left: Linked-polyhedron representation. Right: Ball model showing oxygens atoms only: same scale

(Weakley, 1974).

35.

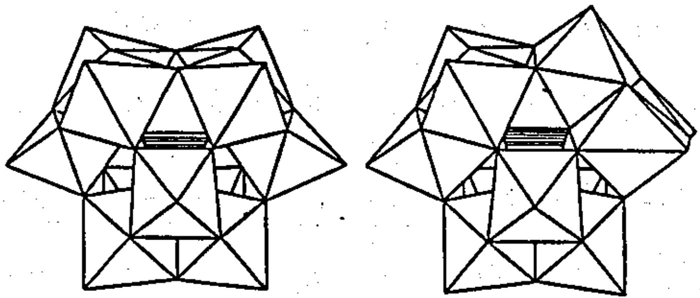

(a) (b)

Polyhedral diagrams of the 12-A heteropoly anions: a, the α-isomer; b, the β-isomer.

(Kasprzak et al, 1982).

The stable α-form has the Keggin structure and the β-form has a modification of this structure. Three M-O octahedra are rotated 60° with respect to the rest of the molecule (see fig. 35a, b). Recently 12-heteropolyanions have been studied by electron spin resonance (Launcey et al, 1980); Fruchart et al 1976) and Raman spectroscopy (Kasprzak 1982) confirming the Keggin structure. Both techniques are able to distinguish between α and β isomers. Truesdale and Smith (1975) have distinguished between the isomers spectrophotometrically, and several workers have done so electrochemically (see below).

9b. Formation and isomers of heteropoly acids.

Strickland (1952) laid down conditions for the formation of molybdosilicic acid which had gone unchanged until Truesdale and Smith (1975a, b, 1976, 1977, 1979) published a series of papers re-appraising the situation. They rejected the work of Strickland and replaced it with their own vigorous study, involving pH and molybdate concentration. Strickland was the first to show that there are two possible forms of molybdosilicic acid, and advanced the theory that if the ratio of hydrochloric acid to molybdate is less than 1.5 then the α form is produced, whilst the β form is produced at a ratio of more than 2.0.

Truesdale and Smith (1975a) criticised this rule of thumb, suggesting it was not possible for it to be applied through the whole range of acid and molybdate concentrations. The theory implies that the reaction is unaffected by variations in acid or molybdate concentration of the reagent. Truesdale and Smith (1975a) found that the optimum pH values for the preparation of the β isomer were 1.0 - 1.8 and 3.8 - 4.8 for the α isomer. Figure 36 depicts the absorbance of molybdosilicic acid at 390 nm against changes in pH. 90 minutes was

Figure 36. The absorbance of yellow molybdosilicic acid formed at various values for pH (Truesdale and Smith, 1975b).

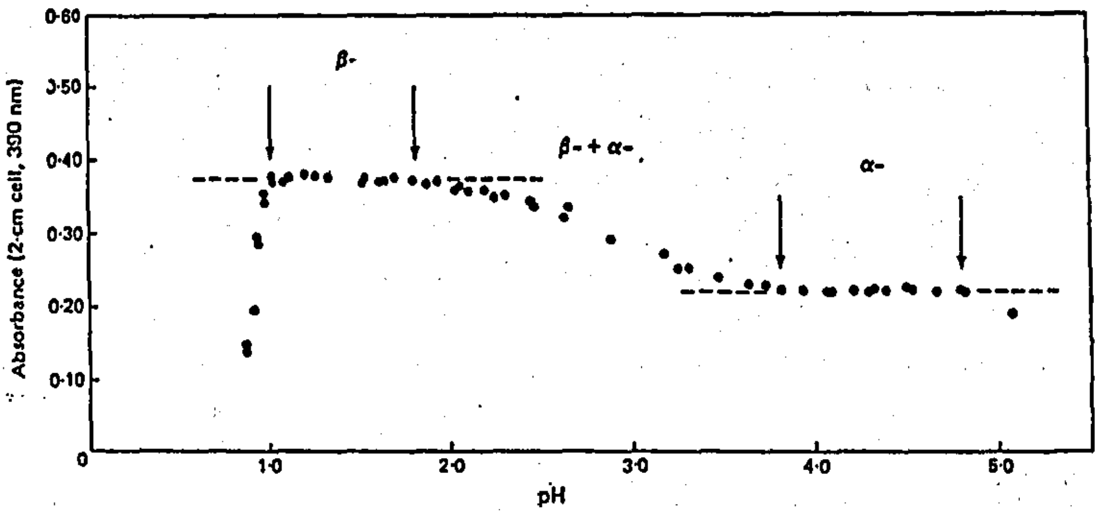

allowed for the completion of α-isomer formation whilst only 5 - 20 minutes were required for the β-isomer. The absorption spectra of α- and β-molybdosilicic acid are very similar, supporting evidence that the structures are not very different. There is no set of conditions at which the absorption of the two isomers are equal in the range 290 - 400 nm. So it is not possible to develop a colorimetric analytical method which is independent of the isomer produced, as suggested by Garrett and Walker (1964). The mechanism of the formation of the α-form is suggested by Truesdale and Smith (1975a) to be via the β-form. However they found that formation via the β form is slower than by direct formation. The conversion of the β-isomer to the β-form is a simple first order reaction with respect to the concentration of the β-form. A solution of β-molybdosilicate at pH 1.8 is buffered to pH 4.2 with acetate to form α-molybdosilicate. Truesdale and Smith (1977) found that sodium chloride would accelerate the conversion. Sodium chloride alters the acid-base equilibrium constant preceding the transformation. The rate of the transformation was found to be zero with respect to molybdate concentration and to decrease as hydrogen ion concentration increases. The α- and β-heteropolymolybdates have been examined polarographically, this is discussed later. The kinetics of heteropolymolybdate formation has been discussed in detail by Hargis (1970), Truesdale and Smith (1979) and Kircher and Crouch (1982b).

Comparatively little work has been published on 12-molybdophosphate, the existence of more than one isomer has only been demonstrated electrochemically. Kircher and Crouch (1982a) when determining the formation constants of molybdophosphates make no reference to the isomerism of 12-phosphomolybdate. They suggest that an equilibrium exists between the 9-, 11- and 12-forms. Chalmers and Sinclair (1965) indicate the existence of two isomers of 12-phosphomolybdate on the evidence of two discontinuities in a plot of optical density against the $[H^+]$:[MoVI] ratio in solution at 1.5 and 1.8. Ploger et al (1974) from electrochemical data propose that 12-phosphomolybdate and 12-Arsenomolybdate only exist as the α-isomers. However Tsigdinos (1978) shows the structure of 12-phosphomolybdate to be the same as β-12-silico-tungstate. Anderson (1958) suggested a mechanism whereas the β-form exists as a transient species degrading rapidly to the α-isomer. The formation of 12-phosphomolybdate is much quicker than 12-silicomolybdate (Chalmers and Sinclair, 1966), but the rate of formation depends on the same parameters (Kircher and Crouch, 1982 a, b):

$$K_j = \frac{[\text{Heteropoly Acid}]}{[H_3PO_4 \text{ or } SiOH_4]\,[\text{Mo VI}]^{12}}$$

The stoichiometry of the formation of 12-molybdophosphoric acid (MPA) is assumed to be governed by the following equation (Crouch and Malmstadt, 1967; Kircher and Crouch, 1982a).

$$X\ H_3PO_4 + Y\text{Mo(VI)} \rightleftharpoons 12\ \text{MPA} + ZH^+$$

Crouch and Malmstadt reported values of X = 1, Y = 6 and Z = 9 derived from experimental results in strong acid conditions. The later work indicates a more complicated relationship. The nature of Mo(VI) has not yet been resolved and is not a simple dimer as first thought. It is suggested that it is a mixture of several octatedrally co-ordinated hydroxy species. The lack of accurate interpretation of the molybdate speciation in solution has restricted the understanding of the kinetics of molybdosilicic acid formation (Truesdale, Smith and Smith, 1979). Hargis (1970) proposed stoichiometry for the formation of 12-silicomolybdate (MSA),

$$Si(OH)_4 + 6\ \text{Mo(VI)} \rightarrow \alpha 12\text{-MSA} + 6H^+$$

and the following mechanism was proposed,

1. $Si(OH)_4 + HMo_2^+ \rightleftharpoons SiO_4.MoO_2^{4-} + 5H^+$

2. $SiO_4.MoO_2^{4-} + 5HMo_2^+ \rightarrow \beta 12\text{-MSA} + 5H^+$

3. $\beta 12\text{-MSA} \rightleftharpoons \alpha\text{-}12\ \text{MSA}.$

This mechanism assumes the molybdate to be in the form of a dimer. The second step is the slow rate determining step, a stepwise addition of 5 molybdate dimers. In the formation of 12-phosphomolybdate Crouch and Malmstadt (1967) suggest the dimer converts to a higher polymer which then reacts with phosphate. The mechanism is given below, and

$$6\ \mathrm{Mo(VI)\ dimer} \rightleftharpoons \mathrm{Mo(VI)\ polymer} + H^{+}$$

$$\mathrm{Mo(VI)\ polymer} + PO_4^{3-} \rightleftharpoons \mathrm{12\text{-}MPA}.$$

it is suggested that this explains why 12-MPA in solution is stable to concentrated mineral acids.

9c. The Chemistry of 12-Heteropolyacids.

(i) Solubility

The solubility of heteropoly compounds is attributed to very low lattice energies and solvation of the cations (Tsigdinos, 1978). The solubility is governed by the packing in the crystal structure, small cations fit easily in between the spheres of the large negative heteropoly anions, larger ions can also be accommodated. Large cations such as Rb^{+}, Cs^{+}, Ag^{+} provide a stable packing, lowering the lattice energy sufficiently to produce insolubility in water. The free 12-heteropoly acids are remarkably soluble in water, dilute acid, alcohols and ethers; for example 100 ml of water at room temperature will dissolve 700 g of 12-molybdosilicic acid. A heteropoly acid solution in an ether (400 g in 100 ml) will form an oil when mixed with water; it is thought that an etherate is formed.

(ii) Hydrates.

Free acids of 12-heteropoly anions form isomorphous 30-hydrates which melt in their own water of hydration at 40-100°C. Salts of the free acids lose water of hydration up to 300°C. The free acids 12-molybdosilicic acid and 12-molybdophosphoric acid can be dehydrated at 180°C and rehydrated at 25°C, their acids are isostructural in the hydrated form.

(iii) Basicity.

12-Heteropolymolybdates have a basicity of 8-n where n is the oxidation state of the central atom. We then expect 12 phosphomolybdates to be tribasic. It has been reported as heptabasic

(Tsigdinos and Hallada, 1970) due to the heteropolyanion being extensively hydrolyzed in solution, especially in dilute solutions. 12-Phosphomolybdate behaves as 6 - 7 basic when titrated against sodium hydroxide. However the free oxides can be stabilized in mixed solvents, for example water-acetone and water-ethanol. When 12-molybdophosphoric is titrated against sodium hydrooxide in 50% Acetone/water it behaves as a tribasic acid. 12-Silicomolybdate is formed from a tetra basic acid. However the neutralisation process is complicated by splitting of the heteropolyanion. Silicomolybdic acid reacts according to the equations below (Myshlyaeva and Krasnoshchekov, 1974).

$$H_4[Si\,Mo_{12}O_{40}] + 4NaOH \rightarrow Na_4\,SiMo_{12}O_{40} \qquad \text{or}$$

$$H_4[Si\,Mo_{12}O_{40}] + 24NaOH \rightarrow 12Na_2MoO_4 + H_4SiO_4 + 12\,H_2O$$

with splitting of the heteropolyanion.

Data for pH in water and organic solvents both show that 12-MSA is a strong acid. A 2% solution gives pH 2.0 and 12-MPA gives pH 3.2 - 3.7, consistent with the phosphorous compound's lower hydrolytic stability. 12-Heteropoly acids with one or more of their central atoms replaced; for example with vanodium atoms show a change in basicity depending on the number of vanodium atoms present (Cheu and Polotebnova, 1973).

(iv) Thermal stability.

12-MPA and 12-MSA following DTA and TGA, have been shown to be stable up to 350° for 12-MPA and 200 - 300 for 12-MSA. Stability is not significantly altered for the salts of heteropoly acids.

(v) Degradation.

Treatment of heteropolymolybdates with alkali results in the degradation to a product with fewer Mo atoms. In the titration of 12-MSA with sodium hydroxide, excess alkali causes complete degradation to simple molybdates. The stability in solution of the 12-heteropolymolybdates differs markedly. 12-MSA is the most stable and can be neutralised intact. Degradation is only affected by excess alkali. 12-MPA on the other hand, has to be maintained in acid solution to avoid hydrolytic anionic degradation, which will occur before neutralisation can be completed. However 12-MPA may also be decomposed by an excess of strong mineral acid.

(vi) Oxidation and Reduction.

Very little oxidation of heteropolyacids has been studied, though a peroxy heteropolymolybdate $(NH_4)H_2(PMo_4O_9(O_2)_2)$ has been isolated (Tsigdinos, 1978). Reduction of MPA's is the basis of the colorimetric methods for phosphate and silicate analysis. A variety of reducing agents have been used to reduce a MPA to a 'Heteropoly Blue' compound, examples are, 1-amino-2-naphthol-4-sulphonic acid (Crouch and Malmstadt, 1967), stannous chloride (Morrison and Wilson (1963) and hydrazine hydrate (Sen and Chatterjee, 1966). The "heteropoly blues" are mixed valence complexes. Pope (1980) has recently reviewed the subject and restricts the term to well defined crystalline molecules or ionic species; but still this encompasses several hundred complexes. The rate of formation of heteropoly blues is dependent on the heteropolyacid concentration and the concentration of the reductant (Hargis, 1970).

$$\frac{d[\text{Hetero Blue}]}{dt} = k\,[\text{12-HPA}][\text{Reductant}]$$

Crouch and Malmstadt indicate some sort of interaction between sulphate and heteropolyacids and that some interference is detected with the colorimetric determinations of phosphate (Guyon and Cline, 1965 and Dehne and Mellon, 1965).

Mixed heteropolyacids like molybdovanadophosphonic acids form heteropoly blues in the same manner. Cheu and Polotebnova (1973) investigated such blue complexes and their redox potentials, which tend to increase with increase in vanadium content of the complex. However these workers suggest that on reduction of the heteropoly acid the blue product contains only molybdenum(V)atoms (no more than three). The vanadium is first reduced in the complex and then eliminated. The reaction is represented below,

$$6(\mathrm{P\ Mo(VI)_{10}V_2O_{40}})^{5-} + 48\mathrm{H}^+ + 27e^- \rightarrow$$

$$\rightarrow\ 5(\mathrm{P\ Mo(VI)_9\ Mo(V)_3O_{40}})^{6-} + 12\ \mathrm{VO}^{2+} + 24\mathrm{H_2O} + \mathrm{PO_4}^{3-}$$

10. Electrochemistry of Heteropoly acids.

The ability of heteropoly acids to undergo oxidation and reduction is their most important property. It is widely used to study their structure and formation, and their salts, also the identification and determination of their constituent elements. This account is mainly concerned with voltammetric methods; electrochemical methods in general have been reviewed by Alimarin et al (1981).

10a. Redox behaviour of Heteropoly acids.

The characteristic of a redox system is the standard potential, (E^o), this is generally calculated from the equilibrium constant of the system. Due to the complexity of MPA systems such calculations have not been carried out. Experimentally the determination of E^o requires the removal of influences of secondary processes and the taking into account of activity coefficients. It is practically impossible to achieve this and the formal potential of whole systems are measured (Ej) with the oxidised and reduced forms at equilibrium.

(i) Reversibility.

There are several factors which affect the reversibility of a system. Heteropolyacids can be irreversibly destroyed or restructured at the electrode by the formation of new compounds, specific adsorption or a chemical reaction in the layer near the surface of the electrode. The principal factor of the heteropolyacid redox system is the symmetry of each octahedron forming the heteropolyacid co-ordination sphere. Those with a Keggin type structure have octahedrons with one terminal bond which are reduced and oxidised reversibly without any change to the original structure. 6-Heteropolyacids in contrast behave irreversibly, the reduced species are thought to be unstable in solution (Tsigdinos and Hallada, 1974). The reversibility of 12-heteropolyacids is indicated by cyclic voltammetric data (see fig. 37). The values of the peak current and the potential at which they occur are almost the same for both reduction and oxidation processes. Secondary processes occurring in aqueous solutions can lead to slight deviations from complete reversibility.

(ii) Redox potentials of Heteropolyacids.

The redox potentials of an HPA can be determined using potentiometric and voltammetric methods. The potentiometric method entails the addition of either the oxidised or reduced form of an HPA to half the amount of titrant required for equivalence. The equivalence point is found according to the titration curve, and hence the potential (E). The voltammetric method produces a value called the half wave potential ($E_{\frac{1}{2}}$) in the case of polarography or the potential at peak maxima in the case of pulse, AC and linear sweep methods.

Typical voltammograms of 12-MPA are shown in figure 38 as cathodic reductions. An HPA in a required state of reduction can be obtained by electrolysis at a controlled potential. The oxidation and reduction of an HPA is a stepwise process (see voltammogram fig. 39).

37.

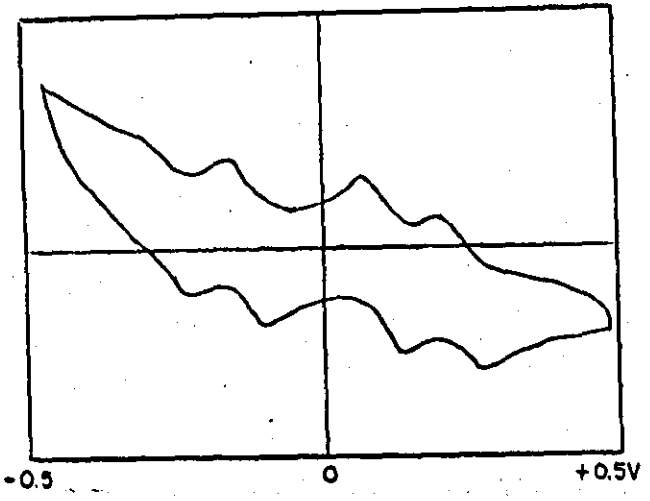

Cyclic Voltammogram of 1 × 10^{-3}M H_3[$PMo_{12}O_{40}$] in 1N H_2SO_4 (1:1 Water-Dioxane).
Y Axis: Current (200 μa/div)
X Axis: Applied Potential (0.1 v/div) versus SCE
Frequency: 10 Hz
Sweep Rate: 20 v/sec

38.

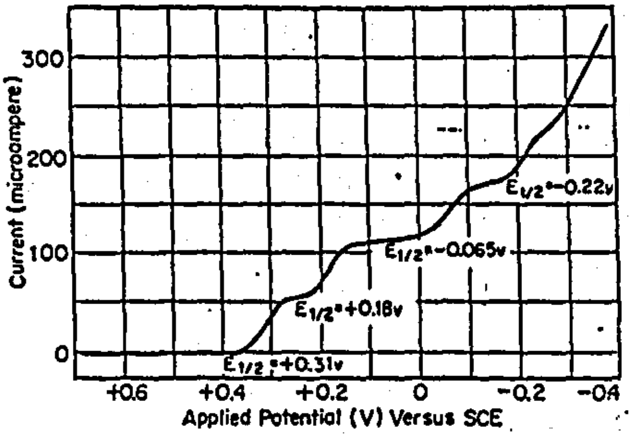

Direct Current Polarogram of 1.06 × 10^{-3}M H_3[$PMo_{12}O_{40}$] in 1M H_2SO_4 (1:1 Water-Dioxane).

39.

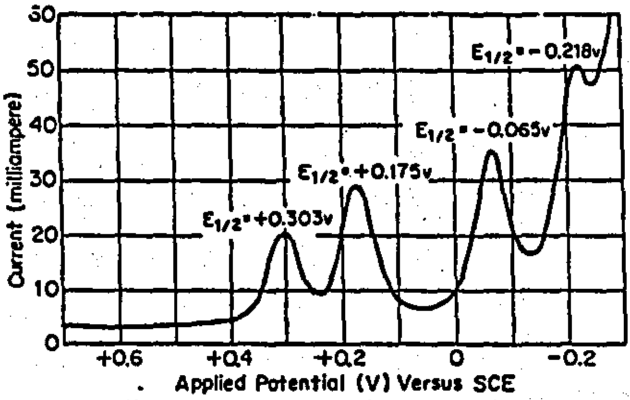

Alternating Current Polarogram of 1 × 10^{-3}M H_3[$PMo_{12}O_{40}$] in 1N H_2SO_4 (1:1 Water-Dioxane).

Figures 37, 38 and 39, depicting the reversibility and stepwise nature of the electrochemical reduction of 12-phosphomolybdic acid.

Each step is a two electron process, the first three represent reductions of the HPA, which are reversible, the fourth step as can be seen from the cyclic voltammogram is not.

10b. Factors Affecting the redox potentials of Heteropolyacids

(i) Influence of ligands.

As previously quoted, it has been found that the redox potential varies with choice of the central atom of the HPA. If the central atom is reduced at a lower potential than the ligand atoms, electrons are added first to the central atom, resulting in formation of complexes of elements in unstable oxidation states (e.g. Cu(I), Co(III)). Heteropolymolybdates are more easily reduced than heteropolytungstates. Mixed anions (e.g. molybdotungstates) will exhibit properties of both types of HPA, the more molybdenum atoms present, the higher the potential. The redox potential increases when a greater oxidising element (e.g. vanadium) replaces either molybdenum or tungsten. If the proportion of vanadium in the complex increases the charge on the anion increases, causing a shift of the potential in the negative direction (hence a decrease in $E_{\frac{1}{2}}$ values).

(ii) Structural Influence.

In all cases HPA α-isomers are reduced at more negative potentials than β-isomers. Contrasting all previous work, Ploger et al (1974) and Umland et al (1973) indicate that α-isomers are more easily reduced and that 12-MPA at a more negative potential than 12-MSA.

(iii) Solvent Effects.

Reversibility is improved in the presence of certain organic solvents which suppress the secondary processes occurring in aqueous solutions. A solution containing 50% acetone, dioxane or ethanol will prevent dissociation and isomerisation of most heteropolyacids.

Generally the inclusion of such solvents does not affect the potential at which heteropolyacids are reduced. A solvent with a high dielectric constant such as dimethyl formamide will not affect the potentials of any dissociation products, which are not detected in a 50% ethanol solution. If the solvent has a long aliphatic chain structure the current or height of the wave may be increasingly reduced as the number of carbon atoms in the structure increases. The diffusion constant is perturbed by changes in the viscosity of the solution.

(iv) Influence of pH.

The hydrogen ion concentration will affect the electrochemistry of heteropolyacids. Protonation in solution will result in the formation of new redox systems. The amount of adsorption of an HPA at the electrode surface can be affected by changes in the pH. This results in complications of the electrode reaction, consequent irreversibility, disproportionation and shifting of redox potentials. Protonation of reduced forms of HPA cause an increase in potential (E_p):

$$E_{p(pH)} = E_p - 0.058\ \mathrm{pH}$$

As pH is increased the peak potential (E_p) shifts in the negative direction. At a high enough pH, the potential becomes independent and the waves become one electron steps (i.e. the 2 electron steps are split). The products of two electron steps are the same as for one 2 electron step. Figure 40 a and b demonstrate the effect of pH on the peak potential and the splitting of the peaks. Fruchart and Souchay (1968) demonstrate this for α- and β 12-MSA in acetic acid at a platinum working electrode.

10c. The effect on reversibility by chemical factors.

A number of processes influencing the equilibrium of an HPA in solution have been discussed.

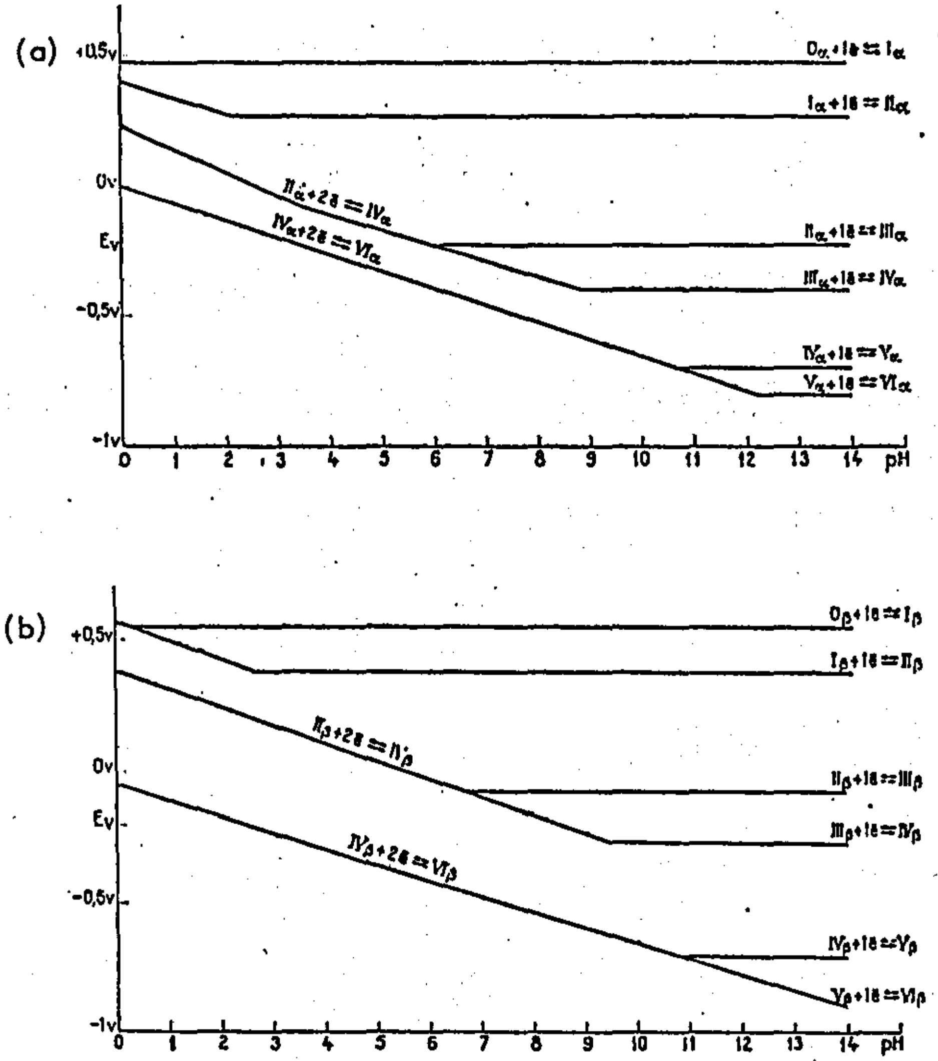

Figure 40. The effect of changing pH on current peak potentials and the splitting of potential peaks for α-(a) and β-(b) molybdosilicic acid (Fruchart and Souchay, 1968).

(1) Dissociation.

The dissociation of HPA may lead to the formation of the original ions, isopolymolybdates (Souchay, 1965) and complexes like molybdotungstates upon the fragmentation of mixed HPAs. Hydrolytic dissociation is perceived by an increase in pH. Molybdosilicic acids are most stable and heteropolytungstates are more stable than heteropolymolybdates. The dissociation products may undergo electrochemical reactions which will complicate and mask the principal reaction being observed.

(2) Isomerism.

An HPA with the Keggin structure is characterised by α-β isomerism with the α-form more thermodynamically stable. As pH is increased the rate constant for β→α transformation increases. As the isomers have slightly different voltammetric waves and the reduced form is more stable in the β form the likelihood of mixed isomers is high. However the system can be stabilised with the use of organic solvents which lower the dielectric constant of the solutions thus inhibiting dissociation and isomerisation.

(3) Heteropoly Chemistry.

The reduction of an HPA results in an increase of negative charge and strong retention of protons. β-Isomers hold protons more tightly than α-isomers despite having identical charge. This is due to the inequivalence of the Mo(VI) atoms in the β-isomers structure, which is attributed to the non-uniform distribution of surface charge. In organic-water solvent mixtures they remain unassociated, in 100% aqueous solutions heteropolyacids are strong electrolytes.

It is possible to get transition from one series of heteropolyacids to another; for example if the pH is increased a 13-HPA will transform into a 11-HPA. It is also known for a 9-HPA to dimerise producing a pseudo 18-HPA.

Catalytic properties of HPA are known, and may result in the irreversible decomposition of solvents. The hydrolysis of butyl acetate is catalysed by 12-MPA as is the decomposition of ketones.

10d. The Effects on reversibility of electrochemical factors.

(1) Electrode Material

The electrochemistry of heteropolyacids has been investigated at both solid and dropping mercury electrodes. The choice of electrode is governed by the restrictions of the system to be investigated. The DME is avoided for heteropolymolybdates, mercury will reduce them and their dissociation products, heteropolytungstates remain unaffected. The current voltage curve in alkaline conditions is practically identical for the platinum and dropping mercury electrode, this is thought just to be coincidence. However the redox potentials of heteropoly compounds (0.1 - 0.6 v. vs. S.C.E.) coincide with the potential range for the double layer of the platinum electrode; ideal conditions for a reversible reaction.

In acidic conditions the wave of an HPA differs considerably when comparing a platinum electrode to a DME. At the DME the electrochemical reaction is slowed from molybdenum and mixed anions. The resulting overvoltage is associated with irreversibility of an HPA at a DME.

(2) Adsorption effects.

Adsorption effects of heteropolyacids have not been reported except at a DME, this is a polarographic effect. The small difference in peak potential between the reduction and oxidation wave of an HPA may be attributed to a degree of adsorption, due to either isomerism or a decrease in adsorption of the reduced form.

(3) Effects in the layer near the electrode.

If a chemical reaction is occurring in the layer close to the electrode, complication of the electrochemical conversion on HPA may occur. For example, a chemical reaction may be proceeding at a faster rate than the diffusion to the electrode.

10e. Voltammetric investigations of Heteropoly Acids.

Recently Alimarin et al (1980) have reviewed the voltammetric work in this field at platinum working electrodes.

The voltammetric wave for 12-MSA and 12-MPA (see fig. 38) represents three 2-electron reduction steps which are normally totally reversible and a fourth step which is irreversible. The general form of the work was found to be similar for all the 12-heteropoly-acids, although it is possible to make qualitative distinctions between them. The fourth step in the wave has not been ascribed to any chemical process to date, it occurs close to the point of evolution of hydrogen and the wave of oxygen. It is possible to distinguish between α and β isomers from their voltammetric behaviour. The three two-electron steps are as follows for 12-MSA,

$$H_4[SiMo_{12}O_{40}] + 2e^- + 2H^+ \rightarrow H_6[SiMo_{12}O_{40}]$$

$$H_6[SiMo_{12}O_{40}] + 2e^- + 2H^+ \rightarrow H_8[SiMo_{12}O_{40}]$$

$$H_8[SiMo_{12}O_{40}] + 2e^- + 2H^+ \rightarrow H_{10}[SiMo_{12}O_{40}]$$

In each step one Mo(VI) atom is reduced to Mo(IV). Launay et al (1974) have followed the transformation of the β-isomer to α-form electrochemically, by recording voltammogram at set times after the addition of the reducing agent, stannous chloride. The pure α and β forms only give two steps in the reduction wave but their mixtures are more complicated (see fig. 41). The isomers of 12-MSA have been studied electrochemically by many workers with consistent results.

Figure 41. Transformation, β → α molybdosilicic acid (Launay et al, 1974).

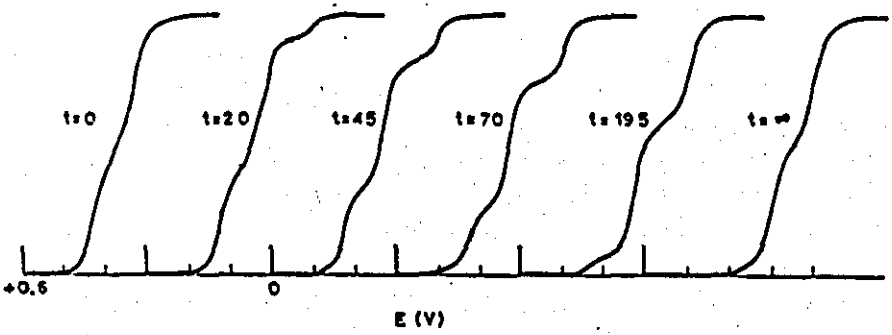

Evolution $\beta \rightarrow \alpha[SiMo_{12}O_{40}]^{4-}$: Each curve is shifted 0.3 V with respect to the preceding one. Times, t, are in min.

The typical potentials (v.) of a voltammetric wave at a platinum electrode are as follows (D.C. vs SCE, Tsigdinos and Hallada, 1974).

Wave Procession	α-isomer	β-isomer
1	0.32	0.42
2	0.19	0.31
3	-0.06	0.19
4	-0.23	-0.12

10f. Analytical Electrochemistry of phosphate and silicate.

Polarography of heteropolyacids at the DME has been applied to the determination of phosphate and silicate despite the DME shortcomings. Recently analytical methods have been published employing mercury electrodes. Fujinaga and Magaosa (1974) extracted 12-MPA and 12-MSA into various organic solvents before polarographic analysis. Iyer et al (1981) preconcentrated 12-MSA on an HMDE at -0.2v followed by stripping at -0.36v, levels of 10^{-7}M SiO_2 are detected by this method. Polarographic methods of analysis have been reviewed by Alimarin et al (1980). The majority of the methods are by normal DC mode, a few are AC and two are differential pulse.

Fogg and coworkers (1978, 1981a, b, c) have used voltammetry at a glassy carbon electrode to determine phosphate and silicate by the differential pulse mode. Scanning from zero in the positive direction they were able to record voltammograms without the need of deoxygenate. Cox and Cheng (1974, 1978) have also used glassy carbon electrodes for the determination of phosphate as 12-MPA using cathodic stripping voltammetry. Most of the methods for the determination of silicate and phosphate can also be applied to arsenic and germanium. The sensitivity and selectivity of the methods can be improved by extraction techniques with specific solvents.

(1) Indirect electrochemical methods.

Bazzi and Boltz (1976) decomposed 12-MSA and 12-MPA and extracted molybdate which is determined at a DME. The complexing nature of tripolyphosphate has been used to reduce polarographic wave heights of octyltin (Shaw and Townshend, 1973) and cadmium (Al-Sulimany and Townshend, 1973), calibrating for tripolyphosphate in the presence of pyro and orthophosphate. Similarly the wave of hexammine cobalt(III) is reduced by complexation with polyphosphates (Matsuura et al, 1974). Pyrophosphate can be determined by complexation of metals, linearly reducing the polarographic wave of copper lead and iron (Reynolds and Rogers, 1949).

(2) Electrochemical Titration.

Amperometric titrations usually involve the precipitation of an HPA with an organic base in a strict stoichiometric reaction. The titrations are carried out according to the reduction current of the HPA on a DME or the oxidation current at a platinum electrode.

Large concentrations of silicate have been determined potentiometrically and lower concentrations in cloudy or coloured solutions, where alternate methods are inapplicable. Generally, the slow establishment of a constant potential and the chemical instability of the reducing titrants limit the application of potentiometric titrations.

Coulometric titration of heteropolymolybdates of silicon, phosphorus and germanium by tin(III) generated at a platinum electrode has been used. The end point in this method is determined photometrically (Alimarin, 1980).

Instrumentation used.

The instrument used throughout this project was the E.G.& G./PARC Model 174A polarographic analyzer. It is capable of performing normal and sampled dc, normal and differential pulse, linear sweep and anodic stripping voltammetry. In the Model 174A the output ramp pulses are summed with the initial potential and a feedback signal from the reference electrode. The potentiostat in turn applies a potential to the auxiliary electrode and drives it to whatever potential is required to make the reference electrode equal and opposite to the sum of the output and initial potentials.

Any current that flows through the working electrode is converted to a voltage which is then amplified and applied to the "Y" axis of an X-Y recorder, in this case a Gould Advance HR2000. The "X" axis is driven by a signal from the scan-potential generator of the Model 174A. In the pulse mode the current is sampled during the last 17ms. of the timing period. The specifications of the instrument are as follows:

(i) Initial Potential. A continuously adjustable from 0 to ± 5v.

(ii) Scan Rate, 0.1 mv/s^{-1} to 500 mv/s^{-1}

(iii) Scan Range, 0.75, 1.5 or 3.0v of either polarity.

(iv) Operation, "Initial", "hold", "scan" and "scan reverse" are the modes available.

(v) Current range, 0.02 μA to 10mA full scale deflection.

(vi) Overload. The malfunction indicator operates whenever the output amplifier, current converter amplifier or the potentiostat are driven to the limits of their capability.

(vii) Modulation. 5, 10, 25, 50 or 100 mv pulses are available for the differential pulse mode.

(viii) Clock. A choice of 0, 0.5, 1, 2 or 5 second controlled drop time when the instrument is used with a DME or pulse times with the relevant modes of operation.

(ix) Offset. A continuously adjustable offset of 0 to ± 1000% of full scale output. This is used to nullify large non-signal differential outputs.

(x) Low pass filter. Filter time constants of 0, 0.3, 1.0 and 3.0 seconds are available. The filter determines the response time of the signal amplifier and is used to smooth over signal fluctuations. It is better to use the sampled mode to remove fluctuations as the low pass filter can produce distortion of the readout. The low pass filter provides an RC network which filters the output signal before it is applied to the recorder.

(xi) Cell selector, three positions, "off", "external cell" and "dummy cell". The dummy cell provides a 10Ω resistor used for instrument check out and trouble shooting.

(xii) Display direction. This allows for a positive output signal of either an anodic or cathodic current.

The injection value used the flow injection system was a Rheodyne Type 50 Teflon Rotary Valve. The valve used was the sample injection model (see fig. 42), it is of convenient assembly (see exploded view, fig. 43) with easily replaceable components. It is possible that the rotor and stator components may become scratched during operation and require replacing. The operation of the valve is facilitated by the rotation of a flat Teflon rotor against a flat Teflon stator. The switching pattern is shown in figure 42. All the wetted parts of the valve are of Teflon construction, the remainder is stainless steel and polypropylene. Flanged tubes are fitted flush to each of the six ports. If a loop is fitted between two ports, say nos. 1 and 4, a sample contained in the loop can be transferred to the main carrier stream applied across parts 2 and 3. The rotor only moves between two positions through 60°.

The electrochemical detector used in the flow injection system was a "Metrohm" detector cell which works on the wall-jet principle (see figures 28 and 30). The cell is made out of a block of polytrifluorethylene with the electrodes inserted in cavities bored into the block. The working electrode is made of glassy carbon designed specifically for this detector cell. The cell, originally designed as a detector for HPLC has a dead volume of less than 1 µl. The Metrohm glassy carbon electrode was also used for static voltammetry, as was a carbon paste electrode manufactured by E.D.T. research.

The carrier stream for the FIA work was driven by an "Ismatic" Mini S peristaltic pump. The barrel has eight rollers and can accommodate three pump tubes providing they are all of the same diameter. The "Ismatec" pump is recommended for FIA work, it generates a low

42.

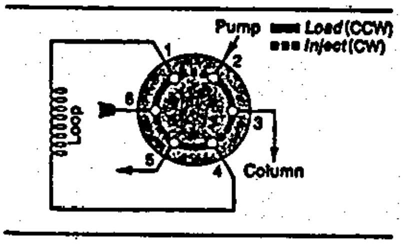

43.

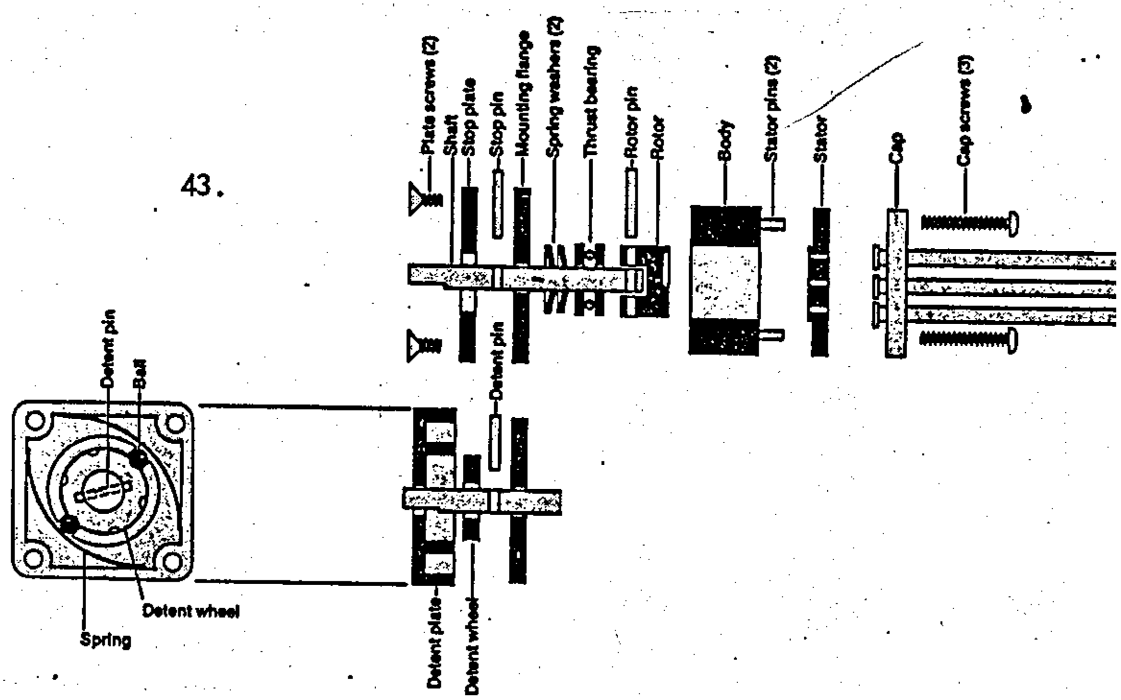

Figures 42 and 43. The switching pattern and exploded view of the Rheodyne sample injection valve (Rheodyne Inc. operating instructions).

amplitude pulsing producing a low level of signal noise at the detector. A more sophisticated pump, the "Gilson Minipulse 2" was used to drive the stream connected with an autoanalysis hydrolysis coil. The Gilson has a ten roller barrel and variable speed control. The "Ismatec" model has very limited means to change the flow rate, having a screw tightening clamp on the pump tube. Different flow rates can be achieved by changing the diameter of the pump tubes.

A "Technicon Autoanalyzer" heating bath was used for air segmented continuous flow hydrolysis of polyphosphates. The autoanalyzer consists of two reaction coils, 7m.in length and 2mm. and 3mm. internal diameter, resting in a silicone oil bath. The autoanalyzer is fitted with a stirrer/heater and can operate at a maximum temperature of 95°. The stream is air segmented, the air segments being facilitated by standard Technicon fittings (bubbler and debubbler).

Experimental and Results

The starting point for the experimental work was the method for determining phosphate and silicate developed by Fogg et al (1981, a, b). Orthophosphate and soluble silicate combine with acid molybdate reagent to form heteropoly acid compounds. These compounds exhibit an anodic voltammogram in the potential range 0 - + 0.6 v. Figures 45 a and b depict the characteristic waves of the above procedure.

1. Hydrolysis of Polyphosphates.

In order to determine total phosphate a necessary hydrolysis step is required to convert all the polyphosphates that may be present in the sample to orthophosphate. The heteropoly acid will only be produced with orthophosphate. Much work has been published concerning the hydrolysis of polyphosphates (see Greenfield and Clift 1975), and no better method than an acid digestion at pH 1.0 has been achieved.

Attempts were made to improve the hydrolysis step by varying pH and acid concentration. The use of high concentrations of acid is not favoured; not only as more care is required in handling, but because high concentrations of acid interfere with the formation of the heteropoly acid and increase the background current of the voltammogram. Alkaline and copper catalysed methods were also tried without any success.

The heteropoly acids and related compounds are known to have catalytic properties, so hydrolyses were carried out in the presence of the acid molybdate reagent in an attempt to self catalyse the hydrolysis reaction. Acid molybdate solution (30 gpl sodium molybdate and 24 gpl tartaric acid in 1M HCl) (10 ml) is added to 10 ml of sample solution (Washing Powder) and digested on a steam bath for 0 to 60 minutes. The extent of hydrolysis is measured as a function of

Figure 46. Voltammetric waves for (a) 12-MPA and (b) 12-MSA used for the determination of phosphate and silicate. The heteropolyacids were formed according to Fogg et al (1981b).

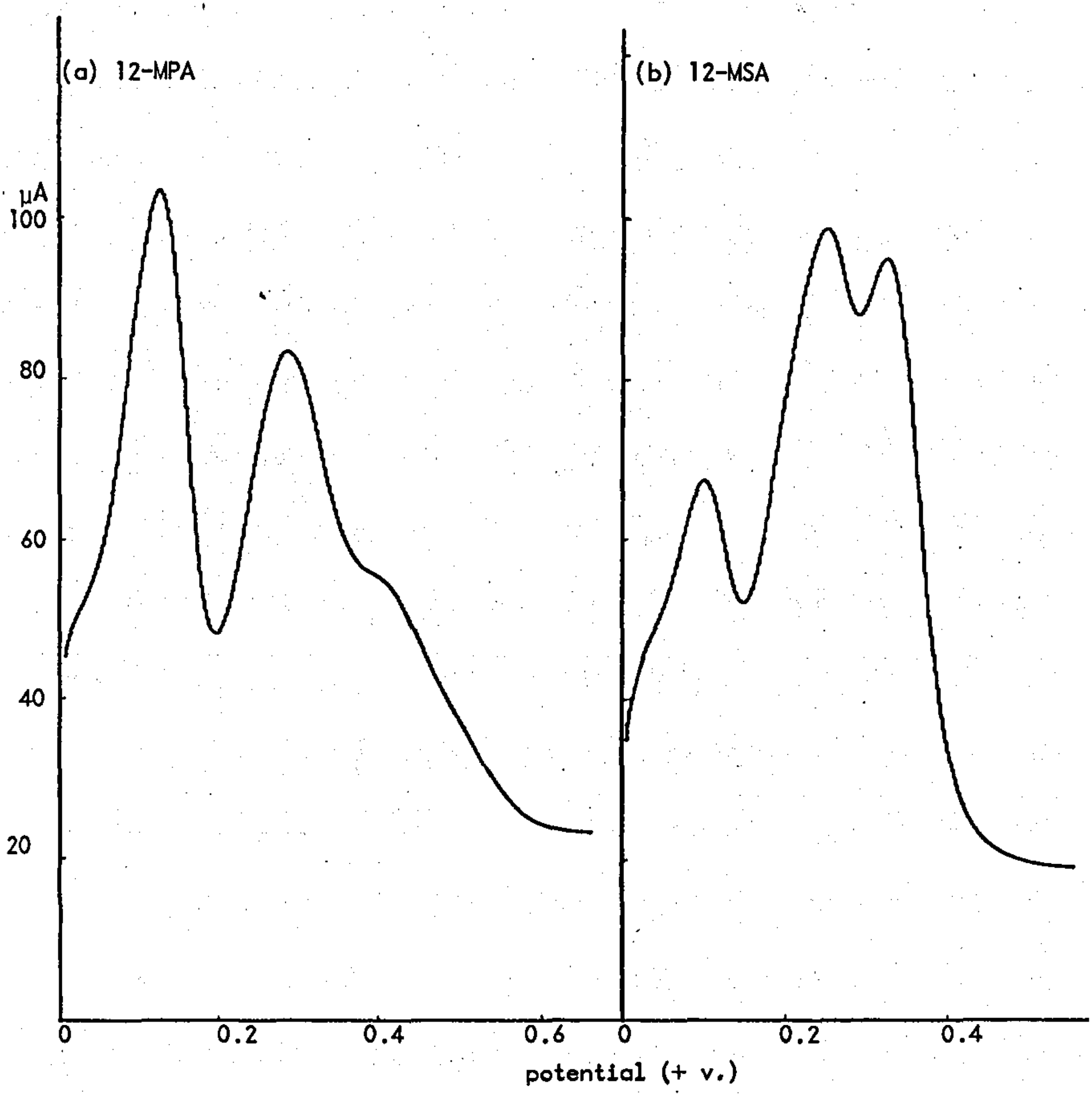

peak height of the voltammogram due to 12-MPA. The sample is diluted to 50 ml and the potential is scanned from 0 to + 0.6 v. The final solution is a dark green colour, in the absence of tartaric acid it is a deep blue. The tartaric acid is present to prevent interference from 12-MSA. The rate of hydrolysis, however, was no faster than any of the previous methods. Hydrolysis was complete within 60 minutes. After cooling to room temperature the solution is ready to be determined. The hydrolysis of tripolyphosphate in solutions of washing powders was achieved by the addition of 2M sulphuric acid (5 ml) to the sample solution (20 ml) and digested on a steam bath for 1 hour. The hydrolysis of tripolyphosphate in washing powders by sulphuric acid is not bettered by the method using molybdate/tartaric acid reagent.

2. Surfactant interference.

The analysis of a washing powder sample was attempted using the phosphate methods from Fogg et al (1981a). The sample had been analysed by colorimetric methods at Unilever Research Ltd., the result of the above method was 50% less than expected. Surfactant compounds are known to be active as "maximum suppressors" in normal mode voltammetry. The effect of surfactant was then investigated on the methods proposed by Fogg et al (1981 a, b, c). In general it was found that the presence of surfactants in the test solution reduced the amplitude of the wave due to the heteropoly acid and thus a low result is obtained. The surfactants used were sodium lauryl sulphate (B.D.H. Chemicals Ltd.) and a sodium alkyl benzyl sulphonate, supplied by Unilever as typical of that used in washing powders.

The investigation was carried out by preparing test solutions as in the prescribed methods containing varying concentrations of surfactant, keeping the phosphate or silicate level constant. The range for the surfactant was 0 - 0.03 gpl for the sodium alkyl benzyl sulphonate (SABS) and 0 - 2.5 gpl for sodium lauryl sulphate (NaLS). The typical level of surfactant in a commercial washing powder is 14% by weight. If a 0.5 g sample was dissolved in water (100 ml) of which 20 ml was hydrolysed and diluted to 100 ml., a test sample of 5 ml of this solution diluted to 50 ml would be 0.048 gpl. in SABS. The effect of the surfactant increased with concentration until a minimum value for the wave height was achieved. All the methods were affected thus except for the method where the test sample was 50% acetone where neither NaLS nor SABS affected the wave height. Table I summarises these results and Figures 46 and 47 illustrate the effect. One of the methods using a reagent of mixed molybdate and vanadate gives a more complex wave where the height of the fourth peak at - 0.02 v. is only slightly affected by the increasing concentration of SABS (Figure 48) or NaLS.

Table 1. Summary of the effect surfactant has on the voltammetric wave of a 12-HPA.

Medium	Surfactant	Conc. at which min. effect is observed (gpl)	% Suppression at this point
100% Water	SABS	0.008	60
100% Water	NaLS	1.150	70
50% Acetone	SABS	-	0
50% Acetone	NaLS	-	0
20% Ethanol	SABS	0.012	20
40% Ethanol	SABS	-	0
100% Water[1]	SABS	0.008	95[3]
100% Water[1]	NaLS	0.001	95[3]
10% Acetone[2]	NaLS	1.150	50
10% Acetone[2]	SABS	0.030	75
100% Water[1,4]	SABS	0.010	75

Figure 46. Wave height due to 12-MSA derived from 2×10^{-4}M silicate in the presence of increasing surfactant concentration.

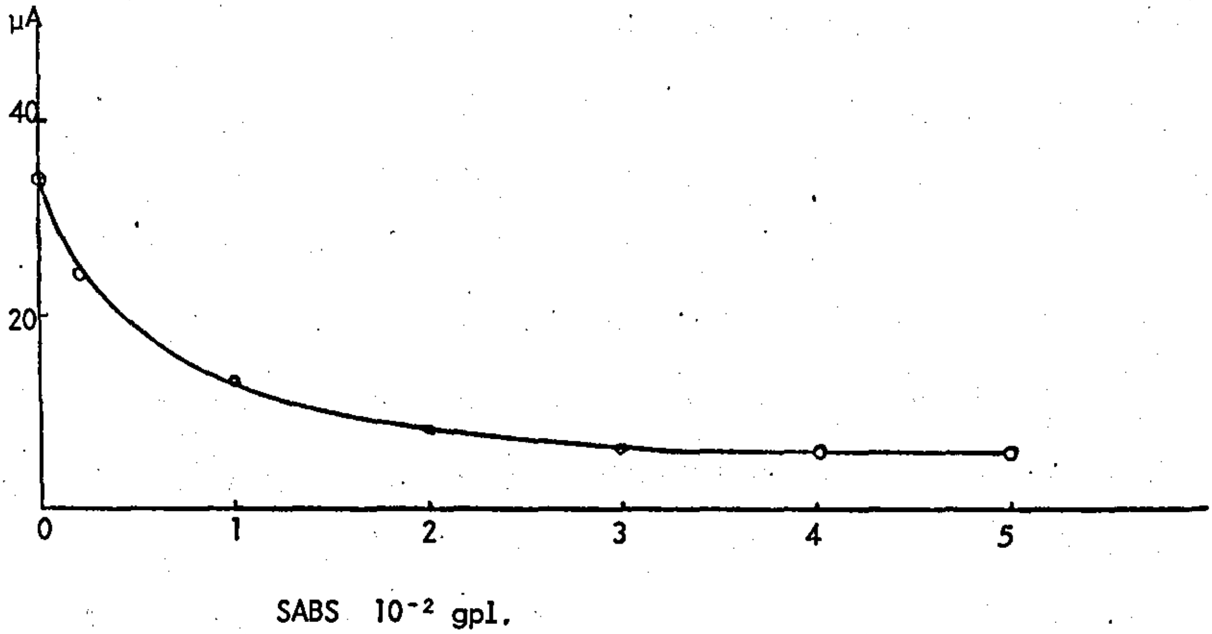

Figure 47. Wave height due to 12-MPA derived from 6×10^{-4}M phosphate in the presence of increasing surfactant concentration.

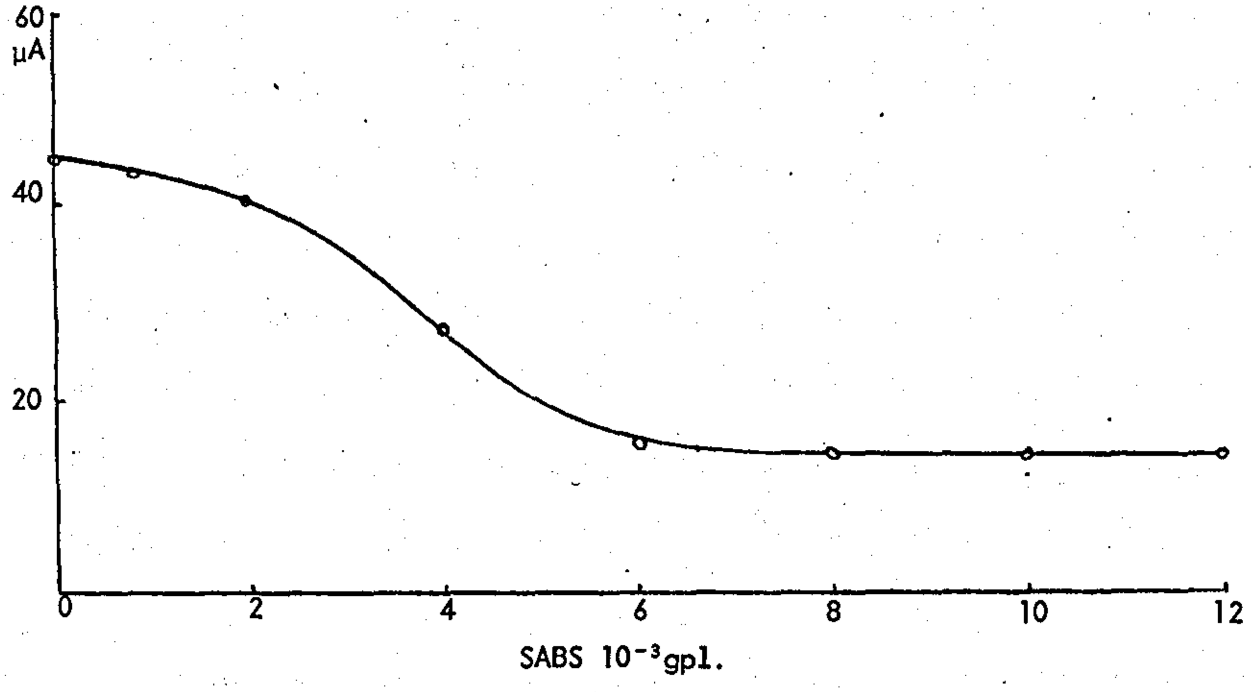

Figure 48. Voltammetric wave of 12-molybdovanadophosphate. (3×10^{-4}M PO_4).

(i) No suppression

(ii) Maximum suppression

(iii) reagent blank

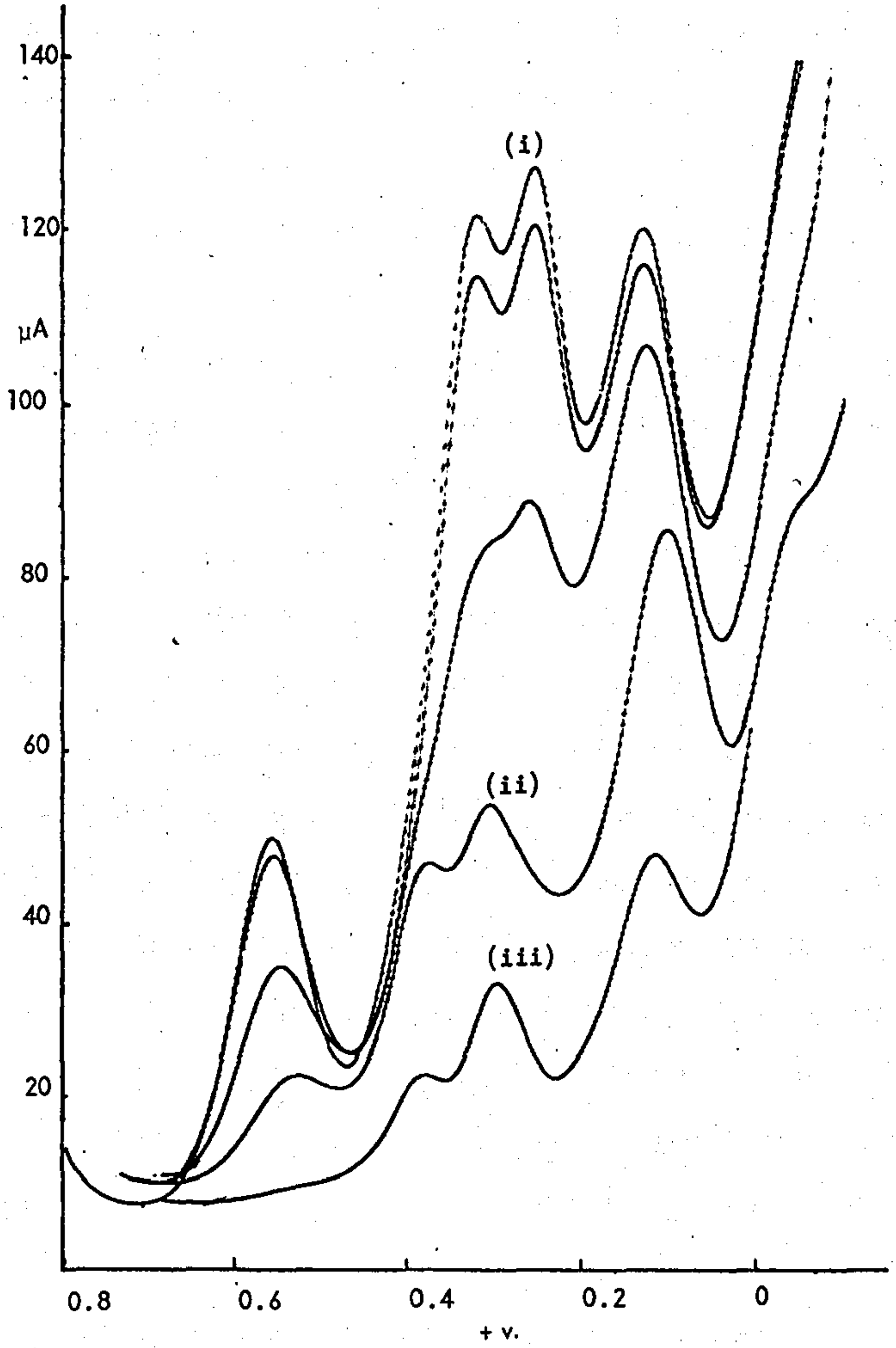

Figure 49. Voltammetric wave for 12-molybdovanadophosphate in 40% Ethanol/water. (Surfactant present without suppression).

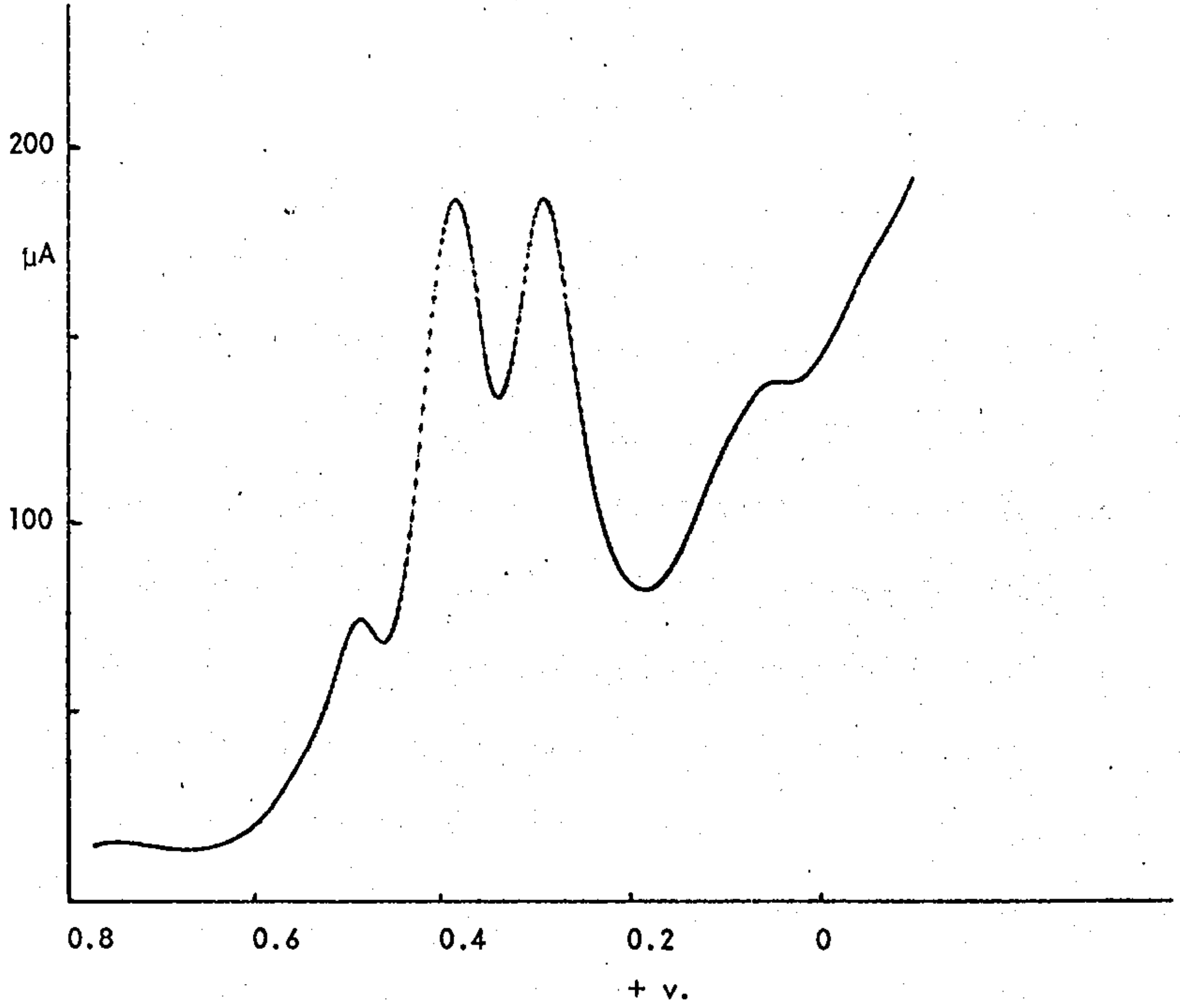

Notes: In all cases the heteropoly acid was 12-molybdpphosphoric except for

1. 12-molybdovanadophosphoric acid and

2. 12-molybdosilicic acid.

3. The first three peaks of the wave are reduced by 95%, the fourth peak by only 40% (SABS) and 30% (NaLS).

4. Normally the test solution is scanned from + 0.8 to 0.2 v. In this case the scan was in the opposite direction. The wave is quite different (Figure 49).

Surfactant was added before and after the formation of the heteropoly compound. The height of the resultant wave was the same in each case. The wave produced in the presence of surfactant has a variability of 2.3% in totally aqueous conditions and 0.38% in 50% acetone.

2.a. Other interferences.

Another constituent of washing powders, sodium perborate, was also found to suppress the wave of a heteropoly acid. In 100% aqueous solution the presence of perborate did not suppress the wave until a level of 0.05 gpl was attained. At higher concentrations the wave is completely suppressed (2.5 gpl) (Figure 50). In the presence of organic solvents (acetone or ethanol) no suppression was observed, sodium perborate is approximately 25% by weight of commercial washing powder. EDTA is also present (> 1%); it was not found to affect the results of silicate and phosphate analysis.

3. The effect of solvent concentration.

The method with a sample solution which was 50% acetone/water was the only determination not to be affected by the presence of surfactant. Thus the modification of other methods was carried out.

Figure 50.

Wave height due to 12-MVPA derived from 6×10^{-4} phosphate in the presence of perborate.

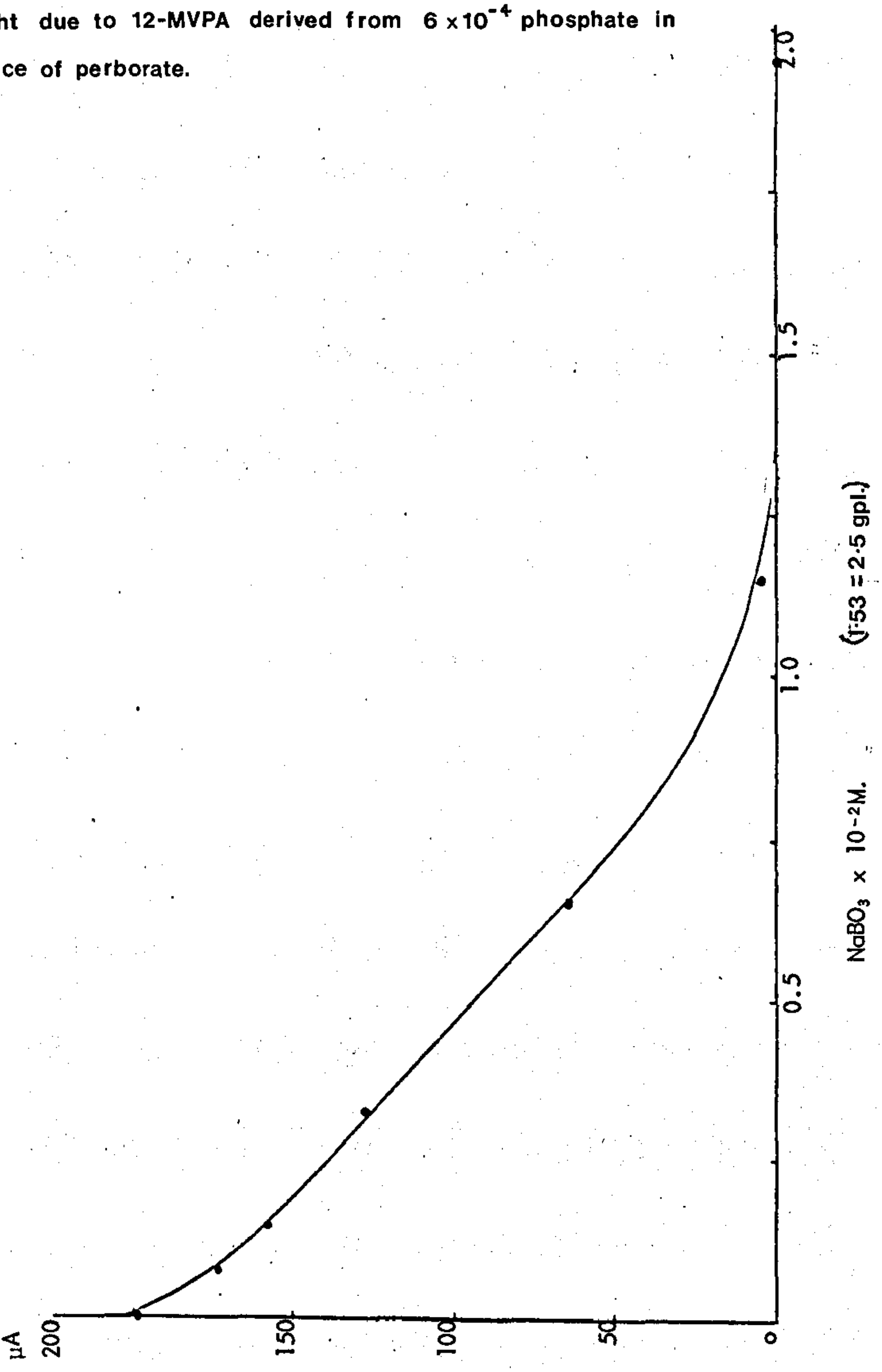

The first to be modified was the 10% acetone method for silicate (Fogg et al 1981 b). The level of acetone in the final test solution was varied from 0 to 50% for silicate samples containing just silicate and silicate plus surfactant. The object was to find how much solvent was required to nullify the suppressing effect of the surfactant. The potential use of ethanol and n-propanol was also studied, the results are given below.

Table 2. Phosphate.	% solvent required to negate surfactant effect.
Acetone	20 and above
Ethanol	40 and above
n-propanol	40 and above
Silicate	
Acetone	35 - 45
Ethanol	46 - 48

3a. Solvent effect on wave shape.

It was observed that when the ethanol concentration of a phosphate test sample was varied, the resultant wave was also altered, the first peak being strongly increased at 10% ethanol then gradually reduced through to 50% ethanol. The second peak gradually increased to a more or less constant level at 50% ethanol, and the appearance of a third peak from 40% ethanol. These variations are shown in figure 51 and 52 depicting the change in ethanol concentration and the wave height due to the heteropolyanion with and without surfactant present. Similarly the variation of acetone concentrations alters the wave, the first peak being almost completely absent at 50% acetone with the

Figure 51. Waves of 12-MPA prepared from 3 x 10^{-4}M phosphate in (a) 100% aqueous (b) 20% acetone and (c) 50% acetone solutions.

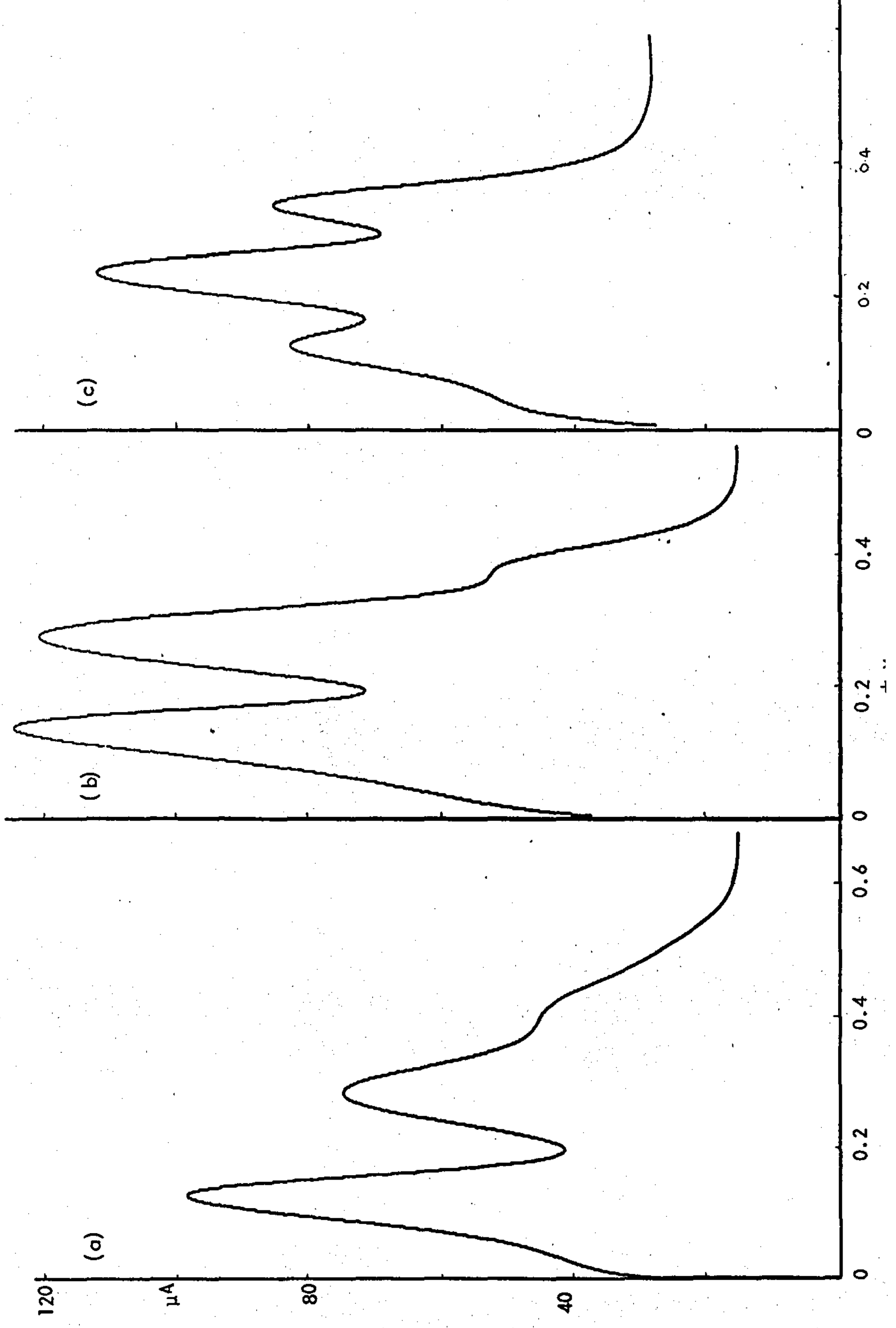

Figure 52. Effect of ethanol concentration on the differential pulse voltammetric peaks of 12-molybdophosphate and on the suppression of the action of sodium alkylbenzenesulphonate.

orthophosphate concentration = 6×10^{-4}M

sodium alkylbenzenesulphonate concentration = 0.02 gl^{-1}

(curves B and D only)

A and B. Peak at +0.14 V, dominant in aqueous solution.

A without detergent, B with detergent.

C and D. Peak at + 0.23 V. C without detergent, D with detergent.

Figure 53. Effect of acetone concentration on the differential pulse voltammetric peaks of 12-molybdophosphate

orthophosphate concentration = 6×10^{-4}M

A. Peak at + 0.14v.

B. Peak at + 0.23v.

C. Peak at + 0.32v.

Figure 56. Effect of ethanol concentration on the differential pulse voltammetric peak at + 0.28 V of 12-molydosilicate and on the suppressive action of sodium alkylbenzenesulphonate.

silicate concentration = 3×10^{-4}M

sodium alkylbenzenesulphonate concentration = 0.020 g l^{-1}

(curve B only)

A without surfactant, B with surfactant.

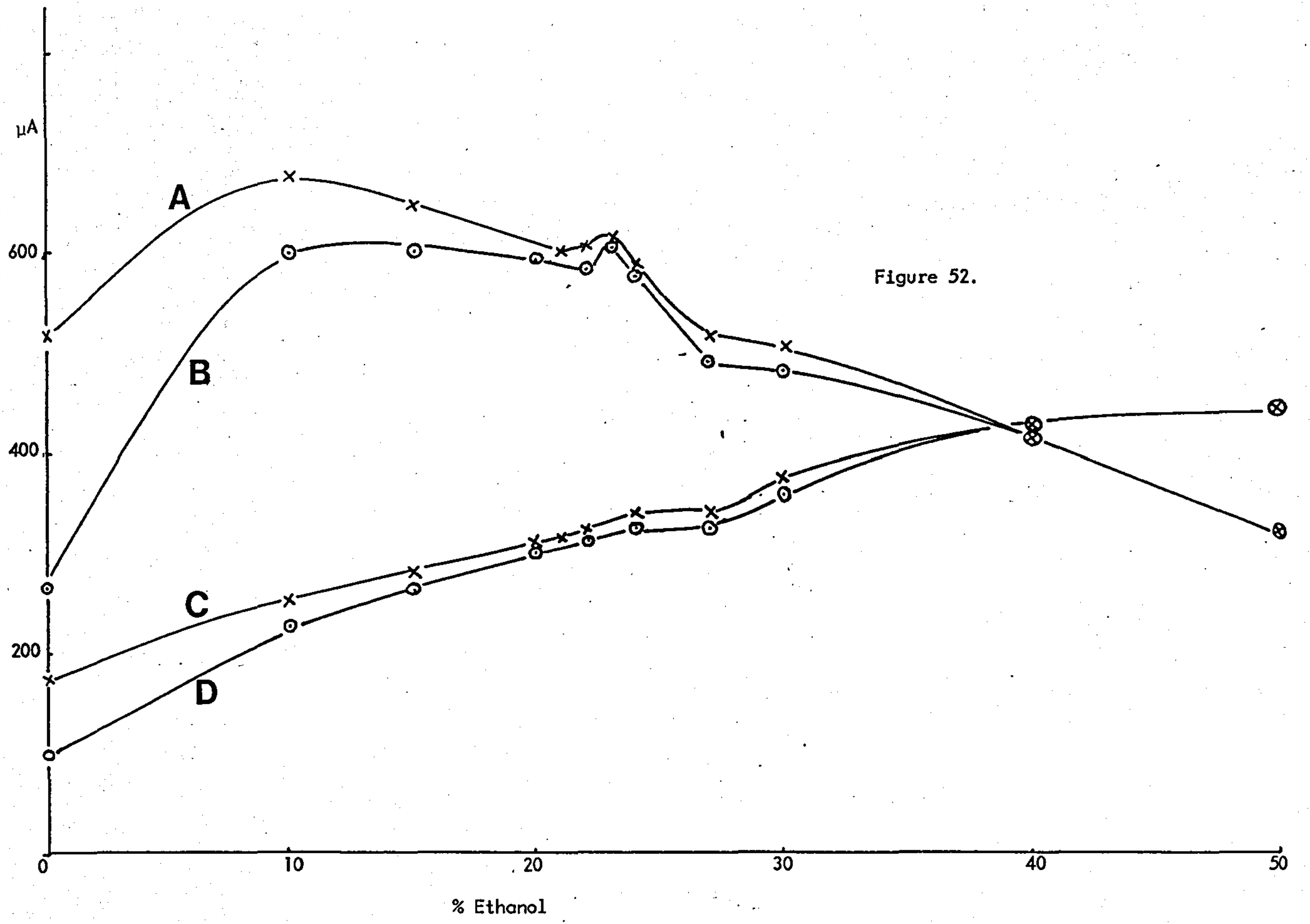

Figure 52.

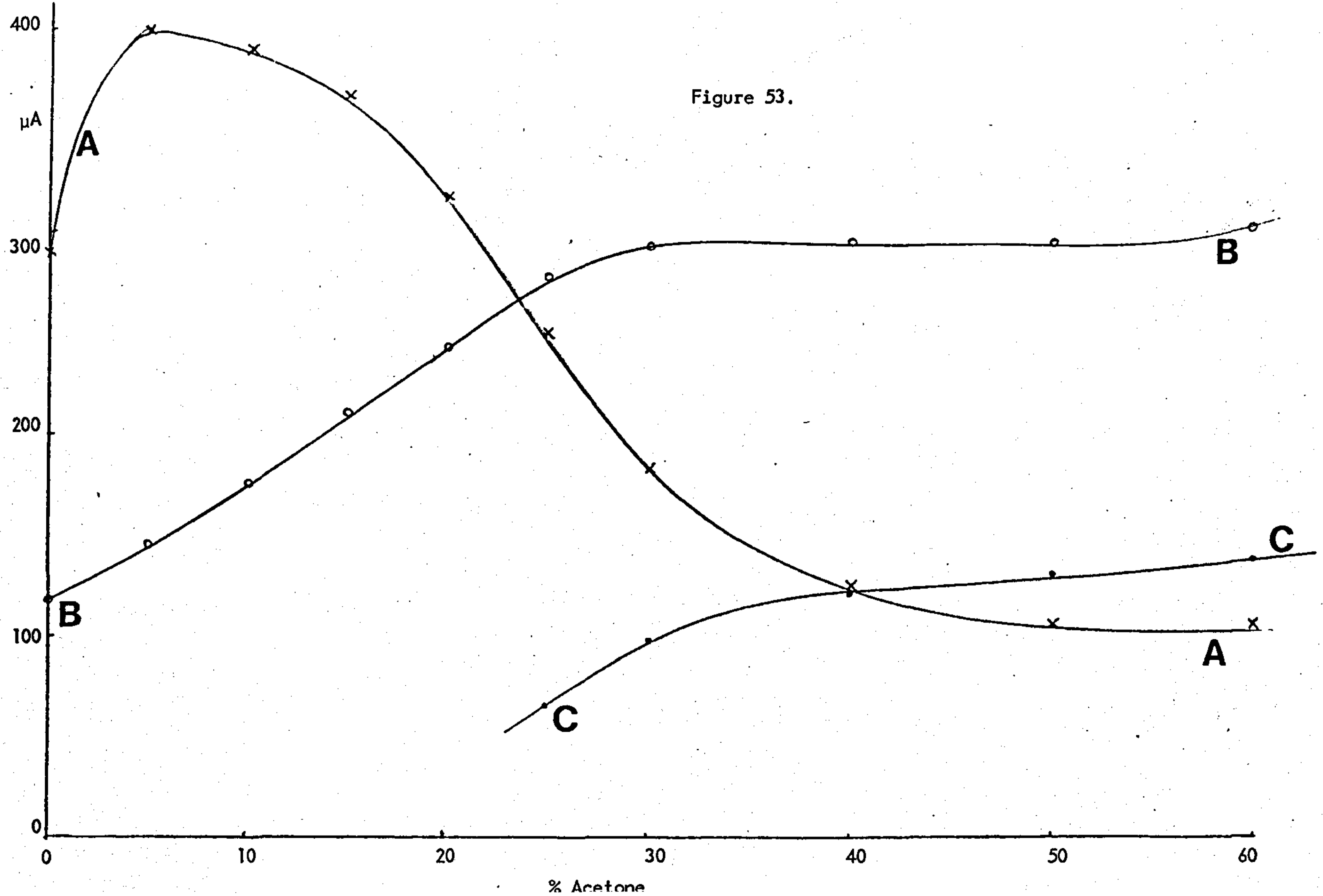

Figure 53.

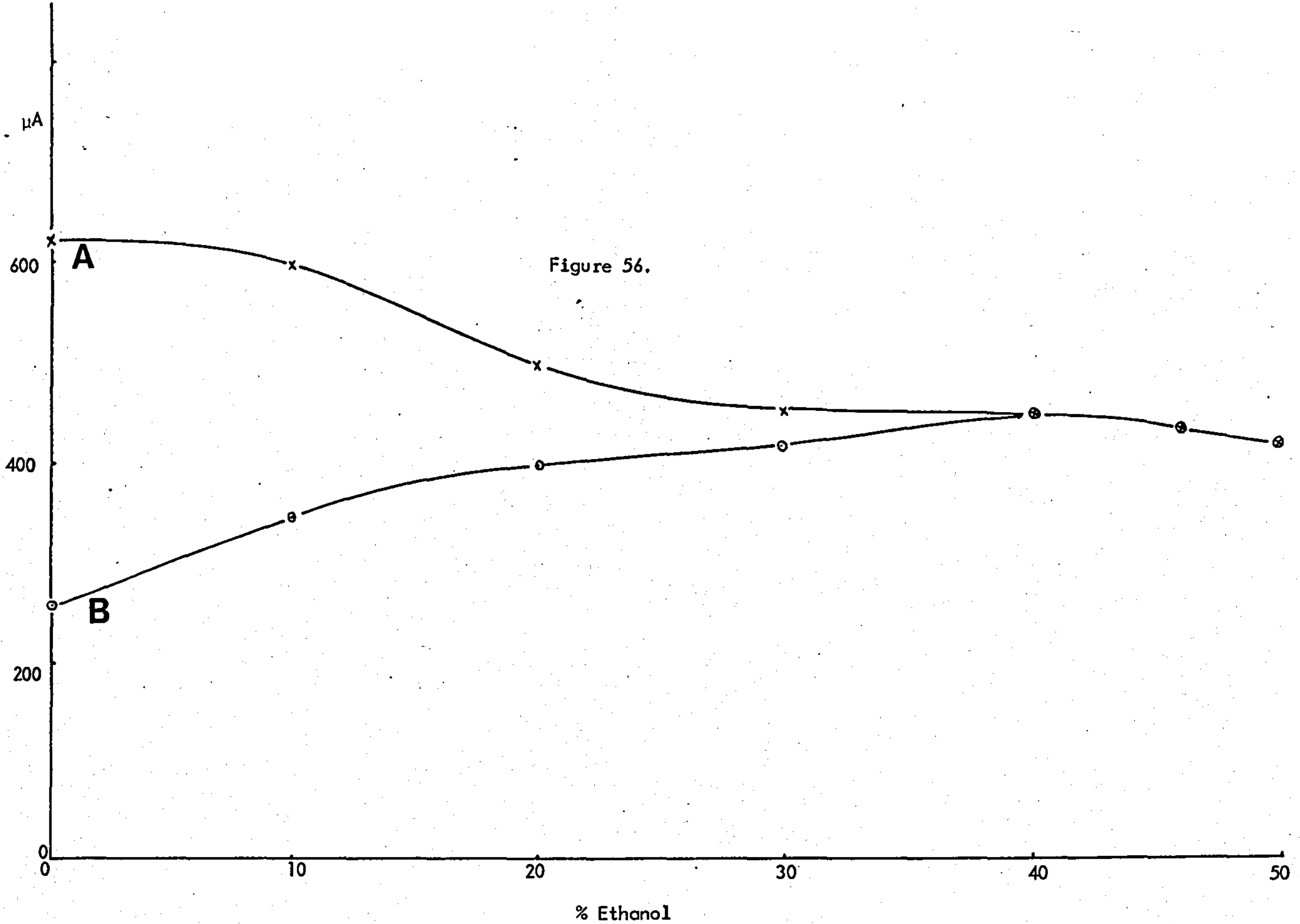

Figure 56.

growth of a third peak from 25% upwards. The second peak is very reduced under 100% aqueous conditions (see Fig. 53). The graph of ethanol behaviour shows a discontinuity at 22 - 23% ethanol, a closer examination of the range 20 - 24% ethanol was carried out to show a break in the curve at 22.4% (Figure 54). Acetone does not exhibit this effect.

The waves for silicate gradually change through the basic shapes as acetone increases in concentration (see Figures 55 a, b, c and table 3). In the presence of surfactant the wave gradually increases in size until its suppressing effect is overcome (Figure 56). The curve is smooth with no discontinuities.

3b. Summary.

The results show that the presence of an organic solvent in the test solution radically changes the shape of the voltammogram for phosphate determinations but not for silicate. The current peaks of the wave are summarised below.

Table 3. Current peaks of voltammograms of heteropoly anions derived from phosphate and silicate.

Anion	Solvent	Current peaks (+ v. unless otherwise shown)			
12-MPA	H_2O	0.14(s),	0.31 (m)		
"	50% Ac_2O	0.14(w),	0.23 (s)	0.32 (w)	
"	50% EtOH	0.14(m)	0.27(s)	0.37(w)	
"	50% nPrOH	0.15(w)	0.26(s)	0.36(w)	
12-MSA	H_2O	0.1(m)	0.25(s)	0.36(m)	
"	50% EtOH		0.24(s)	0.30(m)	
12-MSA	30% Ac_2O		0.23(s)	0.29(s)	0.45(w)
"	50% Ac_2O	0.20(s)	0.28(m)	0.33(m)	0.45(w)
12-MVPA	H_2O	0.13(m)	0.24(s)	0.32(s)	0.56(w)$^+$
"	50% EtOH	0.05(w)	0.29(s)	0.38(s)	0.48(w)$^+$
12-MVSA	H_2O	0.17(m)	0.26(w)	0.36(m)	0.49(w)$^+$

(s) strong, (m) medium, (w) weak.

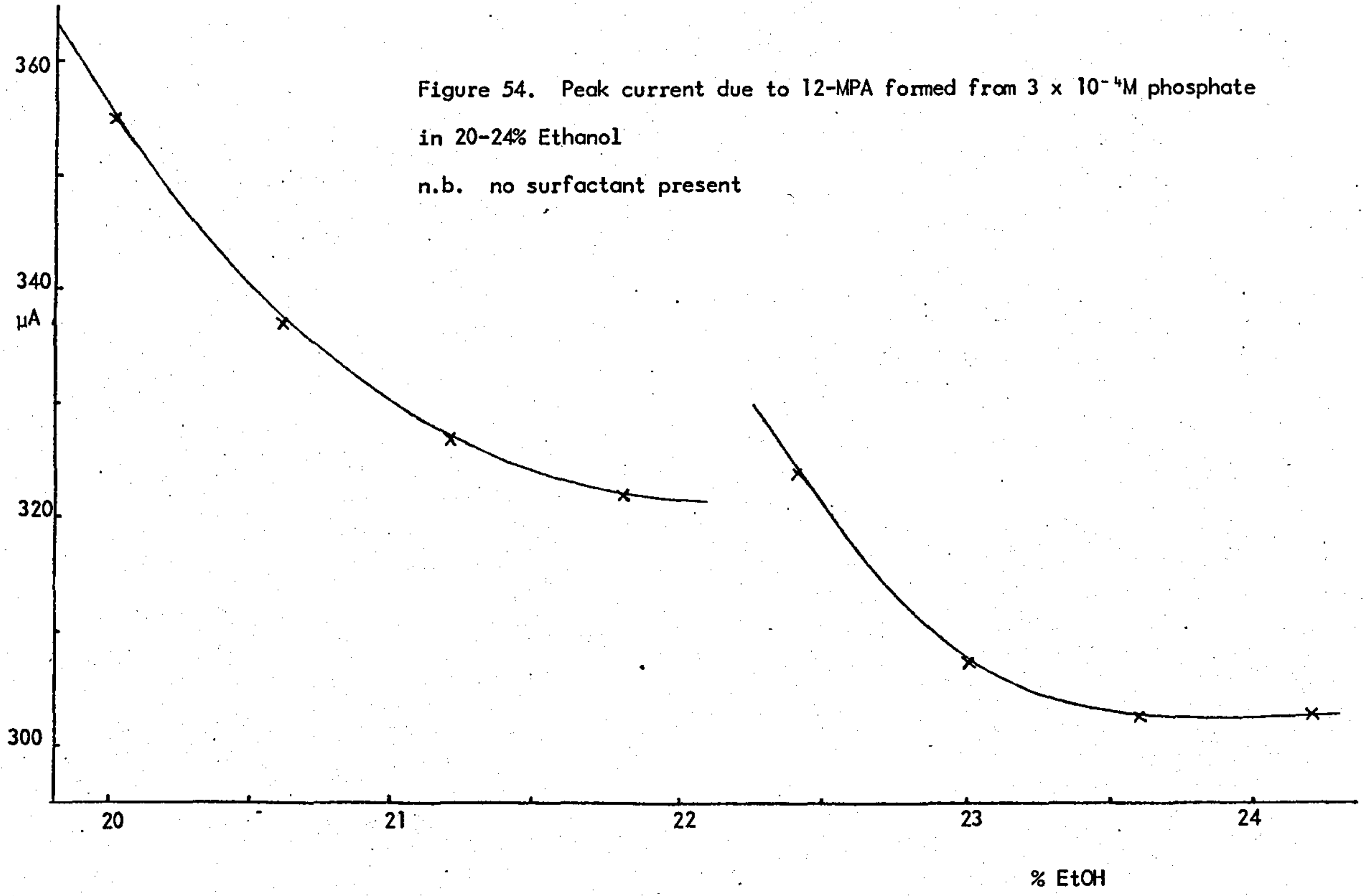

Figure 54. Peak current due to 12-MPA formed from 3 x 10^{-4}M phosphate in 20-24% Ethanol

n.b. no surfactant present

Figure 55. Wave of 12-MSA formed from 3 x 10^{-4}M silicate in various solvents.

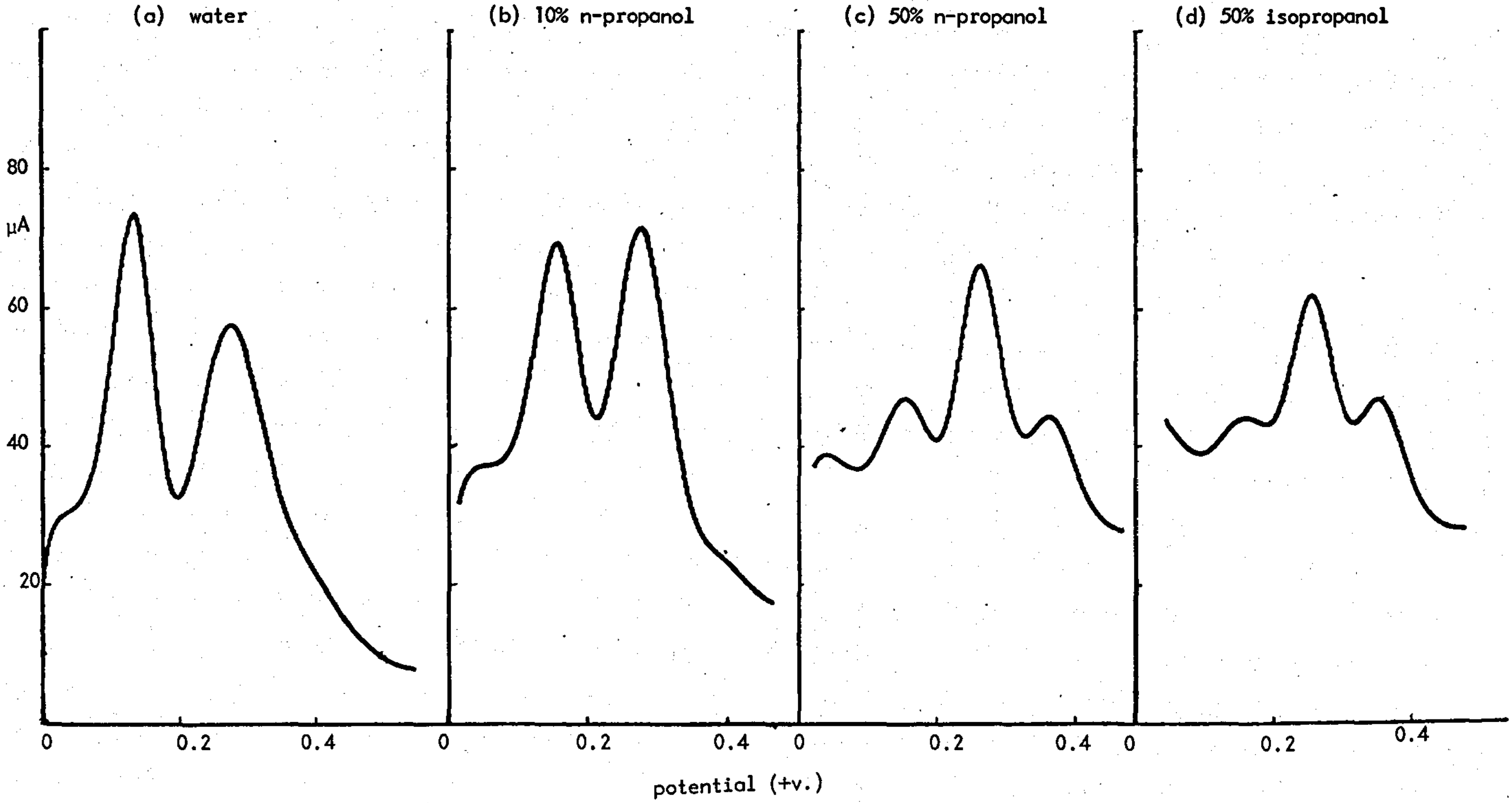

Note (+) These heteropoly anions were prepared from the molybdovanadate reagent (Fogg et al 1981 c). All the waves were recorded by differential pulse voltammetry.

3c. Application of the Revised determination.

The methods of Fogg et al (1981b) for the determination of silicate and phosphate were modified, so that the test solution for phosphate was 40% ethanol and 47% ethanol for silicate. Samples of washing powder were analysed for soluble silicate and total phosphate. The results were in good agreement with the figures for routine colorimetric analyses by Unilever Research (see table 4, section 4a). The calibration curves at 10^{-5}M or lower levels were rectilinear, but at higher concentrations the calibration slopes gradient tailed off towards the end of the range (see fig. 57). The lowest concentration at which a reproducible silicate determination could be made was at 10^{-6}M. The limit of detection is 10^{-7}M for phosphate. The coefficient of variation was 2.5% for the phosphate method and 2.2% for the silicate method. Both figures were arrived at from six separate determinations. The full methods are described later in the experimental section.

4. Flow Injection Analysis.

The methods just described were converted into flow injection techniques.

4a. Preformed flow injection.

A very simple flow system was set up to investigate the behaviour of the detector. The heteropoly anions were prepared as for the static method (see section 3c) and injected into a stream of electrolyte (0.005M H_2SO_4) and detected at a wall jet electrode. The conduit from the injection valve to the detector cell was kept as short as possible (15 cm) to reduce response time and thus keeping dispersion to a minimum

Figure 57. Calibration curves for silicate by static voltammetry at 0.14v.

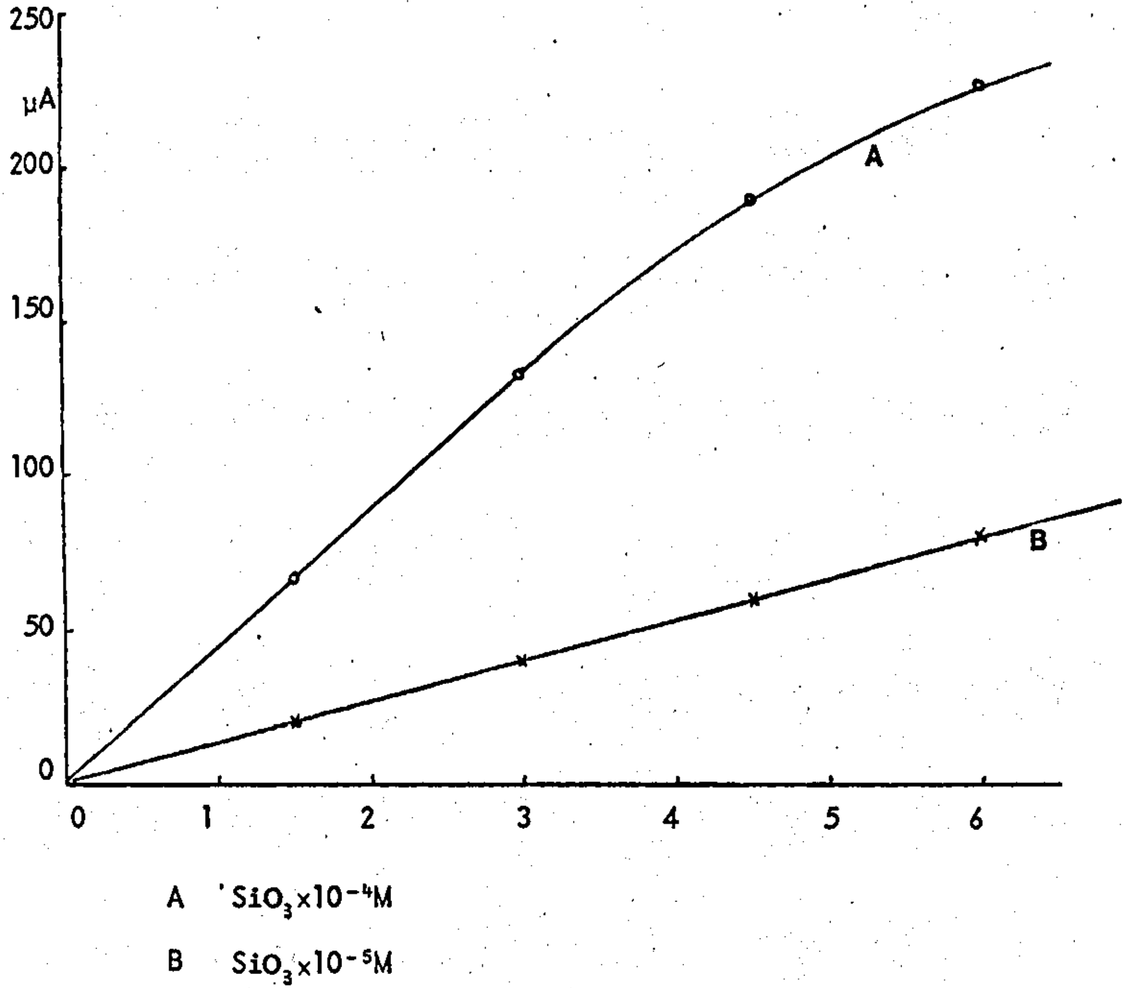

(Fig. 58 below)

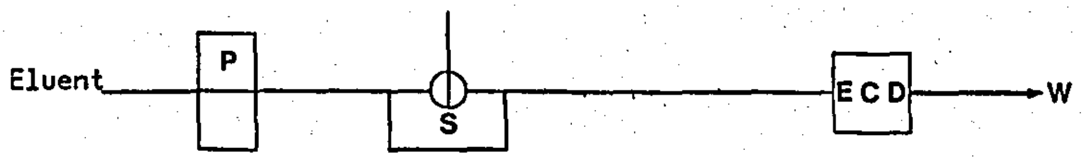

P. Pump
S. Sample Injection
W. Flow to waste
ECD. Electrochemical Detector

Figure 58. Simple Flow Injection System.

The first requirement was to determine the most convenient potential at which to detect the heteropoly species. Injections were made of test solutions derived from 3 x 10^{-4}M phosphate and 2 x 10^{-4}M silicate at potentials from 0 to + 0.5 v. Figures 59 and 60 show the results compared to injections of blank reagent. The figure for phosphate injections shows a plateau between 0.14 and 0.18 v, recording a current of ≈ 15 μA. A small plateau is seen for silicate followed by a steady decrease in the signal from 23 μA at 0.1 v to 0 at + 0.45 v. Determinations of phosphate and silicate in washing powder were carried out by preformed injection detecting at + 0.15 v. The results showed a good comparison with the colorimetric method and an increase in reproducibility compared to the static method.

Figure 59. Current signal due to injections of preformed 12-MPA into a stream of 0.005M H_2SO_4 at increasing potentials.

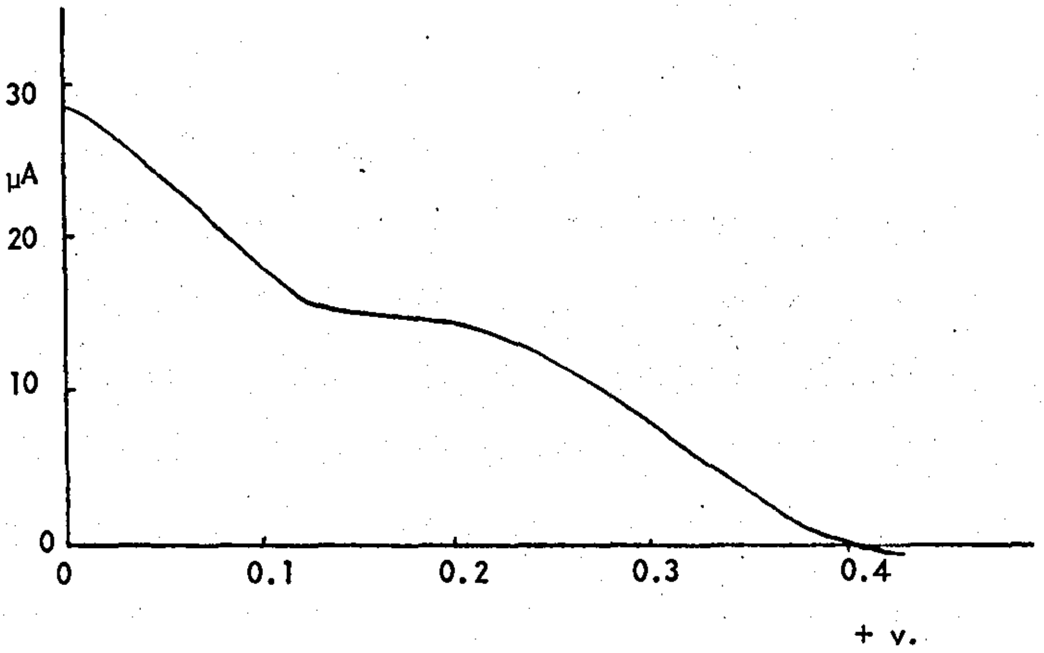

Figure 60. Current signal due to injections of preformed 12-MSA into a stream of 0.005M H_2SO_4 at increasing potentials.

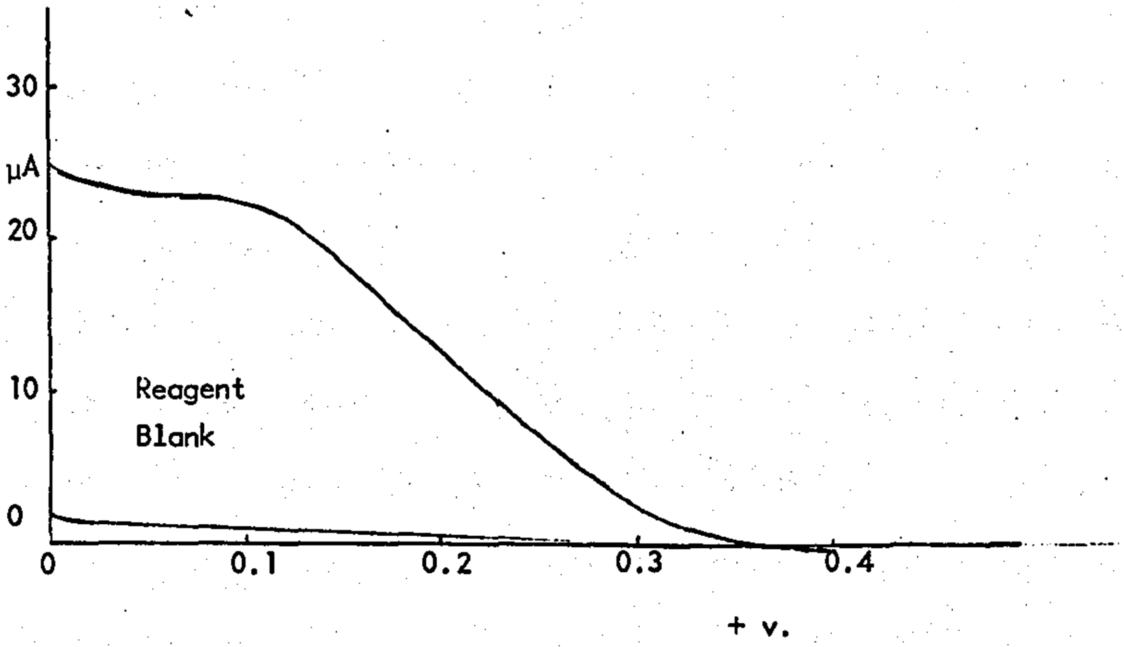

Table 4. Washing powder analysis by the preformed injection method. and static DPP method.

(a) phosphate as % P_2O_5 $^m/_m$

sample	Static	Preform.	Colourimetric.
B	19.7	19.8	19.9
C	18.6	18.2	18.6
D	18.1	18.1	18.5
F	9.6	9.6	9.0

(b) Silicate as % SiO_2 $^m/_m$

sample	Static	Preform.	Colourimetric.
A	3.64	4.10	4.09
B	7.05	6.90	6.91
E	3.62	3.56	3.91
G	6.30	6.07	6.41

The coefficient of variability on six separate determinations for phosphate was 0.9% and 1.2% for silicate. Initially the carrier flow was generated by a gravity food system but this was superseded by a peristaltic pump. This resulted in a faster flow rate and a sharper response at the detector cell.

4b. Development of flow injection system.

A flow system was arrived at for direct injection of phosphate or silicate samples into a stream of reagent blank, which would react in a delay coil before being presented to the detector (see below).

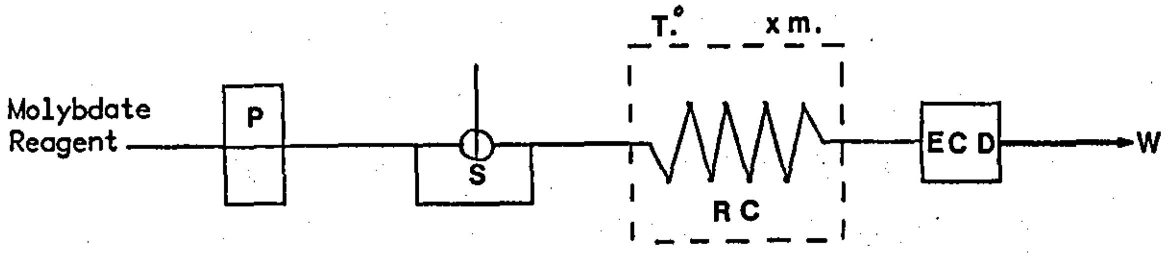

RC. Reaction Coil.

Figure 61. Flow injection system with heated reaction coil.

The flow rate at the detector for the simple system (see Fig. 59) with gravity feed was 3.1 ml/min. and with a Gibson minipuls 2 a maximum of 10.7 ml/min; in all cases the flow is measured with the loop in the stream. The injection loop severely restricts the flow rate; a maximum of 22.2 ml/min was achieved with the injection loop bypassed. For most of the work an "Ismatec Mini S" peristaltic pump was used. When used with a delay coil (3m x 0.58 mm) there was a flow rate of about 3 ml/min. at the detector.

The flow [illegible] of the stream affects the response at the detector. Fast speeds are preferred giving sharp traces and the most stable base line. The slower the flow rate the broader the response band is. More dispersion occurs as the sample bolus is in the coil for longer periods. The rate of flow will drop off when the pump manifold tube begins to wear out, the tube becomes permanently misshapen.

With the pump employed noise due to pulsing was minimal. The appearance of bubbles in the stream, another source of noise, is obviated by degassing at a water pump.

This is more important if the reaction coil is heated. In the preparation of the carrier stream the mixing of organic solvents with water often causes a good deal of effervescence. The use of the low pass filter on the polarograph will also dampen a noisy trace, at 0.3s the filter reduces the signal by less than 1%.

Solutions of 3×10^{-4}M phosphate and silicate were injected and gave the following current values at different settings of the low pass filter (LPF),

LPF s^{-1}	Signal µA	
	PO_4^{3-}	SiO_3^{2-}
0	12.6	3.75
0.3	12.5	3.55
1.0	12.1	3.4
3.0	9.4	2.5

N.B. The use of 3m heated reaction coil for silicate, phosphate at R.T. The choice of peristaltic tube also affected the level of signal noise. The tubing coded blue/blue (2mm i.d.) proved to be the best with a minimum response (injection-signal time) of 12 seconds, using the system in Figure 61, having less noise than the tube coded purple-white (4mm i.d.) (min. response 7 secs.), and a lower response time than the white-orange tube (1mm i.d.) with a response of 27 seconds.

The reaction coils used were made of Teflon and 3 - 6 m in length with an i.d. of 0.58 mm, a small i.d. is required to keep dispersion to a minimum. The coil is immersed in a water bath at 60° or room temperature.

4c. Development of flow injection analysis of phosphate.

Initially phosphate samples were injected in a stream which consisted of blank reagent, i.e. 10 ml of acid molybdate (2% ammonium molybdate in 2.5M H_2SO_4) diluted to 100 ml with distilled water. For actual determinations the stream was 40% ethanol/water and acid molybdate (10 ml). However consecutive work by Fogg and Bsebsu (1982) found that the optimum coil length was 3m. The same workers varied the acid and molybdate level in the carrier stream, finding 0.11M H_2SO_4 was the most effective level for the acid and 0.2% $^{w}/_{v}$ ammonium molybdate. The change in acid concentration is described in Figure 62, showing a maximum at 0.1M. Injections of hydrolysed washing powder samples were made into a stream of 10% Acid Molybdate reagent, 40% Ethanol and 50% distilled water to give results comparable to colorimetric methods, using a 3m reaction coil at room temperature (Table 5). Rectilinear calibration was obtained at the 10^{-5}M and 10^{-6}M level. At higher concentrations the calibration graphs were seen to have a "dog-leg" shape, both halves being linear (see Figure 63).

Table 5. Flow injection determination of phosphate at 0.15 v. as % $^{w}/_{w}$ P_2O_5

Sample	Colorimetric Determination.	Flow injection analysis.
A	22.3	22.8^{+}, 22.1
C	18.6	19.1
D	18.5	18.6, 18.3, 18.8^{+}
F	9.0	10.4, 9.6, 9.5, 9.6^{+}

+ final test solution 10^{-5}M w.r.t. phosphate, all others 10^{-4}M.

In an attempt to increase the sensitivity of the method the reaction coil was held at 60° in a water bath. It was estimated

Figure 62. Current due to 3 x 10^{-4}M silicate at + 0.15v with varying levels of sulphuric acid.

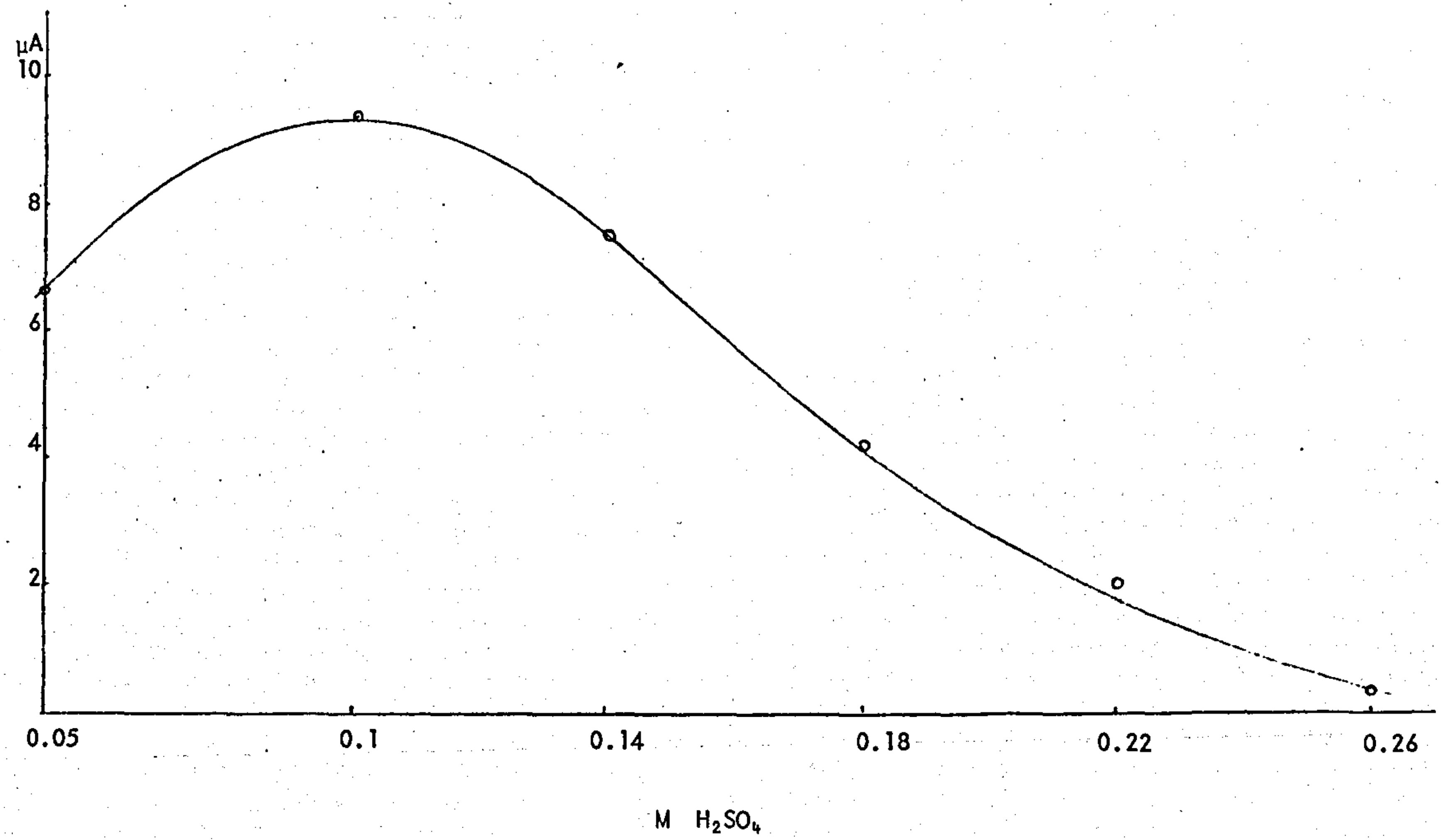

Figure 63. Calibration curves for phosphate FIA at + 0.15v.

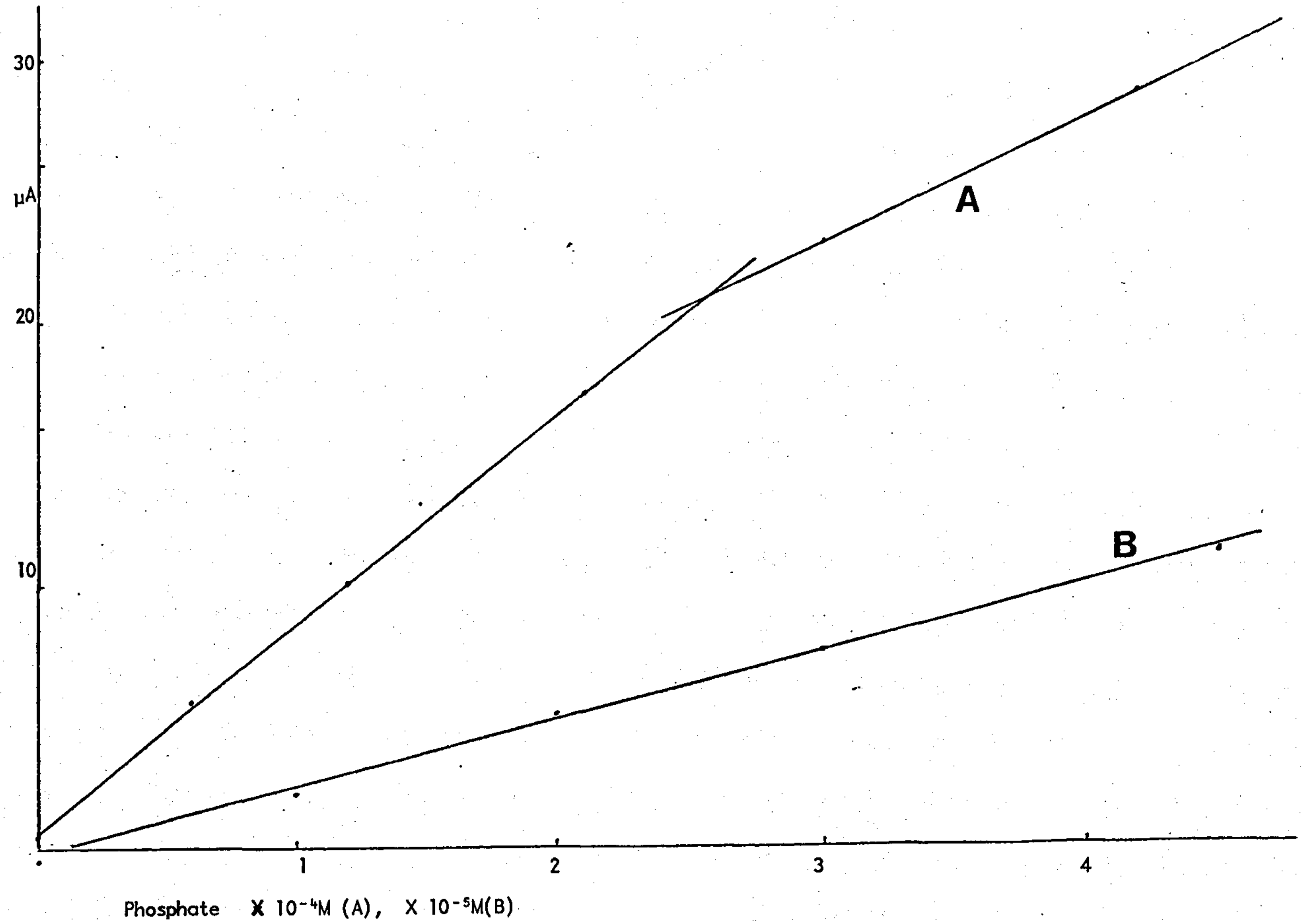

that only 64% of the phosphate was reacting in the coil. The current due to formation of 12-MPA from an injection of 0.1 ml 3 x 10^{-3}M phosphate was 12.6 µA with the reaction coil at room temperature and 20 µA with the coil at 60°. In injection of preformed 12-MPA yielded a current of 31 µA with the heated coil. Some improvement was achieved by lengthening the reaction coil to 6m at 60°C. This resulted in 27 µA compared to the preformed value of 30 µA. However the longer the coil is the less applicable it becomes, as in washing powders the silicate will react sufficiently to interfere with the signal for the phosphate. Injecting 3 x 10^{-5}M phosphate into 6m of coil at 60° could tolerate a maximum of 1.5 x 10^{-6}M silicate present in the test solution. Table 6 compares variations in the flow system for phosphate analysis.

The static voltammetric method includes tartaric acid in the test sample to prevent the formation of 12-MSA. In washing powders the use of tartaric acid is not required in the direct injection mode. The silicate is not concentrated enough to interfere. A reagent stream containing 0.25% tartaric acid reduces the signal by 30% and the signal noise compared to the reagent stream without tartaric acid. The limit of detection using tartaric acid in the reagent stream is 3 x 10^{-6}M. Using tartaric acid means that higher levels of silicate can be tolerated (x 10), however such an excess of silicate is not likely in washing powders.

Fogg and Bsebsu (1982) varied molybdate and acid concentration in the carrier stream of their phosphate FIA method.

Table 6. Variations in the flow system for the analysis of phosphate.

System	Conditions		Molarity M	Coefficient of variation	Current µA
Static (DPP)	-	22°	3×10^{-4}	2.5	245.0
Preform FIA	No Coil	22°	3×10^{-4}	0.9	17.3
"	3m coil	60°	3×10^{-4}	-	31.0
"	6m coil	60°	3×10^{-4}	- +	30.0
Direct FIA	3m coil	22°	3×10^{-4}	1.68	12.6
"	"	60°	3×10^{-4}	1.58	20.0
"	"	22°	4.8×10^{-5}	0.86	2.6
"	"	60°	4.8×10^{-5}	2.34	4.4
"	6m coil	60°	3×10^{-4}	2.77+	27.0
"	"	60°	3×10^{-5}	1.19	3.4
"	"	22°	3×10^{-4}	- +	13.4

+ Peak broadening

It was proposed in this case to use a 40% EtOH instead of 100% aqueous carrier stream the experiments were repeated with slightly different results.

Table 7. Injections of 3×10^{-4}M Phosphate.

Stream conditions	Molarity H_2SO_4	Current μA.
100% aqueous	0.10	16.0
40% EtOH	0.10	4.1
40% EtOH	0.12	17.0

Table 8. Variation of acid and molybdate concentration in the FIA stream for phosphate analysis.

% reagent in stream	H_2SO_4 M	Current μA.
10	0.1	16.5
10	0.11	17.9
10	0.12	18.5
12	0.12	15.4
12	0.13	16.3
12	0.14	16.5
13	0.15	17.5
15	0.17	18.5
20	0.2	17.5
20	0.24	17.5

N.S. 0.1 ml injections of 3×10^{-4}M phosphate with 3m reaction coil at 60 and reagent is 2% acid molybdate

Increasing the molybdate reagent resulted in a sloping baseline, but little increase in current. By adding an extra 1 or 2 ml of 2M H_2SO_4 the baseline is stabilised and some increase in reaction is observed. These results were used when considering the constitution for the reagent stream of the final method (see experimental section) suitable for both silicate and phosphate determinations. The effect of organic solvents to remove suppression of the signal by surfactants also applies to the direct injection mode. No suppression is found if solvent streams of 40% EtOH/water are used. At lower concentrations of ethanol suppression is observed to a lesser extent than with the static system. In 100% aqueous conditions the static method is suppressed by 44% in the FIA mode only 29%.

4d. Development of a flow injection method for silicate.

Initially, silicate samples were injected into a stream of blank reagent from the static method. However very little reaction was observed so the reaction coil was heated to promote sufficient reaction for an analytical method. At room temperature with a 3m reaction coil, the signal from an injection of 3×10^{-4}M silicate was 1.4 µA, at 3×10^{-5}M the signal was totally due to water. Changing the constitution of the reagent stream, i.e. increasing the molybdate concentration or using organic solvents (e.g. 40% EtOH or 50% Acetone) had little effect at room temperature.

The reaction coil was held at 60° in a water bath and an injection of 3×10^{-4}M silicate resulted in a signal of 4.6 µA. This was then repeated holding the bolus of sample in the reaction coil for 2 minutes. An unreliable signal in the range 7 – 10µ A was obtained. The reagent stream used 10 ml in 100 ml water of 2% reagent as the 4% reagent gave an unstable baseline signal. Using a heated coil appeared to increase the noise in the baseline. This was reduced by employing the low pass filter of the instrument at setting 0.3s. The temperature of a 3m. coil was varied and the current resulting from an injection of 0.1 ml 3×10^{-4}M silicate is shown by the graph, Figure 64. The optimum length for the reaction coil was found to be 6m; an 8m coil gave a slightly higher current but the signal is broader and less reproducible, see below (table 9).

Table 9. Current due to 3×10^{-4}M silicate injections with varying of coil length at 60°.

Reaction Coil length	Current µA.
3m	4.65
6m	8.2
8m	8.5
11m	8.5

Table 10. Residence time in rotation coil compared to detector signal (µA)

Time in Coil, s^{-1}.	Current, µA.
65	9.5
40	8.45
29	6.05
23	3.6

N.B. Potential of detector, + 0.15 v.

Table 10 shows the increase in reaction against the time the sample bolus spends in the reaction coil. A compromise has to be found, maintaining a sharp response together with a suitably large current to enable an effective calibration group to be constructed, with gradient approximating to 1. In an attempt to increase the amount of reaction occurring, experiments were carried out with a coil prior

Figure 64. Current derived from injections of 3×10^{-4}M Si O_3^{2-} at increasing coil temperatures.

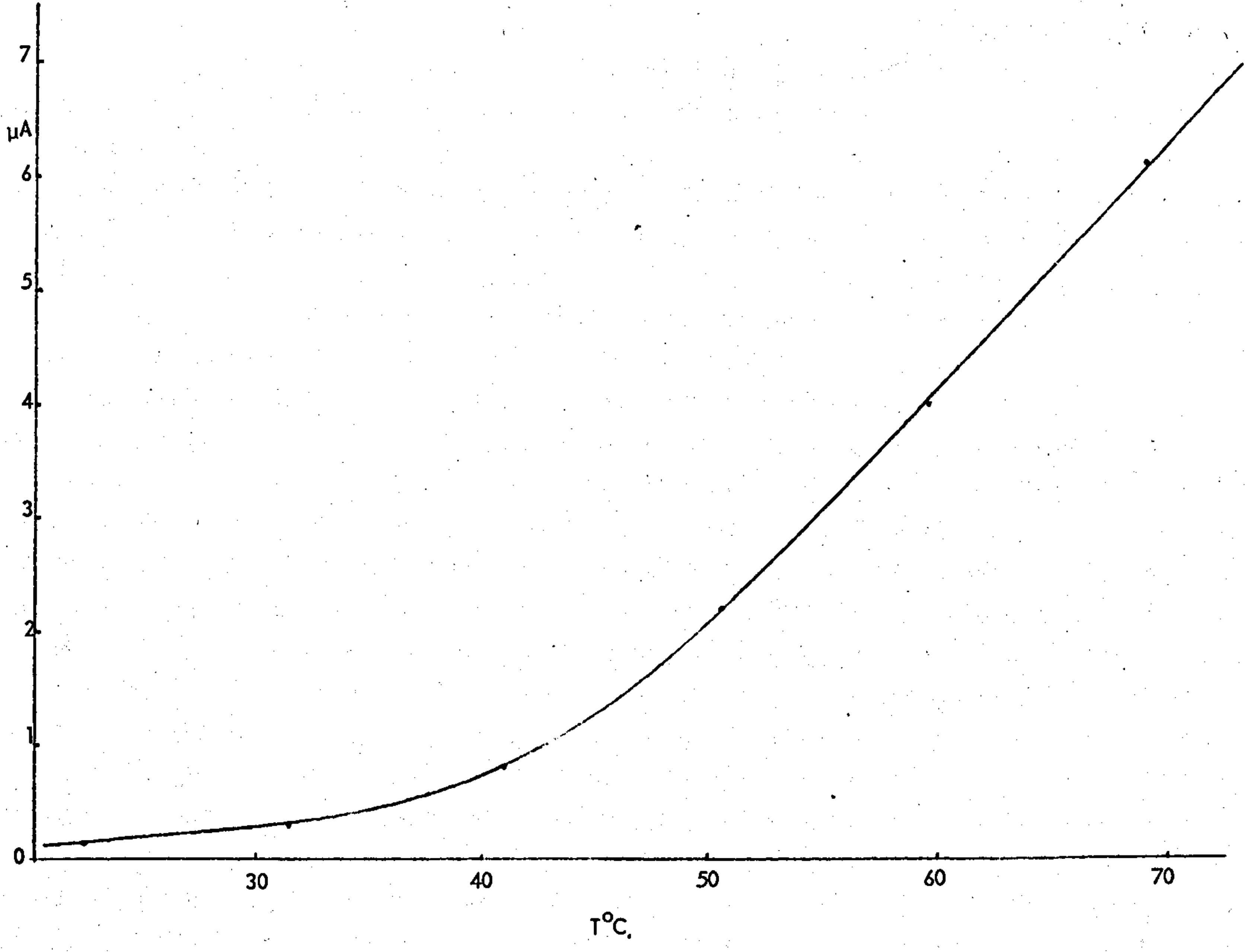

to the injection point in water bath at 60°. 0.5, 1 and 2m lengths of 0.58 mm i.d. tubing were used, currents of 4.68, 4.73 and 4.52 respectively were achieved compared to 4.65 with no pre-injection coil. This was taken as no significant improvement. It was estimated that 41% of of the silicate injected reacted in the 6m reaction coil at 60°C and 23% with the 3m coil. The preformed injection of supposedly completely reacted silicate gave a current signal of 20 μA and 19 μA for the 3m and 6m coils respectively whilst direct injections of silicate solution gave 4.65 and 7.8 μA. Rectilinear calibrations were obtained for 10^{-4}M and 10^{-5}M levels of silicate. The solution injected is 100% aqueous. The signal is only half as strong when injecting a 46% Ethanol solution into a stream which is 46% Ethanol, this effect was also noted with phosphate injections.

The signal at the detector was improved by changing the constitution of the reagent stream in the phosphate determination. A similar study was carried out using silicate injections. The results are set out in the following tables, 11 and 12. Increasing the molybdate reagent in the carrier stream

Table 11. Signal variation from injections (0.1 ml) of 3×10^{-4}M SiO_3 at different stream acid concentrations. (At 0.15 v and 40% EtOH).

Molarity of H_2SO_4	Signal μA.
0.26	0.35
0.22	2.00
0.18	4.20
0.14	7.75
0.10	9.75
0.05	6.6

Table 12. Signal variation from injections (0.1 ml) of 3 x 10^{-4}M SiO_3 at different stream molybdate concentrations. (At 0.15 v and 40% EtOH).

% molybdate reagent	Molarity of H_2SO_4	Signal µA.
10	0.10	9.75
12	0.12	10.20
13	0.13	10.40
15	0.15	11.20
20	0.20	11.10

although increasing the response the baseline was found to be noisier and the peaks are broader, i.e. dispersion is greater. The increase in the acid level of the stream stabilised the baseline which exhibited signal decay for low levels (0.05 and 0.1M). The presence of ethanol increases the signal for both phosphate and silicate. The signal produced by the heteropoly molybdate formed in a 3m coil at 60°C is increased by 27% for silicate and by 10% for phosphate.

4e. Silicate flow injection analysis in the presence of phosphate.

In the static method any heteropoly molybdate produced by phosphate present in the sample is destroyed by the addition of mannitol. A flow system including mannitol for this purpose was devised.

Figure 65. Flow injection system including a stream of mannitol for the removal of interference from phosphomolybdate.

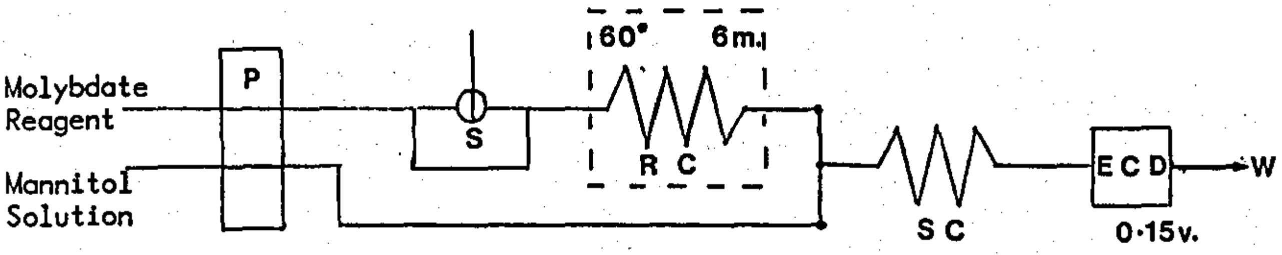

SC. Secondary Coil 2.1 m. at RT.

Flow rates:

Reagent Stream 2.7 ml/min.

Mannitol Stream 0.8 ml/min.

Flow rate at detector 3.4 ml/min.

The mannitol stream (10% w/v) converges with the reagent streams after the formation of the heteropoly molybdates. If the mannitol is included in the reagent stream no signal for the silicomolybdate is observed and the signal due to phosphomolybdate is reduced by 36%. If the coil after the convergence of the streams is heated the signal due to silicomolybdate is reduced. The system requires two separate pumps as the type employed cannot cope with two pump tubes of different diameter required to produce the different flow rates. The flow rate of the mannitol stream was minimised, as the dilution of the main stream would cause excessive reduction in the signal. The mannitol stream also contains ethanol at the same level as the reagent stream. If an injection of 0.1 ml 3 x 10^{-4}M PO_4 is made and the converging stream contains no mannitol then 11.1 µA of signal is recorded; increasing the concentration of mannitol in the converging stream reduces the signal to a constant value after which the signal is unaffected by increasing the level (see table 13 below).

Table 13. Mannitol (%) in converging stream and signal due to phosphomolybdate.

% Mannitol	Signal μA.
0	11.1
0.1	3.5
0.3	1.2
0.5	1.0
0.7	0.9
1.0	0.8
1.2	0.8
2.0	0.8
4.0	0.75
10.0	0.75

The dimensions of the second coil were optimised at 2.8 m in length and 0.8 mm i.d.. The internal diameter has to be greater than the conduits leading to the point of convergance to avoid an increase in back pressure. The length of the coil is the maximum before any substantial reduction in signal and increase in band width occurs. It is evident from the table above that the phosphomolybdate is never completely destroyed; stopping the flow with the sample bolus in the second coil for 3 minutes completely destroyed the phosphomolybdate. However a silicate signal similarly treated was reduced by 10% and the band showed increased dispersion. Hence reproducibility was also reduced. The effect of phosphate on silicate injections was studied using the 6m reaction coil and a test solution of 3 x 10^{-5}M silicate. The silicate solution gave a signal of 1.15 μA which only increased to

1.20 µA in the presence of 6×10^{-5}M phosphate. At higher levels increased phosphate led to a reduction in the signal, for example:

3×10^{-5}M phosphate : 0.25 µA,
3×10^{-4}M silicate : 5.1 µA
3×10^{-4}M silicate + 3×10^{-5}M phosphate : 3.7 µA,
3×10^{-5}M silicate + 3×10^{-5}M phosphate : 1.18 µA,
3×10^{-5}M silicate : 1.15 µA.

On injecting samples which contain unhydrolysed tripolyphosphate some hydrolysis is expected in the heated reaction coil under acidic conditions. A solution of sodium tripolyphosphate (0.02 gpl) is injected into the 6m coil at 60°. A signal representative of 9.2×10^{-7}M phosphate is recorded. Complete hydrolysis would yield 2.1×10^{-4}M phosphate. However colorimetric analysis of the tripolyphosphate showed 0.3% of free ortho-phosphate (corresponding to 8.4×10^{-7}M in the test solution).

It was found that the levels of free phosphate in the silicate determinations of washing powders does not require a treatment from mannitol in the flow injection system. Samples injected containing less than 9.5×10^{-5}M silicate can be determined provided they contain less than 5×10^{-6}M phosphate. Rectilinear silicate calibrations can be obtained for 10^{-5}M solutions and good results were obtained for the determination of washing powders. For example Sample A containing 22.3% phosphate (colorimetric method) gave the following results.

Single 6m coil system :

22.0, 22.3, 22.3, 21.7, 22.1, 22.1; variability, 1.7%.

Double coil mannitol system:

21.9, 22.0, 22.1, 21.7, 22.1, 22.1, 21.8; variability, 0.7%.

The two systems are thus proposed; (a) a single coil system (6m x 0.58 mm) at 60° for silicate samples containing less than 9.5×10^{-5}M silicate and 5×10^{-6}M phosphate. The reagent stream is 0.2% ammonium molybdate in 0.12M sulphuric acid.

(b) The above system is modified by including a stream of 0.1% mannitol converging on the reagent stream after the reaction coil and a further coil following (2.8 x 0.8 mm) at room temperature. This second system enables the same level of silicate to be determined in the presence of high concentrations of phosphate up to 1×10^{-4}M. The flow at the detector is 2.8 ml/min (a) and 3.4 ml/min and the response time lapse is 25 sec. (a) and 32 sec. (b). The working electrode (glassy carbon) in the detector cell is held at + 0.15 v.

4f. Effect of surfactant on flow injection analysis.

Suppression of the current due to the reduction of heteropoly acids occurs in flow injection analysis, but the effect is not so extreme. Figure 66 compares the suppression of DPP wave with the FIA signal for 3×10^{-4}M phosphate. Table 14 (below) is the percentage suppression of 100% aqueous determinations of 3×10^{-4}M phosphate by 0.4 gpl SABS.

Table 14.

Mode of Analysis.	% suppression due to 0.4 gpl SABS.
Differential Pulse	44%
Linear Sweep	51%
Direct FIA	29%
Preform Injection	12%

The same concentration of ethanol obviates the effect of the surfactant as in the static method (40% for phosphate, 46 - 48% for silicate).

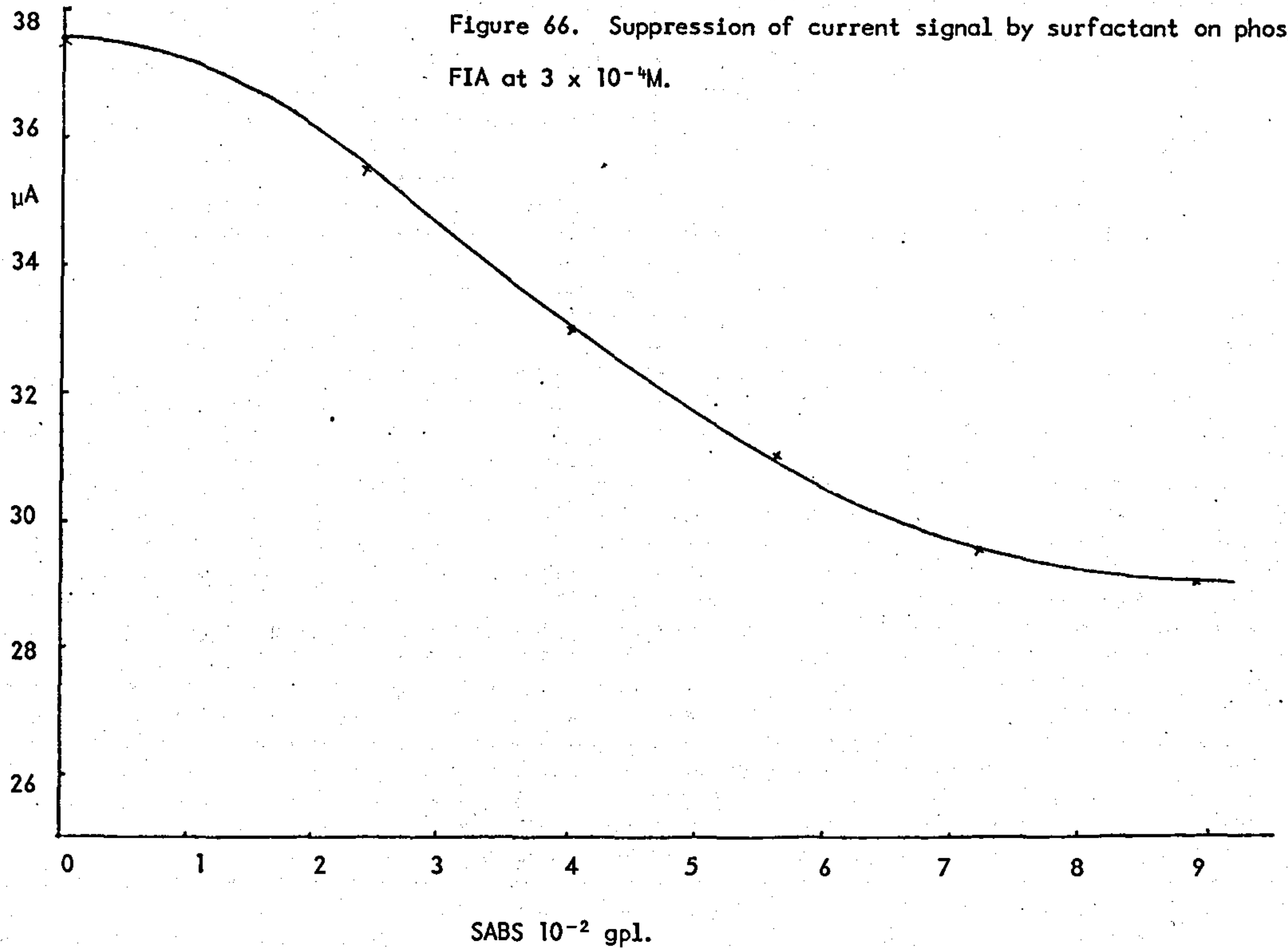

Figure 66. Suppression of current signal by surfactant on phosphate FIA at 3×10^{-4}M.

4g. Reverse injection method.

Work in this laboratory and by Johnson and Petty (1982) reverses the flow injection system, injecting the reagent into a stream of sample. The baseline is very stable and very little adsorption will occur at the electrode. Generally the signal is identical to the normal method of FIA but the response is cleaner and sharper. The stream of sample is 47% and the reagent is 100% aqueous. Six portions of sample A were analysed to give a mean result of 21.95% phosphate with a coefficient of variation of 1.46%.

5. Adsorption at the Working Electrode.

The working electrode in the static methods requires cleaning after each voltammogram has been recorded. Sluicing the glassy carbon electrode in dilute alkali destroys the heteropoly acid adsorbed onto the surface of the electrode. The electrode is then washed with distilled water and wiped with a tissue. This procedure ensures reproducibility of the trace. This treatment of the electrode was not totally successful and occasionally more abrasive action is required to clean the surface. In fact the electrode surface is removed by polishing on a flat cloth with an aluminium/ethanol slurry. Excessive polishing was found to wear down the Teflon sheath holding the glassy carbon disc; this exposed more of the disc and thus increased the surface area of the electrode and the cement which held the disc in place. Increasing the surface of the electrode gave rise to a larger signal from the electrochemical reaction and also increased adsorption. Well used electrodes built up higher background currents and thus became of little use. In some cases it was possible to clean the electrode electrochemically by holding the electrode at a high potential, say + 1 v, in electrolyte to desorb species electrochemically; this was not always successful. Old electrodes were regenerated by more drastic action; removal of the surface of the electrode with a glass lathe, followed by polishing with a series of emery papers of increasing fineness resulted in a flat shiny surface. An electrode treated in this way showed no background current and behaved as new.

In flow injection analysis the electrode behaved satisfactorily if cleaned after every 50 injections. In this case only distilled water is used and followed by wiping with a tissue. If the electrode was washed in alkali the electrode exhibited an initially high background and it took several minutes for the baseline signal to become static.

Carbon paste electrodes were used and found to be initially successful with a generally higher sensitivity and the problem of adsorption negated by the fact that the surface was easily renewed. However when washing powder samples were analysed the surface of the electrode tended to swell and disintegrate, the surfactant in the washing powder reacting with the glycerol or nujol with which the carbon paste is prepared. Carbon paste electrodes were not found to be suitable in the metrohm detector cell used for flow injection analysis. Quite often the surface was damaged on insertion into the cell block, and in the wall jet mode the surface is disrupted by the jet of the carrier stream.

Following some work by Fogg (1981) the adsorption phenomena were studied with the intention of developing an analytical technique. A glassy carbon electrode is held in a solution containing a heteropoly molybdate for a set time and removed washed with 0.1M H_2SO_4 and then a voltammetric scan is performed at this electrode in 0.001M H_2SO_4. Differential pulse scans yielded a high background and linear sweep voltammetry was found more useful. The voltammograms represented those produced earlier for phospho- and silico-molybdate species. A carbon paste electrode was seen to exhibit larger current peaks than a glassy carbon electrode. However the reproducibility of the carbon paste electrode was poor. The scan after soaking the electrode in phosphomolybdate showed three well defined peaks at + 0.24, + 0.10 and - 0.12 v. Silicomolybdate gave one broad peak at about - 0.05v. The voltammogram showed the electrochemical reaction to be 60% reversible. Increased acid molybdate concentration resulted in a higher current recorded, but this was due to a blank signal from the neat reagent.

A 0.2 gpl acid molybdate solution gave a current of 1.7 µA at + 0.1 v. whereas a solution of reagent and 6×10^{-5}M phosphate only yielded 3.0 µA. A calibration of this region, 0 - 6×10^{-5}M phosphate gave a shallow curved graph.

6. Investigation of α and β isomerism of Heteropolyacids.

The conditions for the formation of α and β isomers is reported to be controlled by the acidity of the reaction mixture (Truesdale et al 1977; 1979). Chalmers and Sinclair (1966) maintain that the use of acetone or ethanol stabilises the β form. Differential pulse voltammetry was used to study the formation of α and β heteropolyacids.

The inclusion of ethanol in the reaction mixture gives rise to a voltammogram with two strong current peaks compared to only one for a 100% aqueous reaction mixture. The presence of acetone will also affect the shape of the voltammogram; the results of these solvent effects have already been reported in the section 3.a.

As pH is varied the current peaks change potential and the amplitude of the wave is reduced with increase in pH. The amplitude of the silicomolybdate wave is at a maximum when pH = 1.4 (see Fig. 67). The shape of the wave formed at pH 1.7 is sharp and well defined whilst that formed at pH 4.2 is weak and indistinct. This applies to both 12-MSA and 12-MPA.

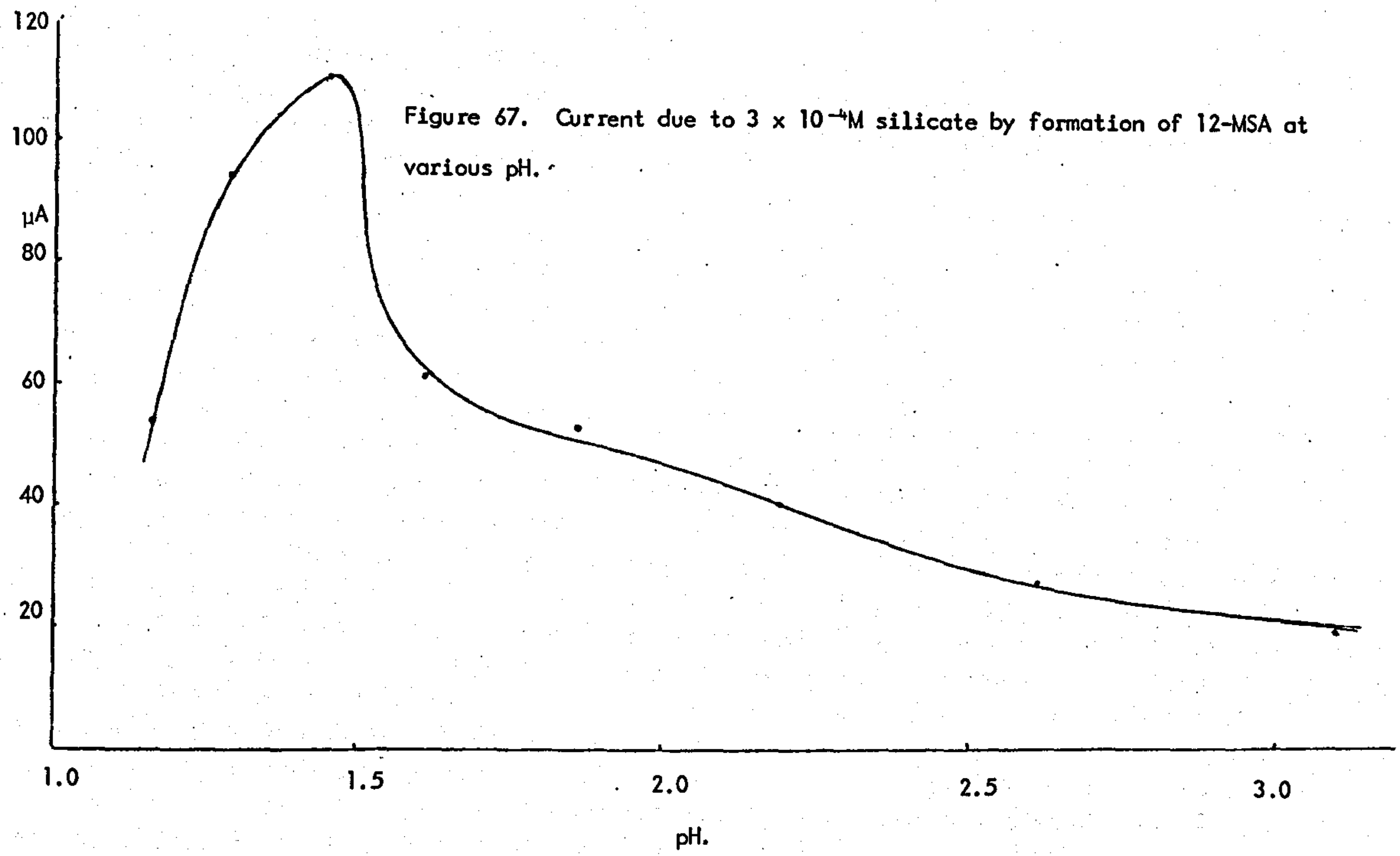

Figure 67. Current due to 3×10^{-4}M silicate by formation of 12-MSA at various pH.

Literature suggests that the β isomer is formed at pH 2.0 or less and the α form at pH 4.0 - 4.4. At high pH values the heteropolyacid will decompose. At pH 1.7 12-phospho- and 12-silicomolybdate were prepared by the addition of 2% acid molybdate (5 ml) to standard solution of ammonium phosphate and sodium silicate. The final solution would be 3 x 10^{-4} M in standard. After formation a differential pulse voltammogram was recorded between 0.6 and - 0.2. The solutions were then adjusted to pH 4.2 and the wave rerecorded after 3, 30 and 60 minutes (see Figs. 68 and 69). Also the heteropolyacids were prepared at pH 4.2 and acidified to pH 1.7 (the reaction time allowed at pH 4.2 was 1 hour) (see Figures 70 and 71). The changes in wave shape are reversible for both 12-MPA and 12-MSA. A flow chart can be constructed for the different forms present in solution. Assuming that the β-isomer exists at pH 1.7 and the α form at pH 4.2, we get the following,

$$\begin{tikzcd}
\beta \text{ in } EtOH/H_2O \arrow[r, shift left] & \alpha \text{ in } EtOH/H_2O \arrow[l, shift left] \\
\beta \text{ in } H_2O \arrow[u] \arrow[r, shift left] & \alpha \text{ in } H_2O \arrow[u] \arrow[l, shift left]
\end{tikzcd}$$

The conversions are all instantaneous except for β12-MPA to α-12MPA, which requires at least 30 minutes.

Figure 68. Wave for α-MSA (a) converted to β-MSA (b).

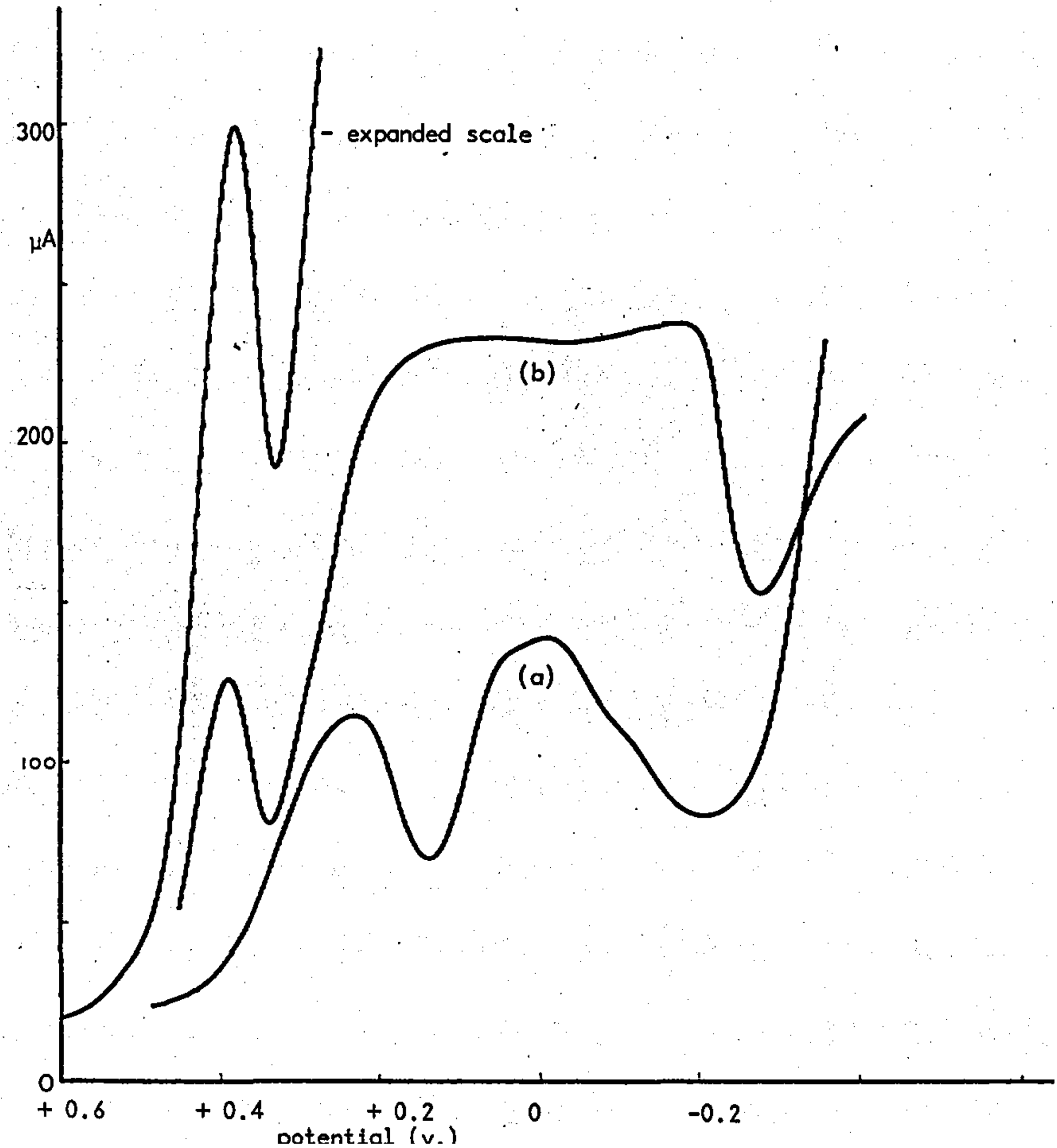

Figure 69. Wave for α-MPA (a) converted to β-MPA (b).

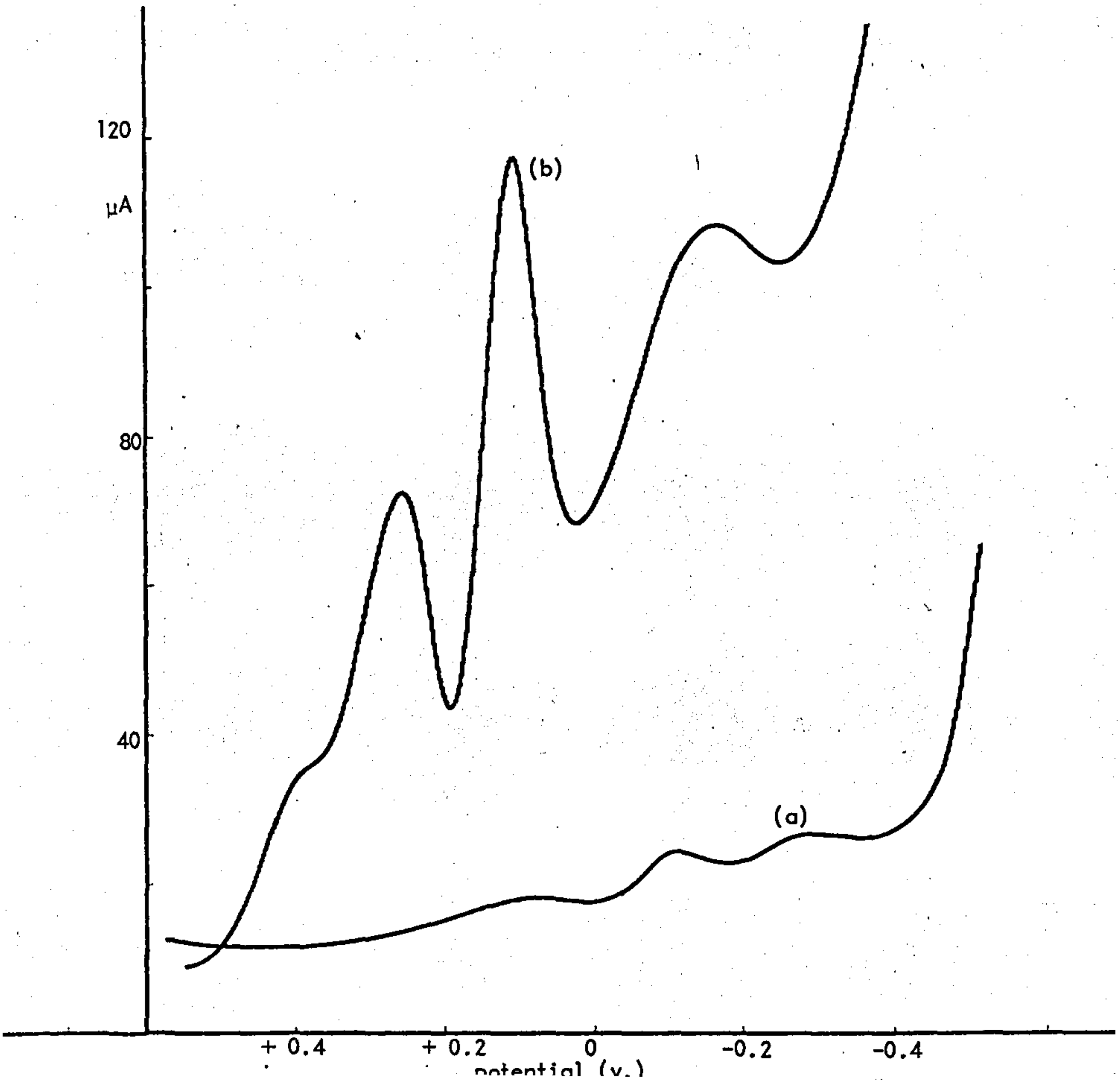

Figure 70. Conversion of β-MPA (b) to α-MPA after 5 minutes (i), 30 minutes (ii) and 60 minutes (iii).

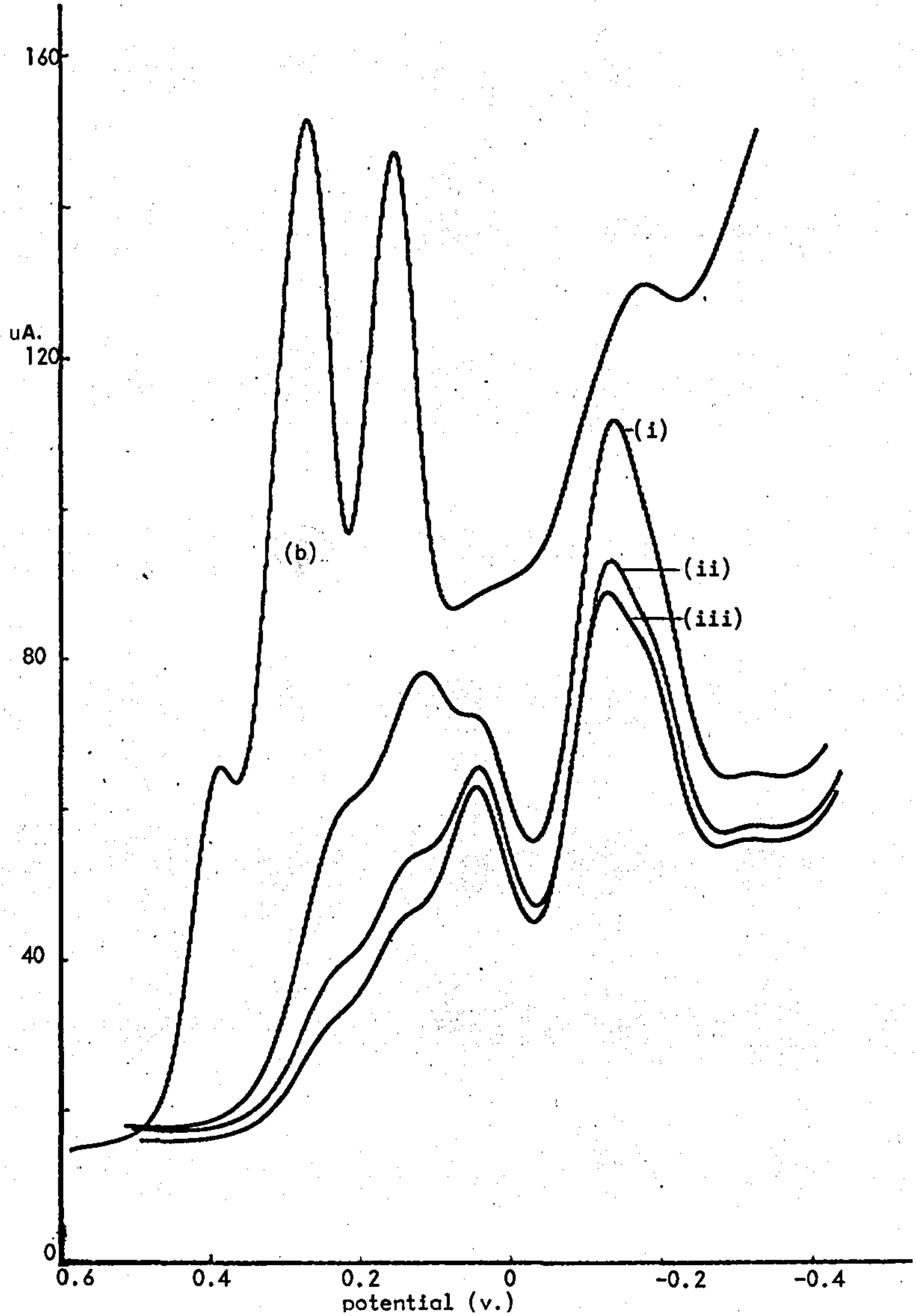

Figure 71. Conversion of β-MSA (b) to α-MSA (a).

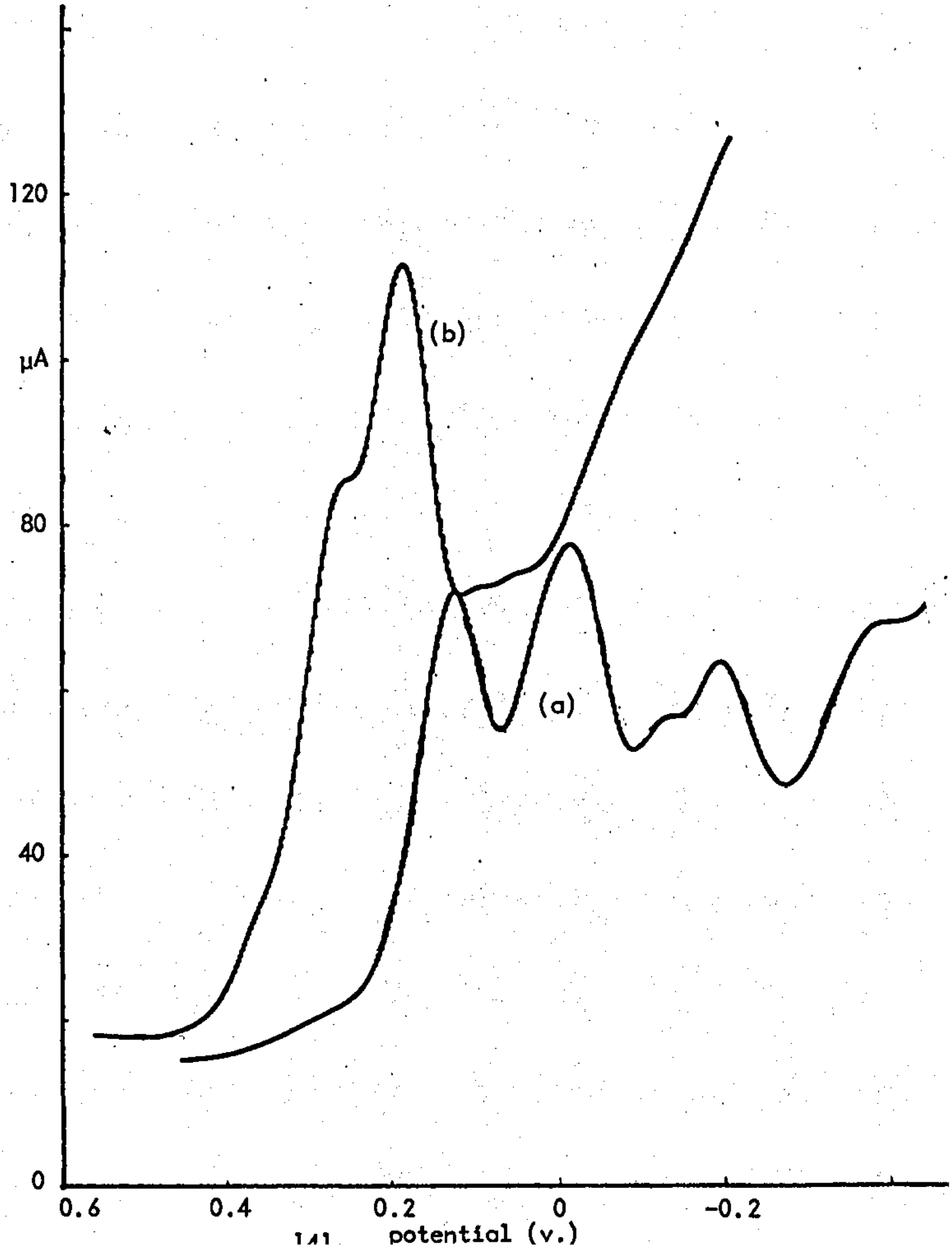

Table 15. Current peaks of the DPV waves of (a) 12-silicomolybdate

Solution Conditions	Potentials of Current Peaks (v.)
40% EtOH pH 1.7	0.19
40% EtOH, pH 4.2	0.12,-0.02, -0.2
H_2O pH 1.7	0.38 (-0.18),
H_2O pH 4.2	0.23,-0.01,
	(b) 12-phosphomolybdate
40% EtOH pH 1.7	0.27, 0.16
40% EtOH pH 4.2	0.04, -0.13
H_2O pH 1.7	0.36, 0.11,
H_2O pH 4.2	0.09, -0.11,

The change in α and β forms is graded with pH change, that is at pH 2.7 mixtures of the isomers will be formed.

7. Simultaneous determination of phosphate and silicate.

The differential pulse voltammograms of 12-MPA and 12-MSA are sufficiently different to suggest that a mixture of phosphate and silicate may be determined simultaneously.

7.a. Static methods.

Fogg et al (1981b) use acid molybdate reagents to produce heteropoly acids, the reagent is 2% molybdate for phosphate and 4% for silicate determinations. However the 4% molybdate reagent is too strong for use with phosphates causing a yellow precipitate of 12-MPA. Conversely the 2% reagent is too weak for any substantial amount of reaction to occur with silicate.

A calibration of phosphate in the presence of silicate was found to be possible (see Fig. 72). The level of silicate should not be higher than 4×10^{-5}M and the level of phosphate no lower than 1×10^{-5} M. 12-MPA in the sample gives rise to a current peak at + 0.09, only background current is observed at this potential for 12-MSA. All voltammetry in this section is in the differential pulse mode. Similarly a rectilinear calibration was also achieved for silicate (not less than 1×10^{-5}M) in the presence of phosphate (not more than 3×10^{-5}M) (see Fig. 73). The current peak at + 0.25 v was used, phosphate only gives a slight peak at this potential. The heteropoly acids were prepared in aqueous conditions with 1 ml of 4% acid molybdate reagent as in Fogg et al (1981b).

7.b. Flow injection systems.

Preformed samples of 12-MPA and 12-MSA give different currents when injected into an electrolyte stream anddetected at a glassy carbon electrode cell. At a potential of + 0.35 the signal for 12-MSA is negligible and the signal from a mixture was totally from 12-MPA. However the signals for 12-MPA and 12-MSA are not additive. It was thus not possible to determine the silicate content of the mixture at + 0.15 v by subtracting the signal due to 12-MPA.

8. Complexing of polyphosphates with metals.

Al-Sulimany and Townsend and Shaw and Townsend used the polarographic wave of metals to analyse for tripolyphosphate. The tripolyphosphate would complex the metal thus reducing the current peaks of the wave.

To solutions containing 1×10^{-3}M Cd^{2+} and 0.1M KCl as supporting electrolyte, sodium tripolyphosphate is added (final concentration in the range $5 - 13 \times 10^{-4}$M). The solutions are deoxygenated for 15 minutes and the wave is recorded at a glassy carbon electrode from

Figure 72. Current due to silicate in the presence of phosphate at 3 x 10^{-5}M.

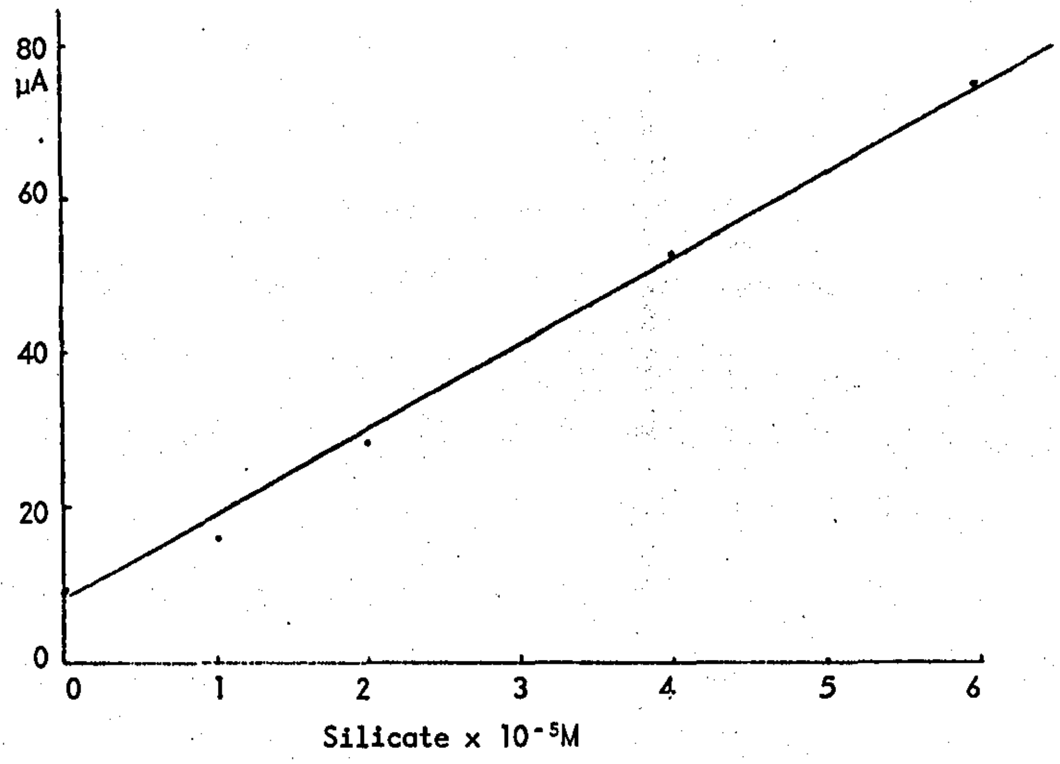

Figure 73. Current due to phosphate in the presence of silicate at 3 x 10^{-5}M

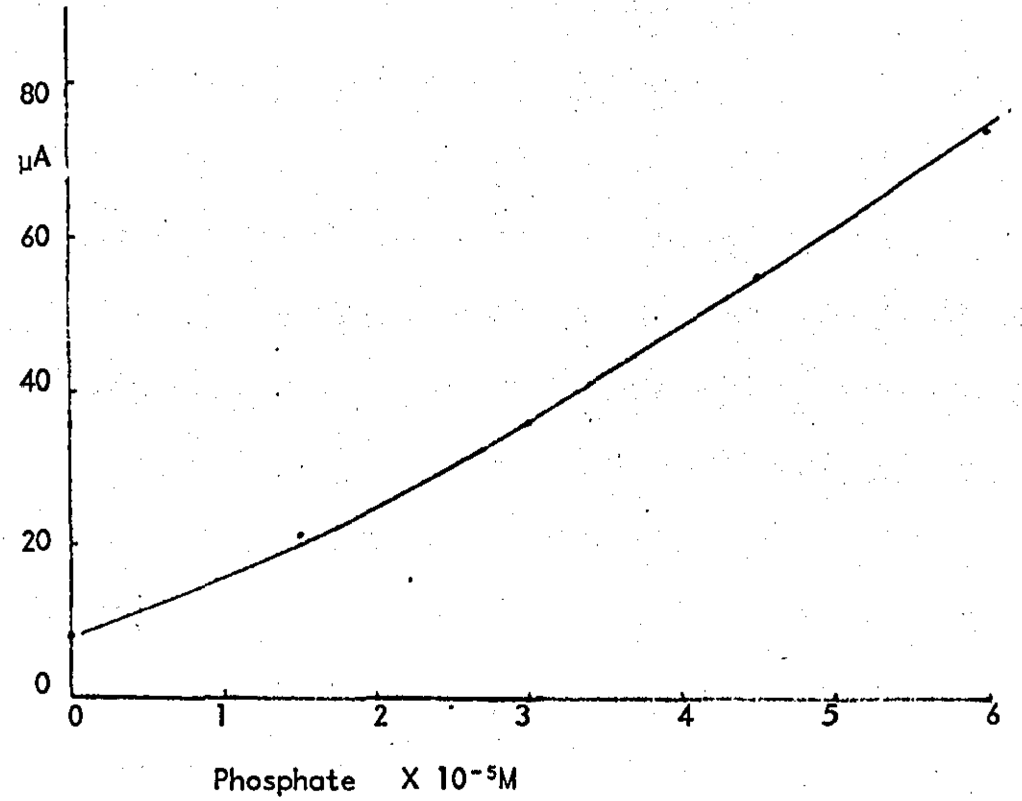

- 0.6 to - 1.2 v. After each wave the electrode is held at - 0.6 v to strip off any plated material for 3 minutes. The wave due to cadmium at - 0.91 v is reduced, but not reproducibly. Sodium pyrophosphate also reduced the cadmium wave, but ortho and trimetaphosphate had no effect.

To a solution of Cu(II) (1×10^{-4}M) various phosphates are added to a level of 1.2×10^{-4}M. Each phosphate affected the differential pulse wave of copper in a different manner or to a greater or lesser extent. Table 16 summarises these results.

Table 16. Reduction of Copper Wave due to phosphate complexation in 0.1M KCl.

Phosphate. Species	Current (μA) at + 0.56 v.	Current (μA) at + 0.95 v.
none	46	54.5
Ortho-	17	8
Pyro-	2	7
Tripoly-	8	18.5
Trimeta-	3	55

9. Automatic Hydrolysis of Polyphosphates.

An attempt was made to combine an air segmented continuous flow hydrolysis coil with the flow injection system developed for the determination of phosphate.

Figure 74. The combination of autoanalysis hydrolysis apparatus with a flow injection system.

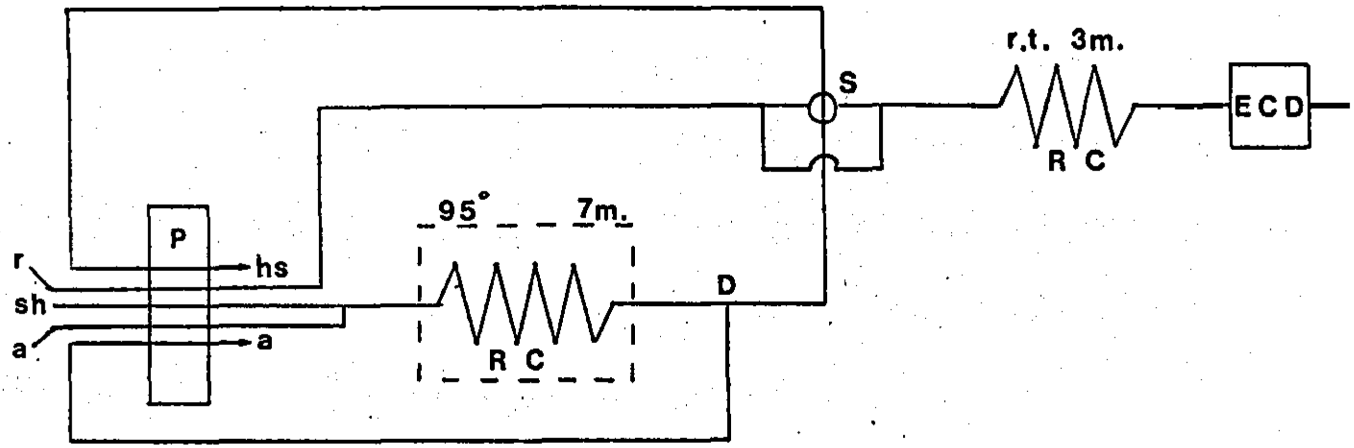

r. reagent stream
sh. stream prior to hydrolysis
hs. hydrolysed stream
a. air.
D. Debubbler

A sample slug is passed into the hydrolysis coil for 10 minutes followed by 10 minutes of distilled water. The sample is resident for 45 minutes in the hydrolysis coil at 95°. At this point the flow is segmented. The output of the hydrolysis coil is controlled by the same pump as the input. The output has to be controlled as the expression of the coil liquid and air-segments entering the coil accelerates the passage of the sample. This results in an increased pressure within the coil. The stream is then debubbled after the pump and passes through the loop of the injection valve of the flow injection system described in Figure 61. The sample slug is identified by a small precursor bolus of 0.5% methylene blue; short sections of glass conduit are required to visualise the slug as the plastic tubing becomes stained. The sample solution is made up in 0.1M sulphuric acid for the hydrolysis. A few drops of detergent solution are added to maintain the integrity of the air segments. The sample stream flowing at 0.25 ml/min is allowed to flow through the injection loop of the valve for 45 seconds. The injection loop is then switched into the molybdate stream; 12 seconds lapse before the signal is recorded. The molybdate reagent is 0.2% with respect to ammonium molybdate and 40% ethanol. No acid is included in this reagent as the sample slug is already 0.1M sulphuric acid. It is possible to make an injection once every 60 seconds. Figure 75 shows a typical series of injection signals.

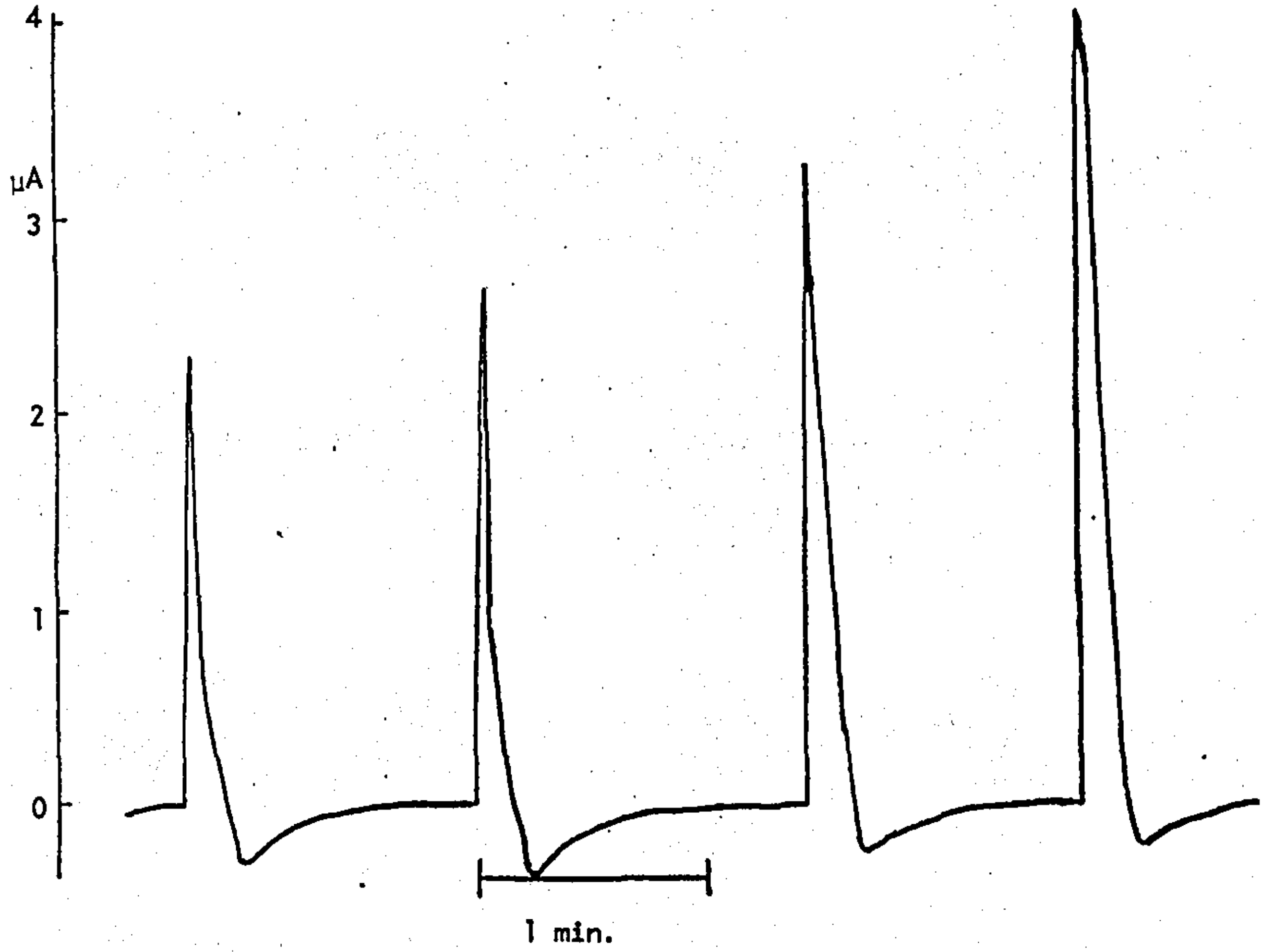

Figure 75. Current signals from 0, 1.5, 3.0 and 4.5 x 10^{-5}M phosphate using flow system including the hydrolysed coil.

The signal for a solution of 8 x 10^{-4}M orthophosphate was 12.4 μA whilst that for 8 x 10^{-5}M was 3.9 μA. The limit of detection is 3 x 10^{-5}M (2.6 μA) as a blank gives 2.3 μA. The use of hydrolysis coil reduces the effective signal by 25%. A sample of phosphate which had not been through the coil gave 16.4 μA as opposed to 12.4 μA for one that had. A series of tests on solutions of sodium tripolyphosphate found that the degree of hydrolysis to be 92% and the coefficient of variation of the signal 1.4%. The total time for the analysis of one sample making three determinations is approximately 75 minutes.

Recommended Analytical Procedures

The procedures described in this section are those finalised for determinations of soluble silicate and total phosphate in commercial washing powders.

1. Static voltammetric procedures.

1a. Reagents

Standard orthophosphate solution, 3 x 10^{-3}M (285 μg ml^{-1} of $PO_4{}^{3-}$)

Dissolve 0.408g of analytical reagent grade potassium dihydrogen orthophosphate in water and dilute to 1 l in a calibrated flask. This solution is 3 x 10^{-3}M in orthophosphate. Less concentrated standard solutions were prepared by dilution.

Standard silica solution, approximately 0.15 mg SiO_2 ml^{-1}

Weigh accurately about 0.15g of quartz into a platinum (or nickel) crucible and fuse it with about 2g of sodium carbonate. Cool the melt, dissolve in water, dilute to 1 l in a calibrated flask and store in polythene. (A 3 x 10^{-3}M solution of sodium metasilicate was also used as a standard solution after comparison with this solution).

Dissolve 15g of sodium molybdate dihydrate and 12g of tartaric acid in water, add 45 ml of concentrated hydrochloric acid and dilute to 500 ml. A brown colour develops in the reagent solution after a few days: discard it three days after preparation.

Ammonium molybdate/sulphuric acid solution

Dissolve 40g of ammonium paramolybdate heptahydrate in 500 ml of water in a polythene beaker and add 500 ml of 1M sulphuric acid solution. Mix and store in polythene.

1b. Dissolution and Hydrolysis of Sample

Dissolve an amount of commercial washing powder containing approximately 50-150 mg of total phosphate (as orthophosphate) and 15-30 mg of soluble silicate (as SiO_2) in about 60 ml of water and heat at 80-90°C in a water bath with stirring until the sample has dissolved. Traces of insoluble silica may remain undissolved. Transfer the solution to a calibrated flask and dilute to 100 ml. Take an aliquot of this solution for soluble silicate analysis.

To 20 ml of the solution contained in a flask add 5 ml of 2M sulphuric acid solution and heat for 1 hour on a boiling water bath to hydrolyse the polyphosphates. Cool and dilute to 100 ml in a calibrated flask. Take an aliquot of this hydrolysed solution for total phosphate determination.

In the present study, 0.5g of detergent powder was taken, a 5 ml aliquot of the unhydrolysed solution was taken for silicate determination, and a 5 ml aliquot of the hydrolysed solution was taken for phosphate determination.

1c. Preparation of calibration graphs and analysis of samples

Determination of silicate

Add aliquots of standard silicate solution (0-10 ml) or an aliquot of unhydrolysed sample solution containing less than 1.8 mg of SiO_2 to a mixture of 10 ml of ammonium molybdate/sulphuric acid reagent and 23 ml of ethanol.

Mix, and after 15 minutes add 10 ml of 10% mannitol solution, mix again, and after a further 15 minutes dilute to 50 ml in a calibrated flask.

Obtain a differential pulse voltammogram of each solution scanning from 0 to +0.6 V or inject 100 μl of the solution into a stream of blank solution prepared as above in larger volume but omitting the silicate. Prepare a calibration graph using the differential pulse peak at +0.31 V or the signal obtained at + 0.15 V (see Figures 76 a, b).

Determination of phosphate

Add aliquots of standard phosphate solution (0-10 ml) or an aliquot of hydrolysed sample solution containing less than 3 mg of orthophosphate to a mixture of 10 ml of sodium molybdate-tartaric acid-hydrochloric acid reagent and 15 ml of ethanol. Mix and after 15 minutes dilute to 50 ml in a calibrated flask.

Obtain a differential pulse voltammogram of each solution scanning from -0.05-+0.5 V or inject 100 μl of the solution into a stream of blank solution prepared as above in larger volume but omitting the phosphate. Prepare a calibration graph using the differential pulse peak at +0.18 V or the signal obtained at +0.15 V (see Figures 77a, b).

1d. Voltammetric Measurements

Voltammograms were obtained using a PAR 174 polarographic analyser (Princeton Applied Research) with three electrode operation (glassy carbon electrode, platinum counter electrode and calomel reference electrode). For differential pulse voltammetry a sweep rate of 5 mV s^{-1}, a pulse height of 50 mV and a pulse frequency of 0.5 s were used. Between scans the glassy carbon electrode was cleaned with 1M sodium hydroxide solution, and occasionally, as required, by polishing with the addition of water or ethanol on a polishing cloth. Voltammograms were recorded with a Gould HR 2000 x-y-t recorder.

2. Preformed Flow Injection Analysis

A Metrohm detector cell (EA 1096) was used with a Metrohm glassy carbon electrode (EA 286) fitted. The detector cell was partially immersed in electrolyte (0.01M sulphuric acid solution) contained in

Figure 76. Silicate calibration in the 10^{-4} range.

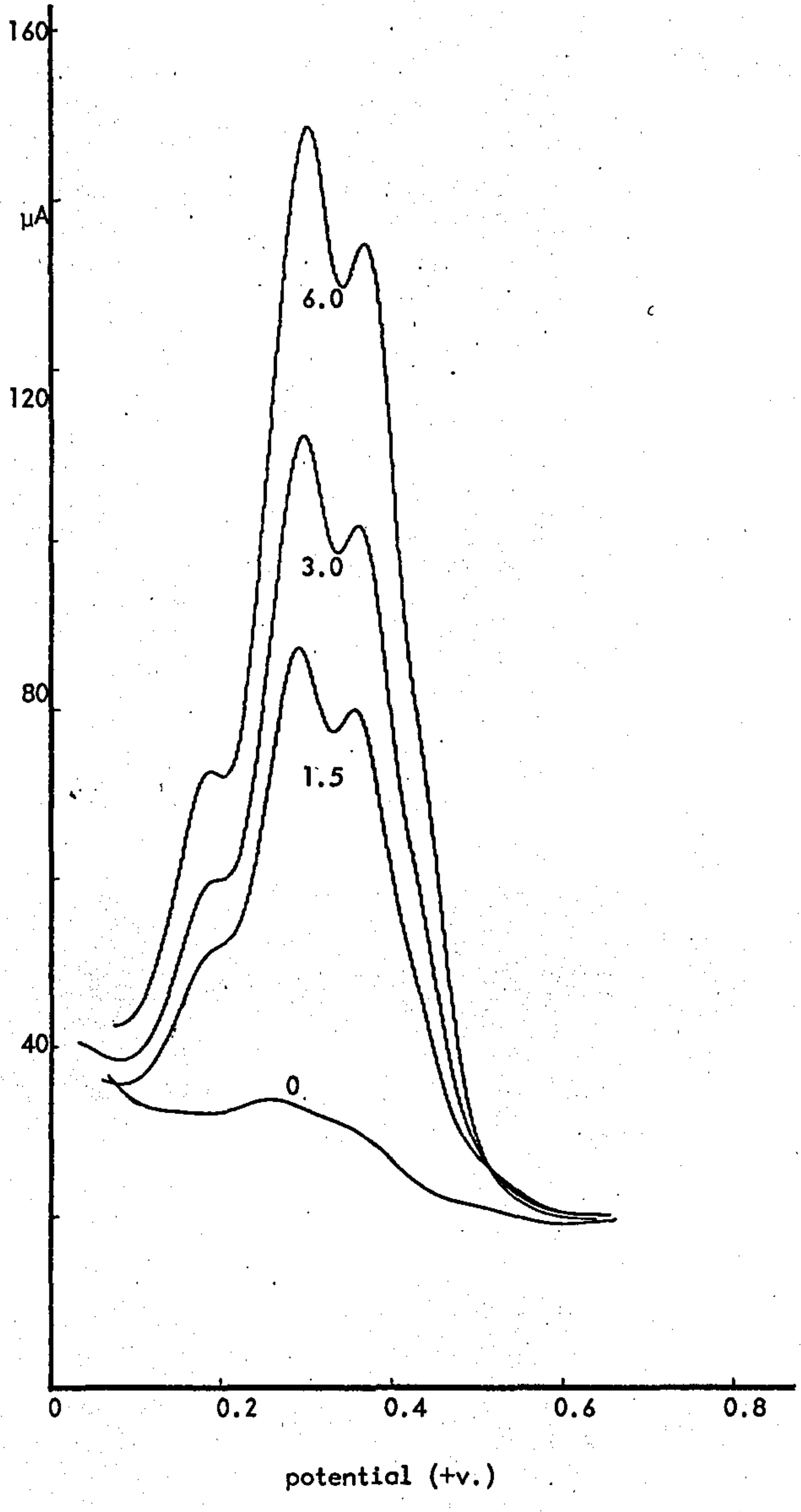

Figure 77. Phosphate calibration in the 10^{-5} M range

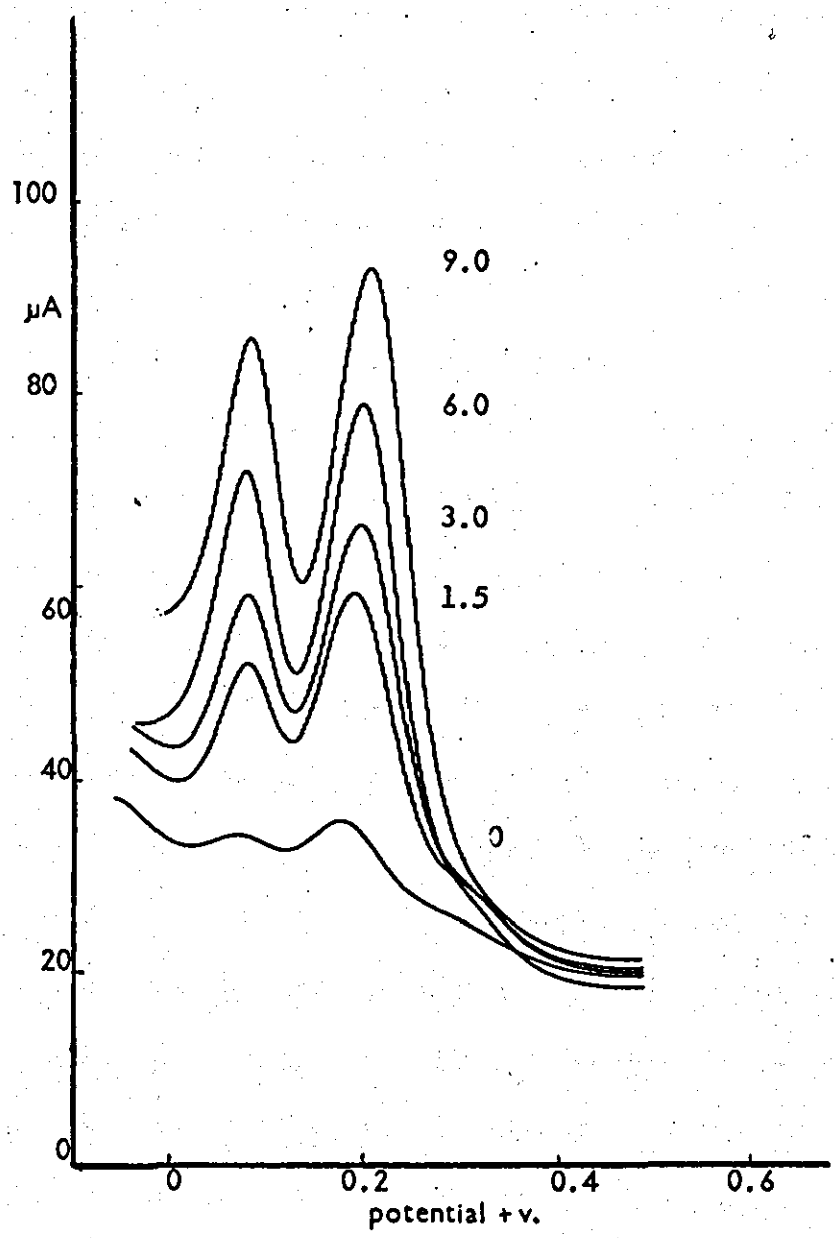

a beaker and contact with the counter and reference electrodes used in the static work was made by means of salt bridges. Eluents were degassed by means of a vacuum pump. Injections were made by means of a Rheodyne sample injection valve (5020) with loop capacity 0.1 ml. The glassy carbon electrode was cleaned with 1M sodium hydroxide solution daily after approximately 50 injections or when changing eluents. The potential of the detector cell was controlled by means of the PAR 174 polarographic analyser; current peaks were recorded with the Gould HR 2000 x-y-t recorder.

3. Direct Flow Injection Analysis

3a. Eluent Constitution

The eluent proposed is suitable for phosphate and silicate determinations. An acid molybdate reagent is prepared by dissolving 2g ammonium molybdate heptahydrate in 30 ml distilled water. To this 55 ml of 2M sulphuric acid is added, the mixture is transferred to a calibrated flask and diluted to 100 ml with distilled water. The eluent is then prepared by diluting 10 ml of the acid molybdate with 46 ml ethanol and 44 ml distilled water.

The stream of mannitol for the silicate determination consists of 10 ml of a 10% aqueous mannitol solution, 46 ml of ethanol and 44 ml distilled water.

3b. Systems Used

In all flow injection determinations the eluent is driven by an "Ismatrec Mini S" peristaltic pump fitted with a blue/blue coded pump tube. The volume of the injected bolus is 0.1 ml in all cases. The potential of the electrochemical detector is +0.15 v for both phosphate and silicate determinations.

Phosphate

The determination of total phosphate uses the system described by

Figure 61, results section 4b. The reaction coil is held at room temperature and is 3m long. If unhydrolysed samples are injected free orthophosphate in the sample is determined.

Silicate, Method A

The determination of soluble silicate in samples containing not more than 1 x 10^{-6}M orthophosphate the system used is the same as for the phosphate method above. The reaction coil is 6m long and held at 60° in a water bath.

Silicate, Method B

This procedure uses the system described in Figure 65 including the stream of mannitol solution. The reaction coil is as above, the second coil is 2.4m long by 0.8 m.m. i.d. and at room temperature. This procedure is suitable for samples containing up to 3 x 10^{-5}M orthophosphate. The mannitol solution is propelled using a purple/yellow coded pump tube.

4. Autohydrolysis of total phosphate

10 Aliquots of unhydrolysed washing powder solution (10 ml) from above are diluted to 100 ml with 5 ml 2M sulphuric acid, 1 ml 0.2% SABS (detergent) and 84 ml distilled water. The stream is driven by a 'Gilson Minipuls' producing a flow rate of 0.25 ml/min. Initially the stream is distilled water. The stream is switched to 0.5% methylene blue for 1 minute then to the test sample for 10 minutes. This is followed by distilled water for another 10 minutes, after which the cycle is repeated for as many times as there are samples. The residence time in the hydrolysis coil is 50 minutes. After the hydrolysis the sample bolus is identified by the preceding slug of methylene blue and directed through the sample loop of the injection valve as in the direct injection method of phosphate (see above). The sample loop is opened to the hydrolysed stream for 45 seconds before injecting into neutral

Figure 78. Preformed injection of 0, 1.5, 3.0 and 6.0 x 10^{-4}M silicate at + 0.15v.

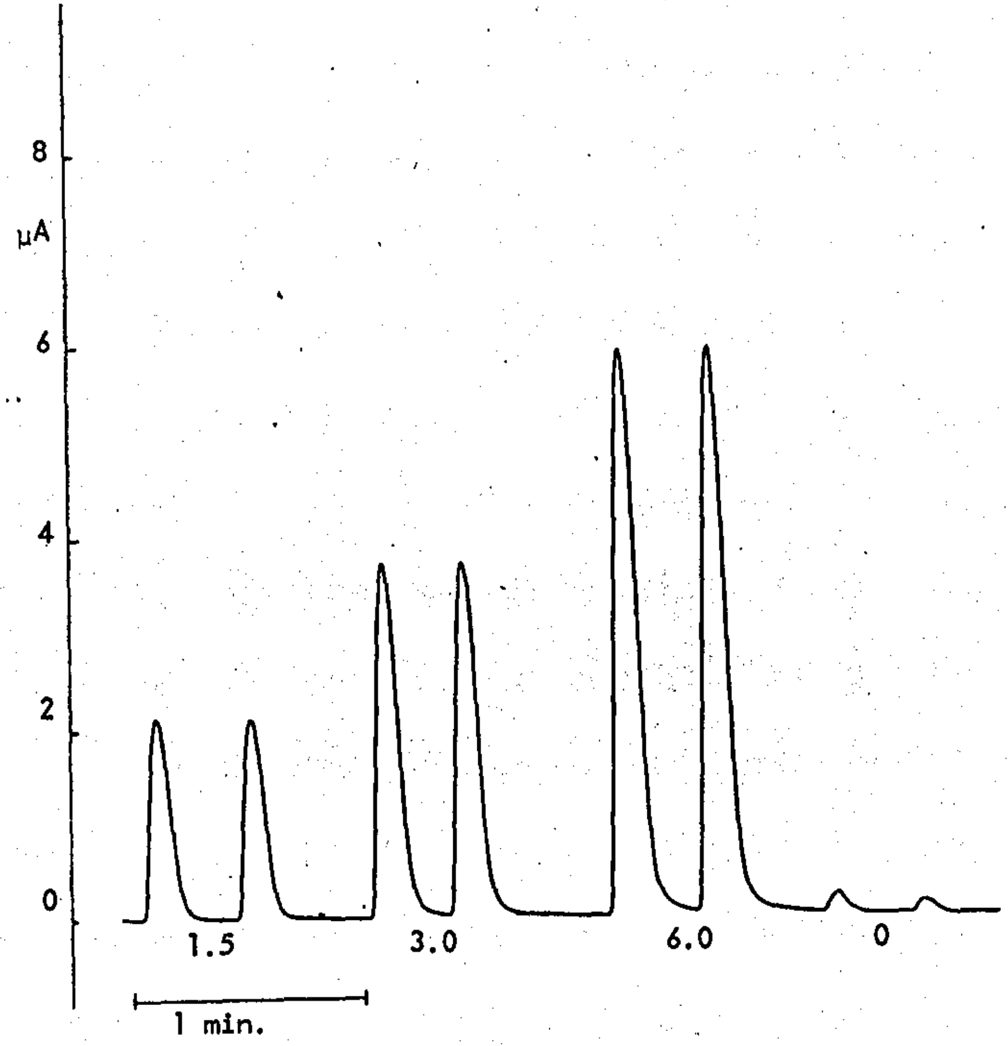

Figure 79. FIA of silicate, (i) 0, (ii) 1.5, (iii) 3.0, (iv) 4.5 and (v) 6.0×10^{-5}M, at + 0.15v.

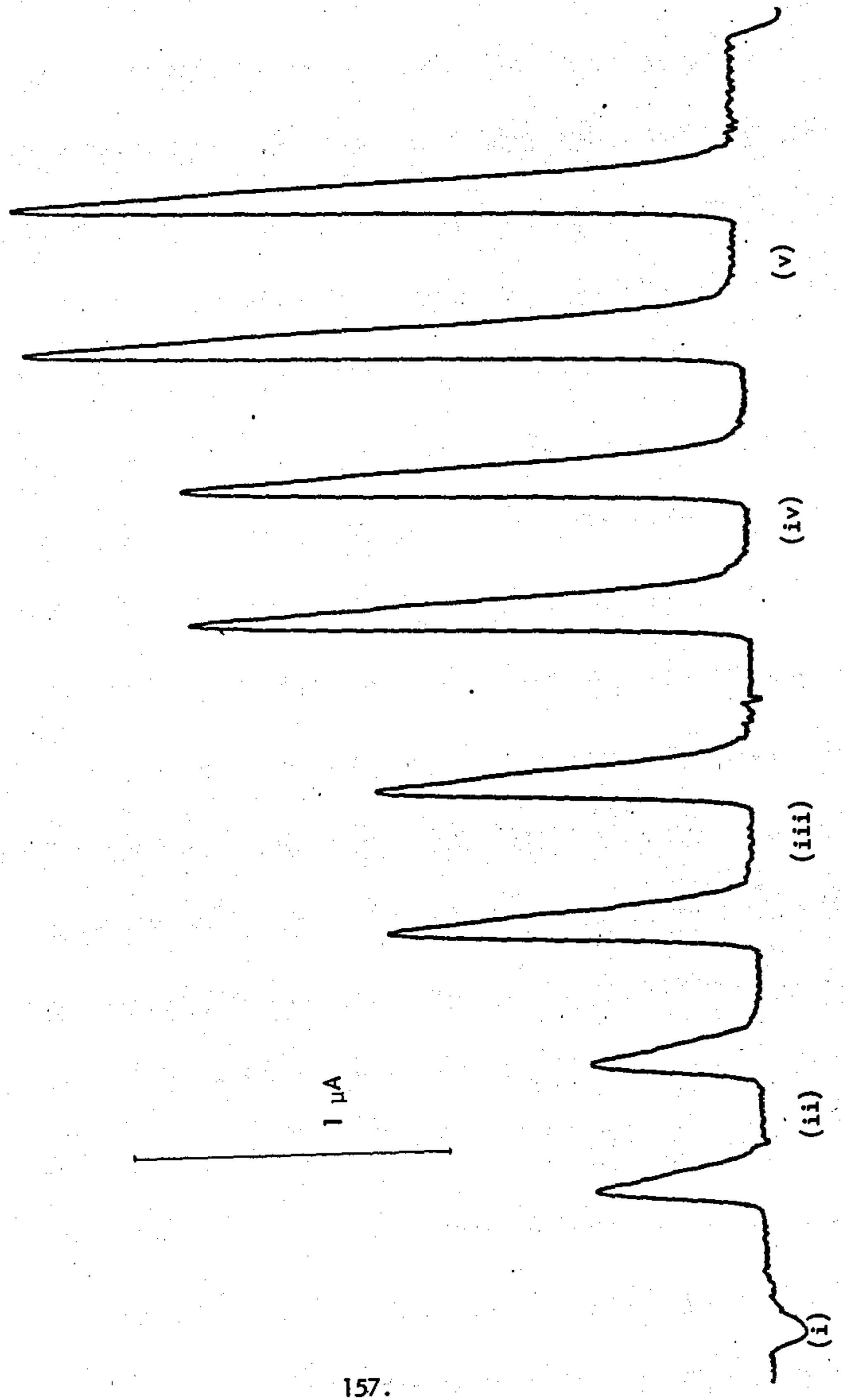

Figure 80. FIA of (0, (ii) 1.5, (iii) 3.0, (iv) 4.5 and (v) 6.0×10^{-5}M phosphate, at + 0.15v.

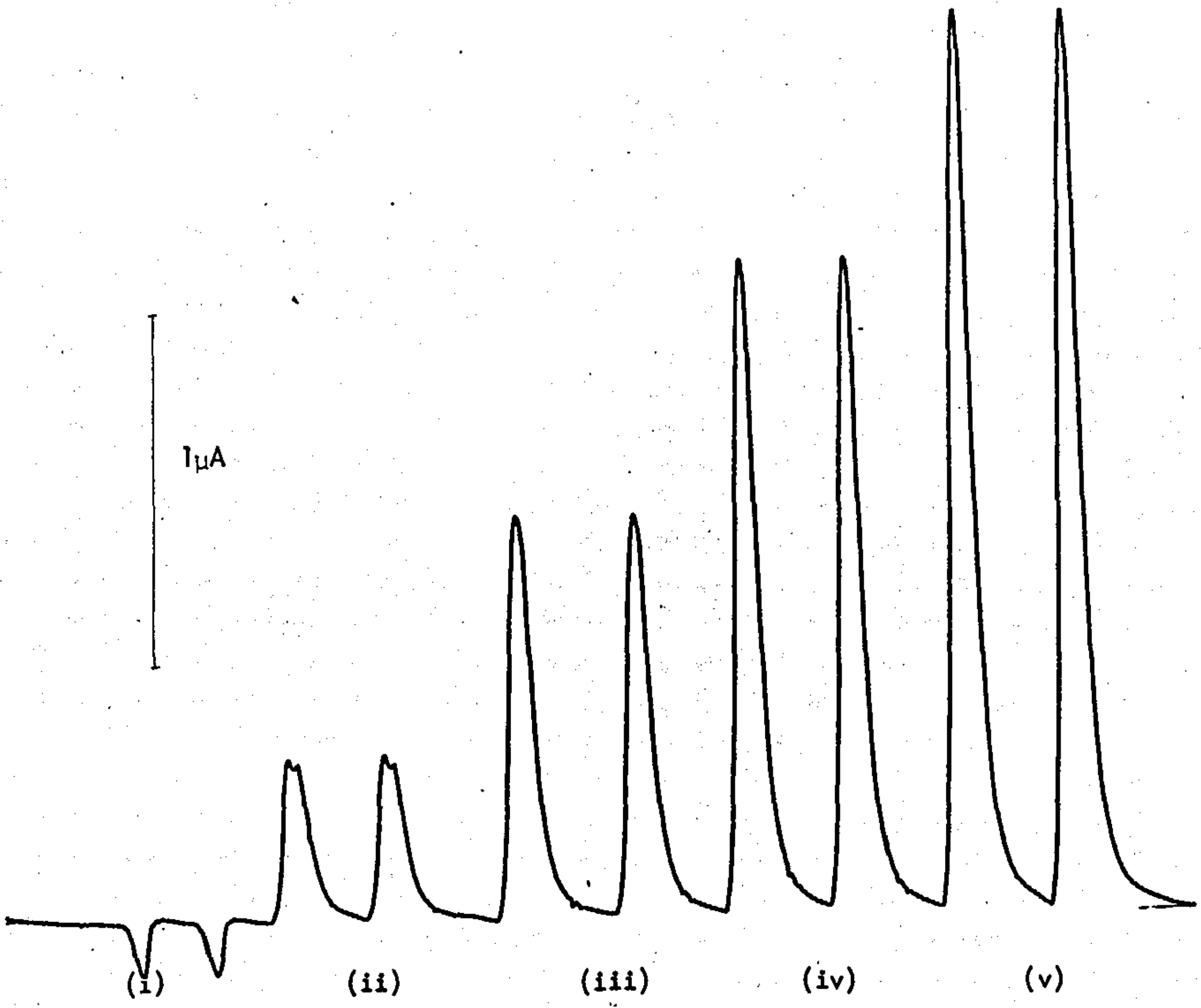

stream of 0.2% ammonium molybdate in 46% ethanol/water.

Figures 78, 79 and 80 depict calibrations for the phosphate method, silicate method B and the autohydrolysis of total phosphate.

Discussion

1. The Hydrolysis of Polyphosphates

The hydrolysis step in the determination of total phosphate is the rate determining factor as regards devising a speedy analytical method. The manual acid digestion still remains the most convenient procedure when analysing a small number of samples. However acid digestion is time consuming and tedius if more than half a dozen samples are to be determined. Autoanalyser systems using air segmentation have been devised, for example, Hirai et al (1980, 1981a), using reaction coils at temperatures in excess of 100°. Consequently the pressure is increased in the reaction coil, this raises a safety problem considering that the eluent can be up to 4M in sulphuric acid. These conditions are required however if the sample residence time in the reaction is to be less than 10 minutes. The results of section 9 show that it is possible to combine an autoanalyser hydrolysis coil with flow injection techniques. The use of flow injection analysis reduces the time required for the formation of phosphomolybdate because of the much faster flow rate (12 seconds in the case of the proposed method). In continuous flow systems the flow rate is generally constant throughout the system, any increase will be due to convergence reagent streams. However only the start up of the continuous flow system is slow, i.e. the time lag until the first sample is detected.

The mixed air segmented/flow injection system used is no faster than the manual digestion followed by flow injection. The equipment available operated at a maximum of 95° and hence a slow flow rate was required for complete hydrolysis. Under conditions of higher temperature a cooling coil would be required before transfer to the flow injection section. This is to guarantee no interference from the silicate in washing powder samples. A cooling coil was not warranted in the system used here. The flow rate was slow enough for eluent to cool sufficiently in the connections and pump tubes between the hydrolysis coil and the flow injection valve. The eluent of the flow injection system in this case is neutral, the sample bolus injected is 0.11M sulphuric acid. ?

Several other methods of hydrolysis have been considered. Hydrolysis in the presence of molybdate reagent was found to be effective. In order to prevent formation of interfering 12-molybdatosilicate, tartaric acid has to be included. The use of tartaric acid will also reduce the signal at the detector.

Catalytic methods using transition metals (e.g. vanadium, Haight et al, 1979) or enzymes (phosphatases, Clesceri and Lee, 1965) offer no practical improvement on acid digestion. Some specific polyphosphatases are available (Bloemers, 1970) and could be useful in determining pyrophosphate content.

2. Static Determinations and the effect of surfactant in washing powder samples.

Although superseded by the flow injection methods devised the static voltammetric determinations are an important point in their development. The surfactant constituent in washing powders was found to be the cause of low results when determining phosphate and silicate by aqueous methods (Fogg et al, 1981b). It is thought that the surfactant molecules are adsorbed onto the electrode surface. In effect a microlayer of surfactant forms on the surface of the electrode rendering it remote to the electrochemically active species in solution (heteropolyacid). Surfactants are long chain alkyl molecules with a charge at one end (negative in this case) associated in solution with a positive species (e.g. Na^+). A plot of surfactant concentration against wave height in aqueous conditions shows the wave height to fall quickly to a low concentration to reach a constant maximum value for any further increases in surfactant. The reduced electrochemical reaction could be due to the surfactant reducing the effective surface area of the electrode by adsorption. The observed current due to an electrochemical reaction is proportional to the area of the electrodes surface in contrast with the solution.

The inclusion of an organic solvent such as acetone or ethanol in the test solutions remove the effect of suppression by the surfactant. The effect is gradually removed by increasing the solvent level until the wave is the same height whether surfactant is present or not. A 40% ethanol/water test solution shows no suppression of the wave for 12-molybdophosphoric acid; 12-molybdosilicic acid requires a 46-48% ethanol/water mixture. Increasing the level of ethanol in the test solution above 40% will gradually reduce the wave height, but the surfactant has no effect on the wave due to 12-molybdophosphoric acid. Above 48% ethanol the wave for 12-molybdosilicic acid is amplified slightly, in the presence of surfactant.

In the presence of ethanol the surfactant molecules will be more soluble than in purely aqueous conditions. The behaviour of the surfactant species will then be different. It is possible that the surfactant molecules will then be more likely to reside in true solution.

Surfactants therefore do not affect the formation of the heteropolyacid; they reduce the amount of electrochemical reaction. It is possible to construct a linear calibration with the totally aqueous methods in the presence of surfactant. Sodium perborate is also present in washing powders and suppresses the voltammetric wave for 12-molybdophosphate only in aqueous conditions. Satisfactory methods for mannitol were also found to reduce the background or blank current.

Under certain conditions a mixture of silicate and phosphate will give a mixed voltammetric wave with current peaks attributable separately to the formation of 12-MPA and 12-MSA. The current peak due to 12-MPA is calibratable in the presence of 12-MSA and vice versa. The calibration curves do not cut the axis at zero. This is due to the current of one heteropoly acid always having some effect on the 'blank' or zero concentration current of the other. This makes the use of this technique inaccurate for analytical purposes, unless the concentration of one of the heteropoly acids is known. However it is possible to determine one in the presence of the other.

3. The effect of solvents and α-β isomerism of heteropoly acids.

Organic solvents, in this case acetone and ethanol, will nullify the suppression of the wave due to heteropoly acids as described above. Also the shape of the wave changes as the content of ethanol increases. Initially at low levels the ethanol will enhance the amplitude of the wave (5-20% ethanol) but generally the solvent will reduce the amplitude of the wave (75-60% ethanol), after 60% solubility problems are encountered. In the presence of organic solvents the polarity of the sample solution will be reduced. This may be affecting the solubility and stability of the heteropoly anions and their diffusion from the bulk solution to the working electrode. Chalmers and Sinclair (1966) propose that ethanol and acetone will stabilise the β-isomer which appear to be less stable to electrochemical reduction. The shape of the wave in aqueous conditions is quite different to that in 40% ethanol. It is thought that in aqueous conditions a mixture of the isomers is obtained. The β form is stabilised by organic solvents and the α form stabilised by a pH of 4 to 7.

When a plot of % ethanol against wave height for 12-phosphomolybdate is constructed the graph displays a discontinuity between 24 and 25% ethanol. It could be that at this point the β isomer, stabilised by the ethanol, becomes the dominating species in solution.

Lower levels of ethanol and acetone are required to obviate the surfactant suppression for phosphate than for silicate. It has been observed (see above) that 12-silicomolybdate behaves slightly differently from 12-phosphomolybdate. The structures of these heteropoly species will be slightly different, as are the parent oxo anions; silicate ($SiO_3{}^{2-}$) and phosphate ($PO_4{}^{3-}$).

The interconversion of the isomers was achieved by manipulation of the pH of the solution. The β form formed at pH 1.7 in 40% ethanol was easily converted to the α form at pH 4.2 and the reverse was true for the α form prepared at pH 4.2 and totally aqueous conditions. These conversions appeared to be reversible. It is likely that the β form when prepared in totally aqueous conditions is not pure due to decomposition to the more thermodynamically stable α isomer. The conversion from β to α is slow in 40% ethanol, but instantaneous in pure water.

4. Electrode Performance.

The glassy carbon electrode was used throughout this work and its convenience of use is apparent compared to the mercury drop. The major disadvantage of the solid carbon electrode is the adsorption of species on the surface. This requires the regular cleaning of the electrode.

In the static determinations the electrode has to be cleaned after every separate determination. Sluicing of the electrode in dilute sodium hydroxide decomposes adsorped acidic molybdate species. It was found that not only the heteropoly acid that was adsorbed, but the acid molybdate also became sorbed onto the electrode surface. In flow injection analysis the electrode is cleaned about every 50 injections and only with distilled water. The surplus water is removed with a tissue followed by a gentle polish. In flow injection analysis the electrode is not poisoned to the same extent; this is probably due to the scrubbing effect of ethanol in the carrier stream.

The abrasive polishing of the electrode with ethanol and alumina is to be used only occasionally. This procedure wears down the plastic sheath and the epoxy resin holding the glassy carbon disc in place. Excessive polishing exposes an increasingly greater area of the glassy carbon, thus modifying the electrode performance.

It was once thought that the adsorption phenomena could be used as an analytical technique for low levels of silicate and phosphate. However it was found that the acid molybdate also adsorbs at the electrode surface. This results in a high blank signal, too high to make analytical use of the idea. An anodic stripping technique has been devised by Iyer et al (1981) for silicate. Silicomolybdate is preconcentrated at a hanging drop at -0.2 v for 2 minutes followed by stripping from -0.2 to -0.8 v. Iyer suggests that the 12-silicomolybdate anion should have adsorptive properties on account of its molecular size. Moreover the reduced form is also strongly adsorbed. The detection limit of this method is noted at 1×10^{-7}M, using the β-isomer stabilised by the presence of methylethyl ketone.

5. Flow Injection Systems

Flow injection analysis is simple, cheap and easy to use. There are however, several parameters which require optimisation before the system becomes operational.

The problem of signal noise in this work was avoided by the degassing of the eluent, small bubbles can form in the stream especially if the reaction is heated. These bubbles when presented to the electrode cause a fluctuation in the baseline signal. The pumps used in this work generated a low amplitude pulsing, use of the low pass filter on the instrument nullified any electrical and pulsing interference. Inclusion of mannitol in the eluent also reduced signal noise. The low pass filter facility of the analyser was found sufficient to reduce noise to give a stable base line. At a setting of 0.3s the observed currents were only reduced by 0.5%. The use of an anti-pulsing chamber between the pump and the injection valve was found to be unnecessary.

The reproducibility of the signal from the detector is important. The integrity of the sample bolus must be maintained, fast flow speeds yield sharp signals with low dispersion. However sufficient time must be allowed for reaction in the coil before the sample reaches the detector. If the sample requires heating of the reaction coil the dispersion will increase and the reproducibility falls off. Larger signals were obtained by slowing the flow rate but this only resulted in getting broader, less well-defined signals. This is not advantageous reducing the effectiveness of the flow injection system. If the reaction coil was too short or of too narrow a bore the sample did not mix thoroughly with the reagent in the eluent. This was manifested as a split signal, the front and rear or the sample bolus reacting more to give a larger signal than the centre of the bolus.

The flow rate of the eluent could be modified by the position of the rotor in the injection valve. When the flow is directed through the sample loop more resistance is encountered and the flow rate is reduced. It is also important that the sample loop is full of undiluted sample before injecting,as the stream has to pass through the sample loop. The bearings of the injection valve are protected with a light grease. This grease can become dislodged and can cause a blockage in the system. A danger of foreign objects fouling the system is ever-present, especially where converging streams are employed. Solid matter showed a tendency to collect in the T-junction employed. The valve is easily dismantled for cleaning. However, this virtue means that the whole system can work loose and affect the sample slug shape. The valve is easily retightened; care is required not to over-tighten. The valve becomes difficult to turn and shearing of the stainless steel locking pin is possible. The Teflon rotor parts may also wear down.

The maintenance of a constant flow rate will be impaired by the ageing of the tubes of the peristaltic pump. The walls of the tube become weakened after a week of heavy use, Though they return to their original shape after use, further use will soon reweaken them. To prolong the lifetime of the pump tubes it is important to release them from the pump barrel when not in use.

The flow rate through the detector is also important, too slow and the signal response will be sluggish and broad. A swift flow rate is required, presenting as much of the sample to the electrode surface in the shortest time possible. A cell used in this work was supplied by Metrohm. If all the three electrodes are in place the flow exits via a small bore duct. This presents a considerable resistance to the flow. The reference and auxiliary electrodes were removed and the cell immersed in a beaker of electrolyte. The reference and auxiliary electrode were connected electrically via salt bridges made from agar gel and saturated potassium chloride. The remoteness of the auxiliary and reference electrode had no effect on the signal. The result was that the flow through the detector is less restricted and able to exit from the cell through the ports provided for the electrodes. The signal observed is increased by approximately four times. However this system is less tidy. Electrochemical cells are available with less restricted flow than the "Metrohm" cell. The product of EDT Research Ltd. has a relatively wide bore exit tube (≃ 3mm) constructed of steel which also acts as the auxiliary electrode.

6. Preformed Injection Analysis of Phosphate and Silicate.

As a prelude to developing the direct injection flow analysis, the heteropoly acids of phosphate and silicate were injected into a stream of very dilute sulphuric acid (0.005M). The potential of the detector was varied to determine the best value at which to detect the heteropoly acids. The polarographic analyser was used in the DC mode and the variation of current against potential was a smooth line decaying to zero at about + 0.4 v. The current due to 12-silicomolybdate decays at a relatively constant rate. The plot for 12-molybdophosphate has a plateau between + 0.1 v and + 0.2 v where the current is constant. The detector potential was set in the middle of this plateau at + 0.15 v. The shapes of these plots do not correspond to a normal DC voltammetric current-voltage trace.

The PARC 174A analyser also has the facility for sampled DC, normal and differential pulse detection. These modes are not suitable for flow injection work. In pulse techniques the potential is only applied for a fraction of a second and in the sampled DC mode the current is only sampled for a fraction of a second. The result of this is that the point at which the concentration of the sample slug is at a maximum may not be detected. The DC mode applies of constant potential observing the whole of the sample slug.

7. Direct Injection of Phosphate.

Direct injection of phosphate would react to form an heteropoly acid in the reaction coil at room temperature. At room temperature there is no interference from silicate which shows very little reaction. However the phosphate determinations are not carried out at elevated temperatures to avoid the silicate present in the washing powder samples from reacting. As the silicate shows negligible reaction at room temperature in a 3m long reaction coil there is no need for tartaric acid to be included in the reagent stream. Under these conditions only 45% of the injected phosphate reacts. The reaction is reproducible and therefore is applicable to an analytical technique. The injected sample solution does not contain ethanol as does the eluent. Injecting sample solution which is also 46% ethanol gives 20% lower signals than if the sample is 100% aqueous. The mixing of the eluent with the sample must be complete, the signal is not suppressed by the surfactant and a sharp response is observed. The mixing of ethanol and water is exothermic and may accelerate the formation of the heteropoly acid.

Recently Johnson and Petty (1982) suggested that if the reagent was injected into a stream of sample the performance is increased. The signal in this work was found to be identical for both methods. The baseline signal was lower and completely free of noise however. This is due to the lack of reagent in the stream, and the electrode surface will be much less affected by adsorption. In the method proposed using acid molybdate as the eluent the baseline is the blank signal. When the sample is the eluent an additional injection has to be made to determine the reagent blank.

8. Direct Injection of Silicate.

The eluent used for phosphate determinations (0.11M sulphuric acid and 2% ammonium molybdate) is satisfactory for silicate determinations as well. The formation of 12-silicomolybdate is facilitated in a reaction coil 6m in length heated in a water bath at 60°. However we can expect phosphate to interfere. At very low levels (say 10^{-7}M) phosphate will not interfere with silicate determinations (10^{-5}M). Frequently the free orthophosphate in washing powders will give higher concentrations than this. The addition of a mannitol stream to the system converging after the reaction coil, serves to remove phosphate interference. The addition of this stream and the use of a wider bore secondary delay coil lengthens the response and broadens the band width. That is, the signal will be lower due to dilution and increased dispersion. The stream of mannitol has to be 46% ethanol as well as the main stream eluent. The secondary coil (2.1 m x 0.8 m.m.) is maintained at room temperature. If it is heated the silicomolybdate will be destroyed along with the phosphomolybdate.

The use of mannitol appears to reduce signal noise and the electrode of the detector is much more stable. It is possible that the mannitol complexes the unused reagent which would otherwise react at the electrode surface. The suppression of signal due to surfactant is not as extensive in the case of the flow system as in the static system. In the static system the surfactant will be in contact with the electrode for the whole determination. In the flowing systems the sample is only in contact with the electrode for a couple of seconds.

It is essential that the sample injected is of non-hydrolysed material when determining silicate. If the sample has been hydrolysed the phosphate signal will swamp that of silicate. Some hydrolysis of the polyphosphate is expected when making silicate determinations, as the coil is heated and the stream is 0.11M in sulphuric acid. In fact very little hydrolysis occurs and does not interfere with the signal for silicate.

9. Final Comment.

The improvement of the hydrolysis of polyphosphates is not very likely. The use of pressurised flow systems in acid at elevated temperatures is the best option open today. The hydrolysis coil would be heated by an oil bath, this is inconvenient from the safety point of view. It is possible that the oil bath can be replaced by a metal heating block. Likely areas for further investigation are, catalytic hydrolysis with transition metals, UV irradiation, enzymatic catalysis. The use of enzymatic methods may facilitate the separation of individual polyphosphates, specific enzymes hydrolysing a particular phosphate. It is possible to separate polyphosphates on ion exchange resins or chelating resins and determine them individually via a hydrolysis coil. It is necessary for the hydrolysis to be complete as certain phosphates will be decomposed to orthophosphate faster than others.

The flow injection systems devised must be compared with the continuous analyser methods in general use today. It is the intention of the author to propose the developed systems as an alternative. The flow injection system proposed is compact and contains no glassware and so is very durable. A possible disadvantage of using plastic components is the likelihood of adsorption onto the walls of the apparatus. In this method there is no chemical reduction step to the "heteropoly blue". Coloured solutions present no problems with the use of an electrochemical detector. A disadvantage of using solid electrodes is that the surface can become contaminated. The electrode is usually easily removed from the system and cleaning is normally a simple and short procedure. Apart from the hydrolysis step, flow injection analysis is much faster than autoanalyser methods; 12 seconds for phosphate and 32 seconds for silicate. The light and robust nature of flow injection equipment make it ideal for use in the field. As the signal is current it could be directly fed into a microprocessor.

It is possible that a small computer might be used to deconvolute the signals obtained simultaneously for one sample injection for phosphate and silicate. The system employed could have dual detectors at different potentials at which the behaviour of phosphate and silicate heteropoly acids is standardised. It is likely that there exist conditions of stream reagent where the signals due to silicate and phosphate are additive.

Flow injection analysis offers a cheap reliable alternative to more traditional methods for use in the laboratory, field or works. The proposal of injecting reagent into a stream of sample is explicable to on-line monitoring. The use of multi-electrode detectors for the determination of mixture components is a likely application.

G.C.CRIPPS,
Loughborough,
September, 1982.

References

Adams, R.N. (1958), Anal. Chem. 30 1576.

Adams R.N. (1969), Electrochemistry at Solid Electrodes, Dekker, New York.

Aiba S. and Ohtake H. (1977), Water Res. 11 159-164.

Alder J.F., Fleet B. and Kane P.O. (1971), J.Electroanal. Chem. 30 427-431.

Alimarin I.P., Dorokhava E.N., Kazanskii L.P. and Prokhorova G.V. (1981), Russ. J. Anal. Chem. 35 1300-1321.

Al-Sulimany F. and Townsend A. (1973), Analyst 98 34-39.

Anderson L.H. (1958), Acta. Chem. Scand. 12 495-501.

Armentrout D.N., McClean J.D. and Long M.W. (1979), Anal. Chem. 51 1039-1045.

Bard A.J. and Faulkner L.R. (1980), Electrochemical Methods, Wiley, New York.

Barker G.C. and Gardner A.W. (1960), Z. Anal. Chem. 173 79-83.

Basson W.D., Von Staden J.F. and Cattin P.M. (1981), Z. Anal. Chem. 307 373-377.

Baykov A.A. and Araeva S.M. (1982), Anal. Biochem. 119 211-213.

Bazzi A. and Boltz D.F. (1976) Anal. Lett. 9 111-1124.

Gorges J., Porthault M. and Vittori O. (1980), J.Chromatog. 204 123-130.

Bennett H. (1977) Analyst 102 153-179.

Bergamin F.H., Zagatto E.A.G., Krug F.J. and Reis B.F. (1978), Anal. Chim. Acta. 101 17-23.

Blaedel W.J. and Todd J.W. (1958), Anal. Chem. 30 1821-1826.

Blank C.L. (1976), J.Chromatog. 117 35-46.

Bloemers H.P.J., Stephenson M.L. and Zamecvik P.C. (1970), Anal. Biochem. 34 66-70.

Boltz D.F. and Howell J.A. (1978), Colorimetric Determination of Non-Metals, Wiley, New York.

Bond A.M. (1980), Modern Polarographic Methods in Analytical Chemistry, Dekker, New York.

Borman, S.A. (1982), Anal. Chem. 54 698A-705A.

Brewer P.G. and Riley J.P. (1960), Anal. Chim. Acta 35 514-519.

Brunt K. (1981), Trace Analysis 1 47-120.

Burmitz J.S. (1980), in Electroanalysis in Hygiene, Environmental, Clinical and Pharmaceutical Chemistry, Ed. Smyth W.F., Elsevier, Amsterdam.

Buyers A.G. (1958), Anal. Chim. Acta 19 118-124.

Chalmers R.A. and Sinclair A.G. (1965), Anal. Chim. Acta 33 384-390.

Chalmers R.A. and Sinclair A.G. (1966), Anal. Chim. Acta. 34 412-418.

Chesney D.J., Anderson J.L., Weishaar D.E. and Tallman D.E. (1981), Anal. Chim. Acta,124 321-331.

Cheu N.V. and Polotebnova N.A. (1973), Russ. J. Inorg. Chem. 18 1157-1159.

Chin D.T. and Chandran R.V. (1981), J. Electrochem. Soc. 128 1904-1912.

Chesceri N.L. and Lee G.F. (1965), Int. J. Air Water Pollution 9 723-742, 743-751.

Corbridge D.E.C. (1978), Phosphorus, Elsevier, Amsterdam.

Costley B.D. and Farr J.P.G. (1968), Chem. and Ind. 1435-1437.

Cox J.A. and Cheng K.H. (1974), Anal. Lett. 7 659-670.

Crawford W.E., Lin C.I. and Huber C.O. (1973), Anal. Chim. Acta, 64 387-395.

Crouch S.R. and Malmstadt H.V. (1967), Anal. Chem. 39 1084-1089.

Dent Glasser L.S. (1982), Chem. Britain 18 33-39.

Dieker J.W., Van der Linden W.E. and Poppe H. (1978), Talanta 25 151-155.

Dieker J.W., Van der Linden W.E. and Poppe H. (1979), Talanta 26 511-518.

Downes M.T. (1978), Water Res. 12 743-745.

E.G. & G./Princeton Applied Research (1979). Model 174A Polarographic Analyzer, operating and service manual.

Evans H.T. (1971), Perspec.Struct. Chem. 4 1-59.

Evseeva M.A., Ashpur V.V., Mashkovich L.A. and Kuteinikov A.F. (1973), Zavod. Lab. 39 1314-1317.

Ewing G.A. (1975), Instrumental Methods of Chemical Analysis, 4th Edition, McGraw-Hill,,Kogakusha, Tokyo.

Fenn R.J., Siggia S. and Curran D.J. (1978), Anal. Chem. 50 1067-1073.

Fleet B. and Little C.J. (1974), J. Chromatog. Sci. 12 747-752.

Fogg A.G. (1981), Unpublished Results.

Fogg A.G. and Bhanot D. (1981), Analyst 106 883-889.

Fogg A.G., Bsebsu N.K. and Birch B.J. (1981a), Talanta 28 473-479.

Fogg A.G. and Bsebsu N.K. (1981b), Analyst 106 1288-1295.

Fogg A.G., Bsebsu N.K. and Birch B.J. (1981c), Analyst 106 369-374.

Fogg A.G. and Bsebu N.K. (1982), Analyst 107 556-570.

Fogg A.G. and Osakwe A.A. (1978), Talanta 25 226-228.

Freed C.R. and Asmus P.A. (1977), Anal. Chem. 49 2379.

Fruchart J.M. and Souchay P. (1968), Compt. Rend. C266 1571-1574.

Fruchart J.M., Herve G., Launay J.P. and Massart R. (1976), J.Inorg. Nucl. Chem. 38 1627-1634.

Fujinaga T. and Nagosa Y. (1978), Z. Anal. Chem. 292 303-304.

Garrett H.E. and Walker A.J. (1964), Analyst 89 642-650.

Grasshoff, K. (1971), in Advances in Automatic Analysis, Vol. 2, pp. 281-289, Thurman, Miami.

Greenfield S. and Clift M. (1975), The Analytical Chemistry of the Condensed Phosphates, Pergamon, Oxford.

Greenfield S. (1959), Analyst 84 380-385.

Griffith E.J. (1959), Ind. Eng. Chem. 51 240.

Griffith E.J., Beeton, A., Spencer J.M. and Mitchell D.T. (Joint Eds.) (1973), Environmental Phosphorus Handbook, Wiley, New York.

Goulden P.P. and Brooksbank P. (1975), Anal. Chim. Acta, 80 183-187.

Hahn H. and Wagenknecht R. (1961), Z. Anal. Chem. 182 343-357.

Haight G.P., Imamura T. and Robinson, P.R. (1979), Fund. Res. Homog. Cat. 3 1033-1043.

Halman M. (Ed.) (1972), Analytical Chemistry of Phosphorus Compounds, Wiley, New York.

Hanekamp H.B., Bos P. and Frei R.W. (1979a), J. Chromatog. 186 489-496.

Hanekamp H.B., Bos P. and Brinkman Th. (1979b) Z. Anal. Chem. 297 404-410.

Hanekamp H.B., Bos P. and Frei R.W. (1982) Trend. Anal. Chem. 1 135-140.

Hargis L.G. (1970), Anal. Chem. 42 1494-1497 and 1497-1500.

Harwood J.E., Van Steenderen R.A. and Kuhn A.L. (1969) Water Res. 3 425-432.

Hirai Y., Yoza N. and Ohashi S. (1979), J. Liq. Chromatog. 2 677-685.

Hirai Y., Yoza N. and Ohashi S. (1980), Anal. Chim. Acta. 115 269-277.

Hirai Y., Yoza N. and Ohashi S. (1981a), J. Chromatog. 206 501-509.

Hirai Y., Yokoyama T., Yoza N., Tarutani T. and Ohashi S. (1981b), Bunseki Kagaku 30 350-351.

Hoffman E. and Saracz A. (1962), Z. Anal. Chem. 190 326-329.

Hori T., Iton T., Okazaki S. and Fujinagu T. (1981) Bunseki Kagaku 30 582-587.

Huffman E.Q. and Fleming J.D. (1960), J. Phys. Chem. 64 240-249.

Illingworth J.W. and Keggin J.F. (1935), J.C.S. 57 575-582.

Imamura T., Hinton D.M., Belford R.L., Gumport R. and Haight G.P. (1979), J. Inorg. Biochem. 11 241-259.

Ivaska A. and Ryan T.H. (1981), Coll.Czech. Chem. Comm. 46 2865-2870.

Iyer C.S.P., Valenta P. and Nurnberg H.W. (1981), Anal.Lett. 14 921-931.

Janata J. and Ruzicka J. (1982), Anal. Chim. Acta. 139 105-115.

Johnson D.L. (1971), Env. Sci. Technol. 5 411-414.

Johnson K.S. and Petty R.C. (1982), Anal. Chem. 54 1185-1187.

Josse J. (1966), J. Biol. Chem. 241 1938-1947 and 1948-1955.

Kasprzak M.S., Leroi G.E. and Crouch S.R. (1982), Appl. Spectroscopy 36 285-289.

Keggin K.F. (1934), Proc. R. Soc. A. 144 75-86.

Kemuda W. (1952), Roczniki Chem. 26 281.

Kircher C.C. and Crouch S.R. (1982a), Anal. Chem. 54 879-884.

Kircher C.C. and Crouch S.R. (1982b), Anal. Chem. 54 1219-1221.

Kirkbright G.F., Smith A.M. and West T.S. (1967), Analyst 92 411-416.

Koen J.G., Huber J.F.K., Poppe H. and den Boef G. (1970), 8 192-199.

Kulaev I.S. (1979), The Biochemistry of Inorganic Polyphosphates, Wiley, Chichester.

Laitenen H.A. and Burdett L.W. (1951) Anal. Chem. 23 1265-1268.

Lankelma J. and Poppe H. (1976), J.Chromatog. 125 375-388.

Launay J.P., Massart R. and Souchay P. (1974), J. Less Comm. Metal 36 139-150.

Launay J.P., Fournier M., Sanchez C. and Pope M.T. (1980), Inorg. Nucl. Chem. Lett. 16 257-261.

Lindquist J. (1974) J. Electroanal. Chem. 52 37-46.

Lund W. and Opheim L.N. (1975), Anal. Chim. Acta, 79 35-45.

Lund W., Harrisdale M. and Greibrook T. (1979), J. Chromatog. 173 249-261.

McDonald A.M.G. and Van der Voort F.H. (1968), Analyst 93 65-71.

Majer V., Veseley J. and Stulick K. (1973), J.Electroanal. Chem. 45 113-125.

Mann C.K. (1957), Anal. Chem. 29 1385-1386.

Marcoux L.S., Prater K.B., Prater B.G., Adams R.W. and Kan L. (1965), Anal. Chem. 37 1446-1447.

Matsuura N., Unomoto K., Takizawa M. and Sasaki Y. (1974), Bull. Chem. Soc. Jap. 47 1172-1175.

Meschi P.L. and Johnson D.C. (1981a), Anal.Chim. Acta. 124 303-314.

Meschi P.L., Johnson D.C. and Luecke G.R. (1981b), Anal. Chim. Acta. 124 315-320.

Meyerhof O., Shatas R. and Kaplan A. (1953), Bioc. Biop. Acta. 12 121-127.

Mueller O.H. (1947), J.A.C.S. 69 2992-2997.

Myshlyaeva L.V. and Krasnoshchekov V.V. (1974), Analytical Chemistry of Silicon, Wiley, Chichester.

Nakamura T., Yamaguchi H. and Ohashi S. (1980), J.UOEH.(University of Occupational and Environmental Health) 2 199-205.

Olson C. and Adams R.N. (1963), Anal. Chim. Acta. 29 358-363.

Osburn Q.W., Lemmel D.E. and Downey R.L. (1974), Env. Sci. Technol. 8 363-366.

Osteryoung R.A. and Osteryoung J. (1981), Phil. Trans. R. Soc. Lond. A. 302 315-326.

Paul J. (1965) Mikrochim. Acta. 830-835.

Parenello M., Bedendo A. and Bertini A. (1977), Riv. Ital. Sostanze, Grasse 54 364-368.

Pierpoint W.S. (1957), Biochem. J. 67 466-472.

Ploger M.L., Pottkamp F. and Umland F. (1971), Z. Anorg. Allg. Chem. 407 211-226.

Pope M.T. (1980) in Mixed Valence Compounds (Brown, D.B. ed.) pp. 365-386, Reidel, New York.

Pottkamp F. and Umland F. (1971), Z. Anal. Chem. 255 367-368.

Pungor E. and Szepesvary E. (1968), Anal. Chim. Acta. 43 289-296.

Pungor E., Feher Zs. and Magy G. (1975), Pure Appl. Chem. 44 595-612.

Ramakrishna T.V., Robinson J.W. and West P.W. (1969), Anal. Chim. Acta. 45 43-49.

Rebertus R.L., Cappell R.J. and Bond G.W. (1958) Anal. Chem. 30 1825-1827.

Reynolds C.A. and Rogers L.B. (1949), Anal. Chem. 21 176-178.

Rogers L.B. and Reynolds C.A. (1949), J.A.C.S. 71 2081-2085.

Roux L. and Boutin J.P. (1975), Agrochimica 19 243-248.

Rucki R.J. (1980), Talanta 27 147-156.

Ruzicka J. and Hansen E.H. (1981), Flow Injection Analysis, Wiley, New York.

Sand J.R., Lin J.H. and Huber C.O. (1976), Anal. Chim. Acta. 87 79-90.

Sarkar R.C. (1981), J. Ind. Chem. Soc. 58 362-363.

Scott R.A.S. and Haight G.P. (1975), Anal. Chem. 47 2439-2441.

Sen B.P. and Chatterjee S.N. (1966), Anal. Chem. 38 536-541.

Shaw S. and Townsend A. (1973), Talanta 20 332-335.

Shen C.Y. and Dryoff D.R. (1962), Anal. Chem. 34 1367-1370.

Silcox D.C. and McCarty D.J.M. (1973), J. Clin. Invest. 52 1863-1869.

Simon S.J. and Boltz D.F. (1975), Anal. Chem. 47 1758-1763.

Souchay P. (1965), Talanta 12 1187-1209.

Strickland J.D.H. (1952), J.A.C.S. 862, 868 and 872.

Strohl A.N. and Curran D.J. (1979), Anal. Chem. 51 1045-1049.

Stulick K. and Pacakova V. (1981a), J. Electroanal. Chem. 129 1-24.

Stulick K., Pacakova V. and Starkova B. (1981b), J. Chromatog. 213 41-46.

Swartzfager D.G. (1976), Anal. Chem. 48 2189-2192.

Takakata Y. and Muto G. (1973), Anal. Chem. 45 1864-1868.

Testa A.C. and Reinmuth W.H. (1961), Anal. Chem. 33 1324-1328.

Thilo E. (1965), Angew. Chem. 4 1061-1071.

Toth K., Feher Zs., Nagy G. and Pungor E. (1981), in Nature, Aims and Methods of Microchemistry (8th Symposium) pp. 301-314, Springer-Verlag, Vienna.

Toy, A.D.F. (1976), Phosphorus Chemistry in Everyday Living, A.C.S., Washington.

Truedell L. and Boltz D.F. (1963), Anal. Chem. 35 2122-2124.

Truesdale V.W. and Smith C.J. (1975a, b), Analyst 100 203-212, 797-805.

Truesdale V.W. and Smith C.J. (1976), Analyst 101 19-31.

Truesdale V.W., Smith C.J. and Smith P.J. (1977), Analyst 102 73-85.

Truesdale V.W., Smith P.J. and Smith C.J. (1979), Analyst 104 897-918.

Tsigdinos G.A. and Hallada C.J. (1970), Inorg. Chem. 9 2488-2492.

Tsigdinos G.A. and Hallada C.J. (1974), J. Less. Comm. Metal 36 79-94.

Tsigdinos G.A. (1978), Topics in Curr. Chem. 76 1-64.

Umland F. Pottkamp F. and Alt. F. (1973), Z.Anorg. Allg. Chem., 395 320-332.

Van der Linden W.E. and Dieker J.W. (1980), Anal. Chim. Acta. 119 1-24.

Wang T. and Dewald H.D. (1982), Talanta 29 453-456.

Weakley T.J.R. (1974), Struct. and Bond. 18 131-176.

Werner J. and Ebert J. (1977), Z. Wasser. Abwasser-Forschung, 10 24-30.

Wightman R.M., Paik E.C., Borman S. and Duyton M.A. (1978), Anal. Chem. 50 1110-1115.

Wilson A.L. (1965), Analyst 90 270-277.

Yamada J. and Matsuda H. (1973), J. Electroanal. Chem. 44 189-198.

Yamaguchi J., Nakamura T., Hirai Y. and Ohashi S. (1979), J. Chromatog. 172 131-140.

Young R.S. (1976), Topics in Phosphorus Chemistry, 8 451-514.

Yoza N., Kouchiyama, Miyajima T. and Ohashi S. (1975), Anal. Lett. 8 641-653.

Yoza N., Kurokawa Y., Hirai Y. and Ohashi S. (1980a), Anal. Chim. Acta. 121 281-287.

Yoza N., Ito K., Hirai Y. and Ohashi S. (1980b), J.Chromatog. 196 471-480.

Zaugg W.S. and Knox R.J. (1966), Anal. Chem. 38 1759-1760.

Zittel H.E. and Miller F.J. (1965), Anal. Chem. 37 200-203.